ENCLOSURE 2

TENNESSEE VALLEY AUTHORITY
BROWNS FERRY NUCLEAR PLANT (BFN)
UNITS 1, 2, AND 3

TECHNICAL SPECIFICATIONS (TS) CHANGES TS-431 AND TS-418
EXTENDED POWER UPRATE (EPU)

STRUCTURAL INTEGRITY ASSOCIATES, INC. CALCULATION PACKAGE 0006982.304, REVISION 1, "COMPARISON STUDY OF SUBSTRUCTURE AND SUBMODEL ANALYSIS USING ANSYS"

Attached is Structural Integrity Associates, Inc. Calculation Package 0006982.304, Revision 1, "Comparison Study of Substructure and Submodel Analysis using ANSYS."

Structural Integrity Associates, Inc.	File No.: 0006982.304
CALCULATION PACKAGE	**Project No.:** 0006982.00

PROJECT NAME:

Extended Power Uprate Main Steam Line Strain Gauge Vibration Monitoring

CONTRACT NO.:

CWA P4463

CLIENT:	**PLANT:** Browns Ferry Units 1, 2 & 3
Tennessee Valley Authority (TVA)	

CALCULATION TITLE:

Comparison Study of Substructure and Submodel Analysis using ANSYS

Document Revision	Affected Pages	Revision Description	Project Manager Approval Signature & Date	Preparer(s) & Checker(s) Signatures & Date
0	1-97, A1-A4, Computer Files	Initial Issue.	K. K. Fujikawa 10/30/08	S. B. Kok 10/30/08 ---------- R. Gnagne 10/30/08 M. Qin 10/30/08
1	1-117, A1-A5, Computer Files	Incorporate NRC RAI and client's comments.	K. K. Fujikawa 01/08/09	S.B. Kok 01/08/09 M Qin 01/08/09

Table of Contents

EXECUTIVE SUMMARY 8
1.0 INTRODUCTION 12
1.1 Background Information 12
1.2 Validation Methodology 12
1.3 Nomenclature 13
1.4 Revision History 14
2.0 STRUCTURE DESCRIPTION AND MATERIAL PROPERTIES 15
3.0 FINITE ELEMENT MODEL DEVELOPMENT 16
3.1 Model Descriptions and Boundary Conditions 17
3.1.1 Full Shell Model 17
3.1.2 Full Solid Model 18
3.1.3 Shell Submodel #1 19
3.1.4 Solid Submodel #1 20
3.1.5 Shell Submodel #2 21
3.1.6 Solid Submodel #2 23
3.2 Finite Element Mesh 25
3.3 Stress Paths 27
4.0 LOAD CASES 29
4.1 Static Analysis Load Cases 29
4.2 Dynamic Analysis Load Cases 30
5.0 STATIC ANALYSIS RESULTS 31
5.1 Static Load Case #1 31
5.1.1 Full Shell Finite Element Analysis 31
5.1.2 Full Solid Finite Element Analysis 32
5.1.3 Substructure Analysis Using Shell Submodel #1 34
5.1.4 Substructure Analysis Using Shell Submodel #2 35
5.1.5 Substructure Analysis Using Solid Submodel #1 36
5.1.6 Substructure Analysis Using Solid Submodel #2 38
5.1.7 Submodel Analysis Using Submodel #1 40
5.1.8 Submodel Analysis Using Submodel #2 45
5.2 Static Load Case #2 50
5.2.1 Full Shell Finite Element Analysis 50
5.2.2 Full Solid Finite Element Analysis 51
5.2.3 Substructure Analysis Using Shell Submodel #1 53

5.2.4 Substructure Analysis Using Shell Submodel #2 ..... *54*
5.2.5 Substructure Analysis Using Solid Submodel #1 ..... *55*
5.2.6 Substructure Analysis Using Solid Submodel #2 ..... *57*
5.2.7 Submodel Analysis Using Submodel #1 ..... *59*
5.2.8 Submodel Analysis Using Submodel #2 ..... *64*
6.0 DYNAMIC ANALYSIS RESULTS 69
6.1 Structural Modal Analysis 70
6.1.1 Shell Model Modal Frequencies *70*
6.1.2 Solid Model Modal Frequencies *71*
6.2 Structural Damping Values 72
6.3 Time History Analysis Integration Time Step 72
6.4 Dynamic Load Case #1 73
6.4.1 Full Shell Finite Element Time History Analysis *73*
6.4.2 Full Solid Finite Element Time History Analysis *77*
6.4.3 Substructure Time History Analysis Using Shell Submodel #2 ..... *82*
6.4.4 Substructure Time History Analysis Using Solid Submodel #2 ..... *85*
6.4.5 Submodel Analysis Using Submodel #2 ..... *87*
6.5 Dynamic Load Case #2 92
6.5.1 Full Shell Finite Element Time History Analysis *92*
6.5.2 Full Solid Finite Element Time History Analysis *96*
6.5.3 Substructure Time History Analysis Using Shell Submodel #2 ..... *101*
6.5.4 Substructure Time History Analysis Using Solid Submodel #2 ..... *104*
6.5.5 Submodel Analysis Using Submodel #2 ..... *106*
7.0 SUMMARY STRESS REDUCTION FACTORS 111
7.1 Static Analysis SRF 111
7.2 Dynamic Analysis SRF 112
8.0 DISCUSSIONS 113
8.1 Static Analysis 113
8.2 Dynamic Analysis 114
8.3 Submodeling Validity 115
9.0 CONCLUSIONS 116
10.0 REFERENCES 117

Appendix A - Computer Files A1

List of Tables

Table 2-1 Key Dimensions 15
Table 5-1 Full Solid Model Baseline Analysis SRF for Static Load Case #1 33
Table 5-2 Substructure Analysis (Submodel #1) SRF for Static Load Case #1 37
Table 5-3 Substructure Analysis (Submodel #2) SRF for Static Load Case #1 39
Table 5-4 Submodel Analysis (Submodel #1) SRF for Static Load Case #1 44
Table 5-5 Submodel Analysis (Submodel #2) SRF for Static Load Case #1 49
Table 5-6 Full Solid Model Baseline Analysis SRF for Static Load Case #2 52
Table 5-7 Substructure Analysis (Submodel #1) SRF for Static Load Case #2 56
Table 5-8 Substructure Analysis (Submodel #2) SRF for Static Load Case #2 58
Table 5-9 Submodel Analysis (Submodel #1) SRF for Static Load Case #2 63
Table 5-10 Submodel Analysis (Submodel #2) SRF for Static Load Case #2 68
Table 6-1 Shell Model Structural Vertical (Y direction) Modal Frequencies 70
Table 6-2 Shell Model Structural Horizontal (Z direction) Modal Frequencies 70
Table 6-3 Solid Model Structural Vertical (Y direction) Modal Frequencies 71
Table 6-4 Solid Model Structural Horizontal (Z direction) Modal Frequencies 71
Table 6-5 Full Solid Model Time History Analysis SRF for Dynamic Load Case #1 81
Table 6-6 Substructure Time History Analysis using Solid Submodel #2 SRF for Dynamic Load Case #1 86
Table 6-7 Submodel Analysis (Submodel #2) SRF for Dynamic Load Case #1 91
Table 6-8 Full Solid Model Time History Analysis SRF for Dynamic Load Case #2 100
Table 6-9 Substructure Time History Analysis using Solid Submodel #2 SRF for Dynamic Load Case #2 105
Table 6-10 Submodel Analysis (Submodel #2) SRF for Dynamic Load Case #2 110
Table 7-1 Summary SRF for Static Load Case #1 111
Table 7-2 Summary SRF for Static Load Case #2 111
Table 7-3 Summary SRF for Dynamic Load Case #1 112
Table 7-4 Summary SRF for Dynamic Load Case #2 112

List of Figures

Figure 3-1 Full Shell Model 17
Figure 3-2 Full Solid Model 18
Figure 3-3 Shell Submodel #1 19
Figure 3-4 Solid Submodel #1 20
Figure 3-5 Shell Submodel #2 21
Figure 3-6 Solid Submodel #2 23
Figure 3-7 Shell Finite Element Model Mesh 25
Figure 3-8 Solid Finite Element Model Mesh 26
Figure 3-9 Solid Finite Element Model Stress Paths (Side View) 27
Figure 3-10 Solid Finite Element Model Stress Paths (Top View) 28
Figure 5-1 Full Shell Model Stress Plot for Case #1 (Full Shell Model Baseline Analysis) 31
Figure 5-2 Full Solid Model Analysis Stress Plot for Load Case #1 (Full Solid Model Baseline Analysis) 32
Figure 5-3 Substructure Analysis using Shell Submodel #1 Stress Plot for Load Case #1 34
Figure 5-4 Substructure Analysis using Shell Submodel #2 Stress Plot for Load Case #1 35
Figure 5-5 Substructure Analysis using Solid Submodel #1 Stress Plot for Load Case #1 36
Figure 5-6 Substructure Analysis using Solid Submodel #2 Stress Plot for Load Case #1 38
Figure 5-7 Submodel Analysis using Submodel #1 Applied Displacements for Load Case #1 40
Figure 5-8 Submodel Analysis using Submodel #1 Stress Profile Comparison for Load Case #1 41
Figure 5-9 Submodel Analysis using Submodel #1 Shell Model Stress Plot for Load Case #1 42
Figure 5-10 Submodel Analysis using Submodel #1 Solid Model Stress Plot for Load Case #1 43
Figure 5-11 Submodel Analysis using Submodel #2 Applied Displacements for Load Case #1 45
Figure 5-12 Submodel Analysis using Submodel #2 Stress Profile Comparison for Load Case #1 46
Figure 5-13 Submodel Analysis using Submodel #2 Shell Model Stress Plot for Load Case #1 47
Figure 5-14 Submodel Analysis using Submodel #2 Solid Model Stress Plot for Load Case #1 48
Figure 5-15 Full Shell Model Stress Plot for Case #2 (Full Shell Model Baseline Analysis) 50
Figure 5-16 Full Solid Model Analysis Stress Plot for Load Case #2 (Full Solid Model Baseline Analysis) 51
Figure 5-17 Substructure Analysis using Shell Submodel #1 Stress Plot for Load Case #2 53

Figure 5-18 Substructure Analysis using Shell Submodel #2 Stress Plot for Load Case #2 54
Figure 5-19 Substructure Analysis using Solid Submodel #1 Stress Plot for Load Case #2 55
Figure 5-20 Substructure Analysis using Solid Submodel #2 Stress Plot for Load Case #2 57
Figure 5-21 Submodel Analysis using Submodel #1 Applied Loads for Load Case #2 59
Figure 5-22 Submodel Analysis using Submodel #1 Stress Profile Comparison for Load Case #2 .. 60
Figure 5-23 Submodel Analysis using Submodel #1 Shell Model Stress Plot for Load Case #2 61
Figure 5-24 Submodel Analysis using Submodel #1 Solid Model Stress Plot for Load Case #2 62
Figure 5-25 Submodel Analysis using Submodel #2 Applied Loads for Load Case #2 64
Figure 5-26 Submodel Analysis using Submodel #2 Stress Profile Comparison for Load Case #2 ... 65
Figure 5-27 Submodel Analysis using Submodel #2 Shell Model Stress Plot for Load Case #2 66
Figure 5-28 Submodel Analysis using Submodel #2 Solid Model Stress Plot for Load Case #2 67
Figure 6-1 Full Shell Model Time History Analysis Vertical Transient Displacements for Load Case #1 73
Figure 6-2 Full Shell Model Time History Analysis Nodal Stress Intensity for Load Case #1 74
Figure 6-3 Full Shell Model Time History Analysis Vertical Displacement Plot for Load Case #1 (Full Shell Model Baseline Analysis) 75
Figure 6-4 Full Shell Model Time History Analysis Maximum Stress Intensity Plot for Load Case #1 (Full Shell Model Baseline Analysis) 76
Figure 6-5 Shell and Solid Model Time History Analysis Vertical Transient Displacement for Load Case #1 77
Figure 6-6 Shell and Solid Model Time History Analysis Stress Intensity for Load Case #1 78
Figure 6-7 Full Solid Model Time History Analysis Vertical Displacement Plot for Load Case #1 (Full Solid Model Baseline Analysis) 79
Figure 6-8 Full Solid Model Time History Analysis Maximum Stress Intensity Plot for Load Case #1 (Full Solid Model Baseline Analysis) 80
Figure 6-9 Substructure Time History Analysis using Shell Submodel #2 Nodal Stress Intensity for Load Case #1 82
Figure 6-10 Substructure Time History Analysis using Shell Submodel #2 Vertical Displacement Plot for Load Case #1 83
Figure 6-11 Substructure Time History Analysis using Shell Submodel #2 Maximum Stress Intensity Plot for Load Case #1 84
Figure 6-12 Substructure Time History Analysis using Solid Submodel #2 Maximum Stress Intensity Plot for Load Case #1 85
Figure 6-13 Submodel Analysis using Submodel #2 Applied Displacements for Load Case #1 87

Figure 6-14 Submodel Analysis using Submodel #2 Stress Profile Comparison for Load Case #1 ... 88

Figure 6-15 Submodel Analysis using Submodel #2 Shell Model Maximum Stress Intensity Plot for Load Case #1 ... 89

Figure 6-16 Submodel Analysis using Submodel #2 Solid Model Maximum Stress Intensity Plot for Load Case #1 ... 90

Figure 6-17 Full Shell Model Time History Analysis Horizontal Transient Displacement for Load Case #2 ... 92

Figure 6-18 Full Shell Model Time History Analysis Nodal Stress Intensity for Load Case #2 ... 93

Figure 6-19 Full Shell Model Time History Analysis Horizontal Displacement Plot for Load Case #2 (Full Shell Model Baseline Analysis) ... 94

Figure 6-20 Full Shell Model Time History Analysis Maximum Stress Intensity Plot for Load Case #2 (Full Shell Model Baseline Analysis) ... 95

Figure 6-21 Shell and Solid Model Time History Analysis Horizontal Transient Displacement for Load Case #2 ... 96

Figure 6-22 Shell and Solid Model Time History Analysis Stress Intensity for Load Case #2 ... 97

Figure 6-23 Full Solid Model Time History Analysis Horizontal Displacement Plot for Load Case #2 (Full Solid Model Baseline Analysis) ... 98

Figure 6-24 Full Solid Model Time History Analysis Maximum Stress Intensity Plot for Load Case #2 (Full Solid Model Baseline Analysis) ... 99

Figure 6-25 Substructure Time History Analysis using Shell Submodel #2 Nodal Stress Intensity for Load Case #2 ... 101

Figure 6-26 Substructure Time History Analysis using Shell Submodel #2 Horizontal Displacement Plot for Load Case #2 ... 102

Figure 6-27 Substructure Time History Analysis using Shell Submodel #2 Maximum Stress Intensity Plot for Load Case #2 ... 103

Figure 6-28 Substructure Time History Analysis using Solid Submodel #2 Maximum Stress Intensity Plot for Load Case #2 ... 104

Figure 6-29 Submodel Analysis using Submodel #2 Applied Horizontal Loads for Load Case #2 ... 106

Figure 6-30 Submodel Analysis using Submodel #2 Stress Profile Comparison for Load Case #2 ... 107

Figure 6-31 Submodel Analysis using Submodel #2 Shell Model Maximum Stress Intensity Plot for Load Case #2 ... 108

Figure 6-32 Submodel Analysis using Submodel #2 Solid Model Maximum Stress Intensity Plot for Load Case #2 ... 109

EXECUTIVE SUMMARY

Purpose

This purpose of this calculation is to address the United States Nuclear Regulatory Commission (NRC) requests for additional information (RAI) #199/156 (Reference 3) and #201/162 (Reference 7) pertaining to Tennessee Valley Authority (TVA) Browns Ferry Units 1 and 2 extended power uprate (EPU) licensing application.

This calculation documents a comparison study of TVA's submodel analysis (referred to as submodel analysis) and the typical submodel analysis (referred to as substructure analysis). The objective is to establish if the submodel analysis is a valid approach for establishing the Stress Reduction Factor (SRF), which is used to factor the local shell stress, which has been computed without the benefit of modeling the weld.

Approach and Scope

In this comparison study, the analyses are performed using a structure consisting of two plates: a horizontal plate (6" wide by 20" long by ¼" thick) welded along the 6" edge to a vertical plate (10" wide by 40" tall by ½" thick) centrally at mid height location using ¼" double-sided fillet weld. It is also assumed that the fillet weld is provided at both ends of the horizontal plate, with rounded transition from the end fillet weld to the side fillet weld. The top and bottom edges of the vertical plate are fixed. This configuration is subjected to finite element modeling and analysis using full shell, full solid, shell submodel and solid submodel techniques to determine comparative SRFs. Additional details for all models are provided in Section 3.1.

The load cases include:

1. Load Case #1: Apply a load that generates primarily bending stress through the thickness of the horizontal plate.
2. Load Case #2: Apply a load that generates primarily membrane stress in the horizontal plate.

The analysis cases include:

1. Static analysis by applying a static uniform load at the free edge of the horizontal plate.
2. Dynamic time history analysis by applying a harmonic uniform load at the free edge of the horizontal plate.

The computed SRFs include:

1. Full Solid Model Analyses: The full solid model is the same size as the full shell model except that it is generated using solid elements and includes detailed modeling of the welds. SRF for a load/analysis case is the ratio of the maximum linearized membrane plus bending stress at the weld from the full solid model to the maximum stress from the full shell model for the same load/analysis case. These SRFs provide a baseline against which the accuracy and conservatism of both the substructure and submodel techniques may be judged.
2. Substructure Analyses: The substructure analyses apply boundary displacements along the perimeter of substructure models generated with shell elements. The boundary displacements are extracted from the full shell model analysis results along the lines that coincide with the substructure model boundaries. The same displacements are then applied to substructure models generated using solid elements and including detailed modeling of the welds. SRF for each load and analysis case is the ratio of the maximum linearized membrane plus bending stress from the solid substructure model to the maximum stress in the joint from the full shell model.
3. Submodel Analyses: The submodel analyses apply displacements or loads to a submodel generated using shell elements to match stress intensity along the weld line common to both the full shell and submodel. These loads or displacements are then applied to a submodel of the same size as the shell submodel but generated using solid elements and including detailed modeling of the weld. SRF for a load/analysis case is the ratio of the maximum linearized membrane plus bending stress at the weld from the solid submodel to the maximum stress from the full shell model.

Key SRF Comparison

Static Analysis SRF Comparison

Load Case #1	SRF
Full Solid Model Baseline Analysis	0.59
Substructure Analysis (1)	0.69
Submodel Analysis (1)	0.66

Load Case #2	SRF
Full Solid Model Baseline Analysis	0.89
Substructure Analysis (1)	0.91
Submodel Analysis (1)	0.89

Note: (1) SRF is computed using submodel #2. The SRF computed using submodel #1 is provided in the calculation, but, has been excluded in this executive summary for brevity.

Dynamic Analysis SRF Comparison

Load Case #1	SRF
Full Solid Model Baseline Time History Analysis	0.59
Substructure Time History Analysis (1)	0.68
Submodel (Static) Analysis (1)	0.66

Load Case #2	SRF
Full Solid Model Baseline Time History Analysis	0.89
Substructure Time History Analysis (1)	0.91
Submodel (Static) Analysis (1)	0.89

Note: (1) SRF is computed using submodel #2.

The solid model baseline analysis does not include any inherent approximation or assumption that is associated with the substructure and submodel analyses. The SRFs computed using the solid model baseline analysis provide an accurate benchmarks for comparison.

The comparison of the SRF provided in the above tables show that:

- The SRFs computed using the full solid to full shell model comparison confirm that shell model stress results are conservative for configurations which represent the double fillet welds used in many BFN Steam Dryer plate-to-plate joints. This is indicated by the computed SRFs of 0.59 and 0.89 for Load Cases 1 and 2, respectively (i.e., both < 1.0). Furthermore, these SRFs were found to be invariant for both static and dynamic analyses.

- The SRFs computed using the substructure analysis are generally higher than the SRFs computed using the solid model baseline analysis. The SRFs are higher because in a substructure analysis

the displacements from a more flexible shell model are applied onto the boundaries of a more rigid solid model, which models in the detailed weld configuration. This stiffness discrepancy between the shell and the solid models causes higher stresses to be computed in the solid model, thus resulting in higher SRF for the substructure analysis.

- The SRFs computed using the submodel analysis technique either match (Load Case 2) or provide a conservative bias (12% - Load Case 1) when compared to full model SRFs. Furthermore, these SRFs are invariant for static and dynamic analyses.

Conclusion

In conclusion, the comparisons above show that the SRFs computed using the submodel analysis approach are accurate and acceptable, and therefore, validate the submodel analysis approach adopted for the steam dryer stress analysis.

1.0 INTRODUCTION

1.1 Background Information

This calculation addresses United States Nuclear Regulatory Commission (NRC) request for additional information (RAI) #199/156 (Reference 3) pertaining to Tennessee Valley Authority (TVA) Browns Ferry Units 1 and 2 extended power uprate (EPU) licensing application.

In the stress assessment of the Unit 1 steam dryer, TVA has employed submodel analysis approach to determine a stress reduction factor (SRF) and apply it to the shell analysis stress in the full shell model steam dryer analysis. NRC has noted that the submodel analysis approach is different from a typical substructure analysis approach, as employed in the general purpose finite element code such as ANSYS (References 4 and 5). This calculation validates the submodel analysis approach by specifically addressing the following issues:

An analysis of the problem using a typical substructure analysis approach.

1. An analysis of the problem applying the submodel analysis approach, by applying "loads" to match the stress intensity along a line common to the full shell model and the shell submodel.
2. An analysis of the problem applying the submodel analysis approach, by applying "displacements" to match the stress intensity along a line common to the full shell model and the shell submodel.
3. A comparison of the results obtained in (1) using the typical substructure analysis approach with those in (2) and (3) using the submodel analysis approach.

1.2 Validation Methodology

The submodel analysis approach will be validated using two analysis options: (1) static analysis and (2) dynamic time history analysis. In both the static and dynamic time history analyses, the submodel analysis approach will be compared with the typical substructure analysis approach.

In addition to the requested comparison of the two approaches, the following additional analyses are performed to provide more benchmark comparison:

- Perform a static analysis using a full solid model, which models in the detailed weld configuration. This full solid model analysis provides the most accurate information, since this does not include any inherent assumption or approximation associated with substructure or submodel analysis techniques.
- In the static analysis, two submodels are developed: one submodel is 1/2 the size of the full model, and the other is 3/4 the size of the full model. The two different sized models will provide some additional data for comparison, and establish if the size of the submodel influences the analysis results.

1.3 Nomenclature

The key terminology used in the calculation is defined as follows.

Submodel

This refers to a subpart of the full model that has been developed for use in either the substructure analysis or the submodel analyses.

Substructure Analysis

Substructure analysis refers to a typical analysis approach, as employed in the general purpose finite element codes such as ANSYS. In this approach, the displacements from the full model analysis are interpolated and mapped onto the nodes on the appropriate submodel boundaries. These nodal displacements along the boundaries and any loads applied to the local region determine the solution of the submodel.

Submodel Analysis

In a submodel analysis, two submodels are created: one is based on shell elements and the other solid elements. The shell submodel is used to match the stress profile in the submodel with the corresponding stress profile of the full shell model. This matching of stress profile is an iterative process. This is performed by applying loads or displacements, typically along a line. When a close match of the stress profile is achieved, the established loads or displacements can then be applied to the corresponding solid submodel stress analysis. Appropriate boundary conditions are required to be applied to the submodel boundaries. A stress reduction factor (SRF) is calculated by comparing the solid submodel result to the corresponding full shell model result. The SRF is then applied to the appropriate stresses in the full model shell analysis.

Stress Reduction Factor (SRF)

This refers to the ratio of the maximum solid submodel linearized stress intensity and the maximum full shell model stress intensity, at the location of interest. Mathematically, SRF is defined as "Solid Submodel Maximum Linearized $P_m + P_b$ Stress Intensity (along solid submodel stress paths) / Full Shell Model Maximum $P_m + P_b$ Stress Intensity".

1.4 Revision History

Revision 1

This revision addresses the following issues:

- Incorporates the action items pertaining to the submodel analysis documented in NRC's Round 23 Draft RAI (Reference 7). The action items include: a) Perform a full solid finite element analyses for the two dynamic load cases listed in Section 4.2. b) Compare the resulting weld stresses from the full shell finite element analyses with the full solid finite element analyses to establish the Stress Reduction Factors. c) Compare the Stress Reduction Factors computed in b) with the Stress Reduction Factors computed using TVA's submodeling approaches, and assess the validity of TVA's submodeling approach.
- Use a structural damping of 1%, which is consistent with the damping value used in the steam dryer analysis (Reference 6).
- Use the appropriate mass density for the dynamic analysis. In the Revision 0 of this calculation, the material weight density was inadvertently used in the dynamic analysis.

2.0 STRUCTURE DESCRIPTION AND MATERIAL PROPERTIES

Structure Description

With reference to Figure 3-1, the structure used for this study consists of:

- A 10" x 40" x 1/2" thick vertical plate.
- A 6" x 12" x 1/4" thick horizontal plate.
- The 1/4" horizontal plate is welded to the 1/2" vertical plate using double-sided 1/4" fillet weld. The fillet weld is wrapped around at both ends of the horizontal plate.
- The vertical plate is restrained at the top and at the bottom. The vertical edges of the vertical plate are not restrained.
- A-240, Type 304 stainless steel material properties at 550°F (Reference 1) are assumed for all components.

Table 2-1
Key Dimensions

Component	Thickness / Size (in)	Modeled Dimensions (in x in)
Vertical Plate	1/2"	10" (width) x 40" (height)
Horizontal Plate	1/4"	6" (width) x 12" (long)
Weld (1)	1/4"	Along the entire connection.

Note: (1) The fillet weld is modeled in the solid finite element models, on both sides.

Material Properties

Modulus of Elasticity	=	25.55E6	psi (Reference 2)
Poisson's Ratio	=	0.30	
Mass Density	=	0.735E-3	$lb\text{-}s^2/in^4$

3.0 FINITE ELEMENT MODEL DEVELOPMENT

There are a total of 6 finite element models used in this study:

1. The full shell model (see Figure 3-1). This model is used to establish the Shell Baseline Analysis.
2. The full solid model (see Figure 3-2). This model is used to establish the Solid Baseline Analysis.
3. The shell submodel #1 (see Figure 3-3). This shell submodel is 1/2 the size of the full shell model. This model is used in the submodel analysis to match the stress intensity along the weld line.
4. The solid submodel #1 (see Figure 3-4). This solid submodel corresponds to the shell submodel as shown in Figure 3-3. This model is used to establish the stress reduction factor (SRF).
5. The shell submodel #2 (see Figure 3-5). This shell submodel is 3/4 the size of the full shell model. This model is used in the submodel analysis to match the stress intensity along the weld line.
6. The solid submodel #2 (see Figure 3-6). This solid submodel corresponds to the shell submodel as shown in Figure 3-5. This model is used to establish the stress reduction factor (SRF).

A typical finite element mesh of the shell model is shown in Figure 3-7, and a typical finite element mesh of the solid model is shown in Figure 3-8.

Detailed weld configurations are modeled in the solid finite element models. The top two edges of the vertical plates are fixed, and the two vertical edges are free, i.e. not restrained(see Figure 3-1).

The boundary conditions are identified for each of the finite element model in the figures.

3.1 Model Descriptions and Boundary Conditions

3.1.1 Full Shell Model

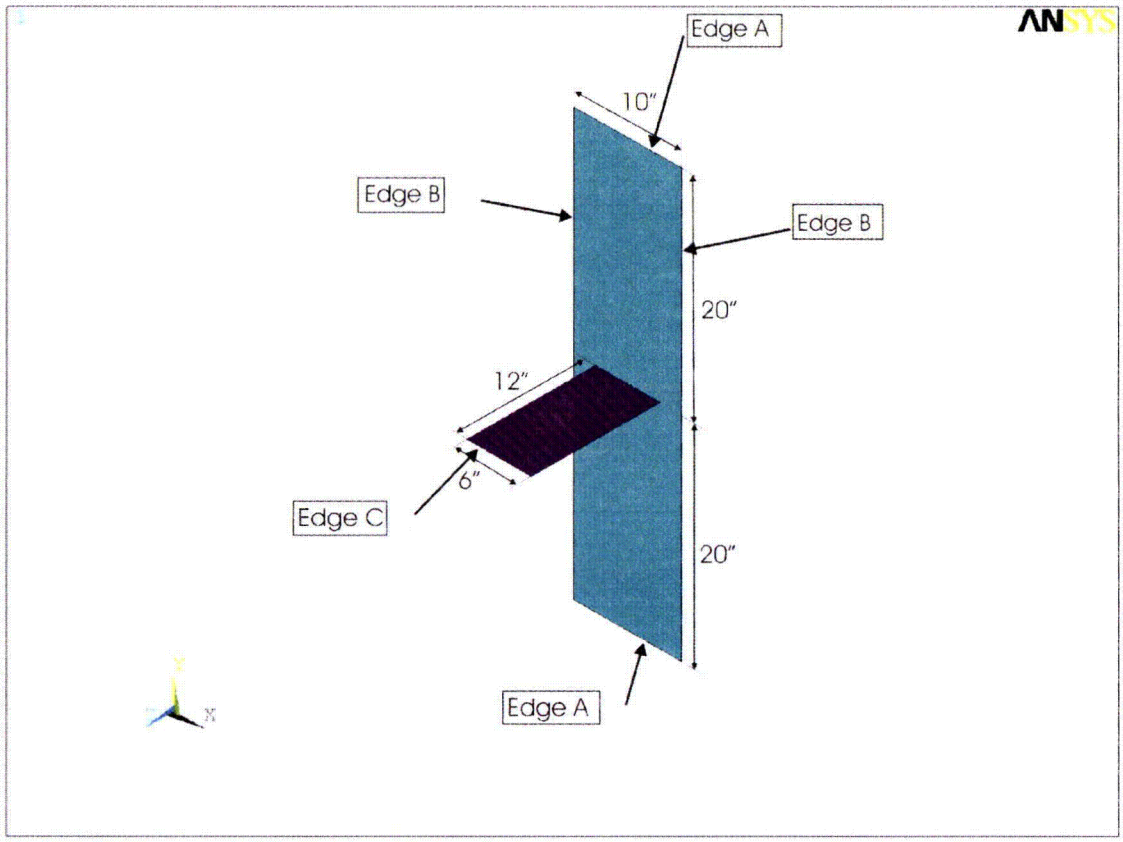

Figure 3-1
Full Shell Model

Boundary Conditions

Edge A: Fixed

Edge B: Free (i.e., not restrained)

Edge C: Applied Load

3.1.2 Full Solid Model

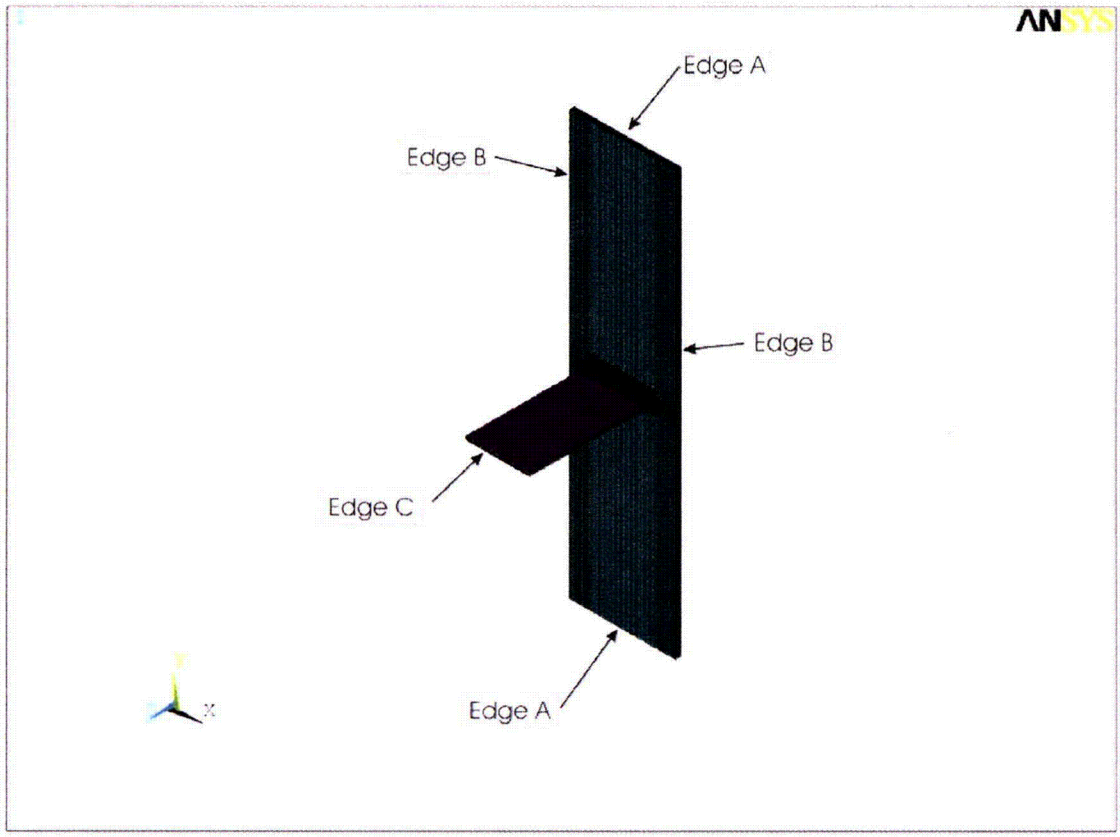

Figure 3-2
Full Solid Model

Boundary Conditions

Edge A: Fixed

Edge B: Free (i.e., not restrained)

Edge C: Applied Load

3.1.3 Shell Submodel #1

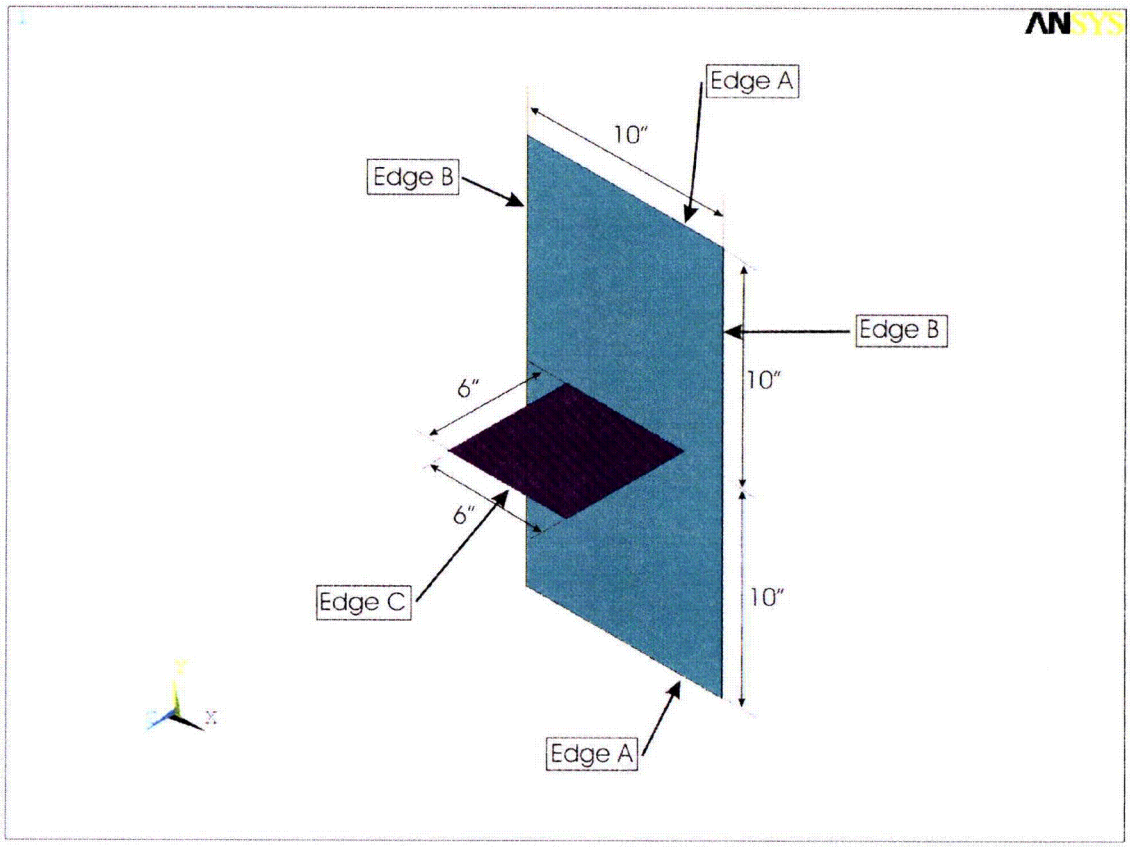

Figure 3-3
Shell Submodel #1

Substructure Analysis Boundary Conditions

Edge A: Applied Displacements

Edge B: Free (i.e., not restrained)

Edge C: Applied Displacements

Submodel Analysis Boundary Conditions

Static Load Cases #1

Edge A: Fixed

Edge B: Free (i.e., not restrained)

Edge C: Applied Displacements

Static Load Case #2

Edge A: Restrained in X and Z translations

Edge B: Free (i.e., not restrained)

Edge C: Applied Load.

3.1.4 Solid Submodel #1

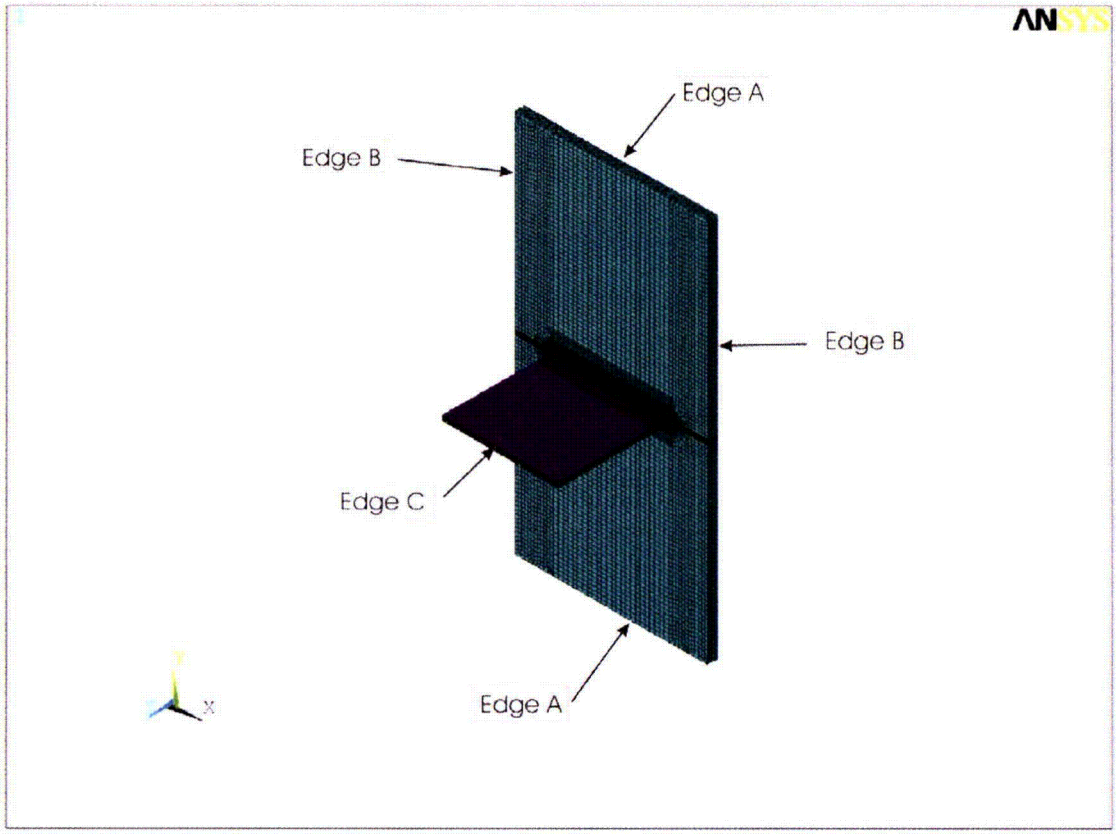

Figure 3-4
Solid Submodel #1

Substructure Analysis Boundary Conditions

Edge A: Applied Displacements

Edge B: Free (i.e., not restrained)

Edge C: Applied Displacements

Submodel Analysis Boundary Conditions

Static Load Cases #1

Edge A: Fixed

Edge B: Free (i.e., not restrained)

Edge C: Applied Displacements

Static Load Case #2

Edge A: Restrained in X and Z translations

Edge B: Free (i.e., not restrained)

Edge C: Applied Load.

3.1.5 Shell Submodel #2

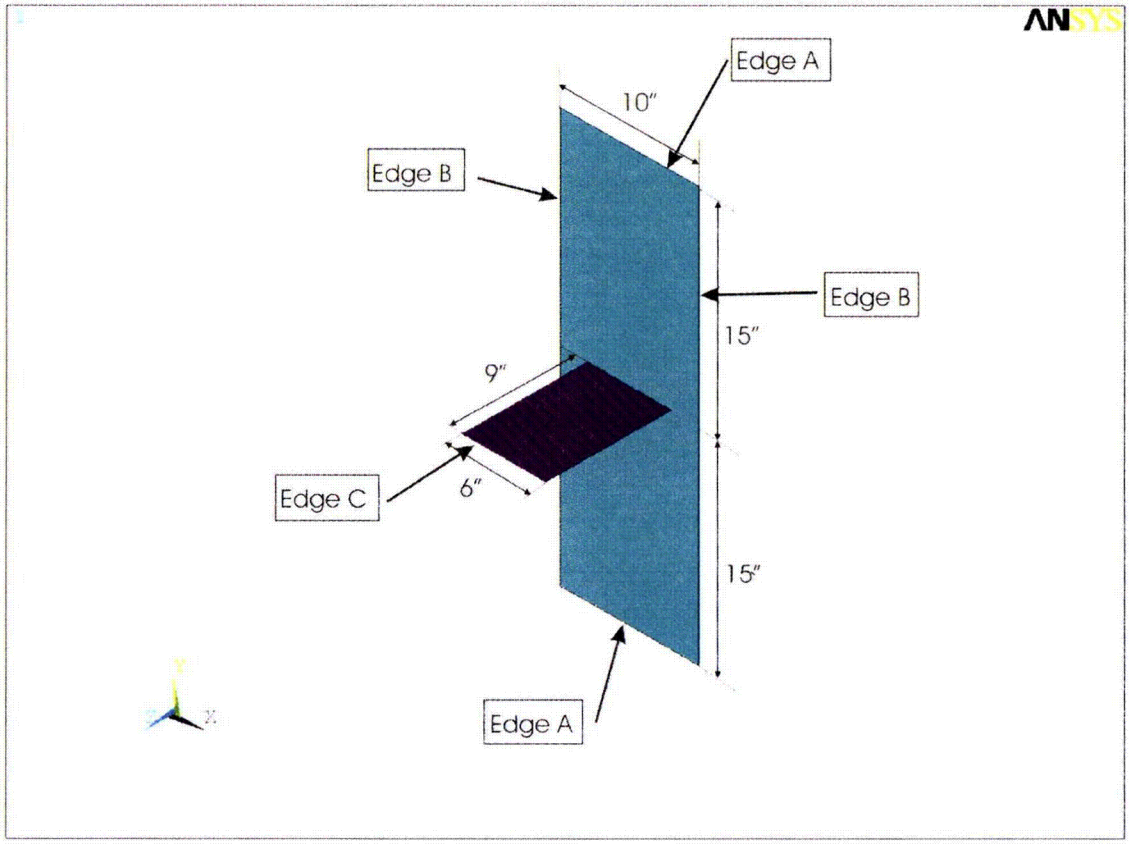

Figure 3-5
Shell Submodel #2

Substructure Analysis Boundary Conditions

Edge A: Applied Displacements

Edge B: Free (i.e., not restrained)

Edge C: Applied Displacements

Submodel Analysis Boundary Conditions

Static Load Cases #1

Edge A: Fixed

Edge B: Free (i.e., not restrained)

Edge C: Applied Displacements

Static Load case #2

Edge A: Fixed

Edge B: Free (i.e., not restrained)

Edge C: Applied Load

Dynamic Load Cases #1

Edge A: Fixed

Edge B: Free (i.e., not restrained)

Edge C: Applied Displacements

Dynamic Load Case #2

Edge A: Fixed

Edge B: Free (i.e., not restrained)

Edge C: Applied Load

3.1.6 Solid Submodel #2

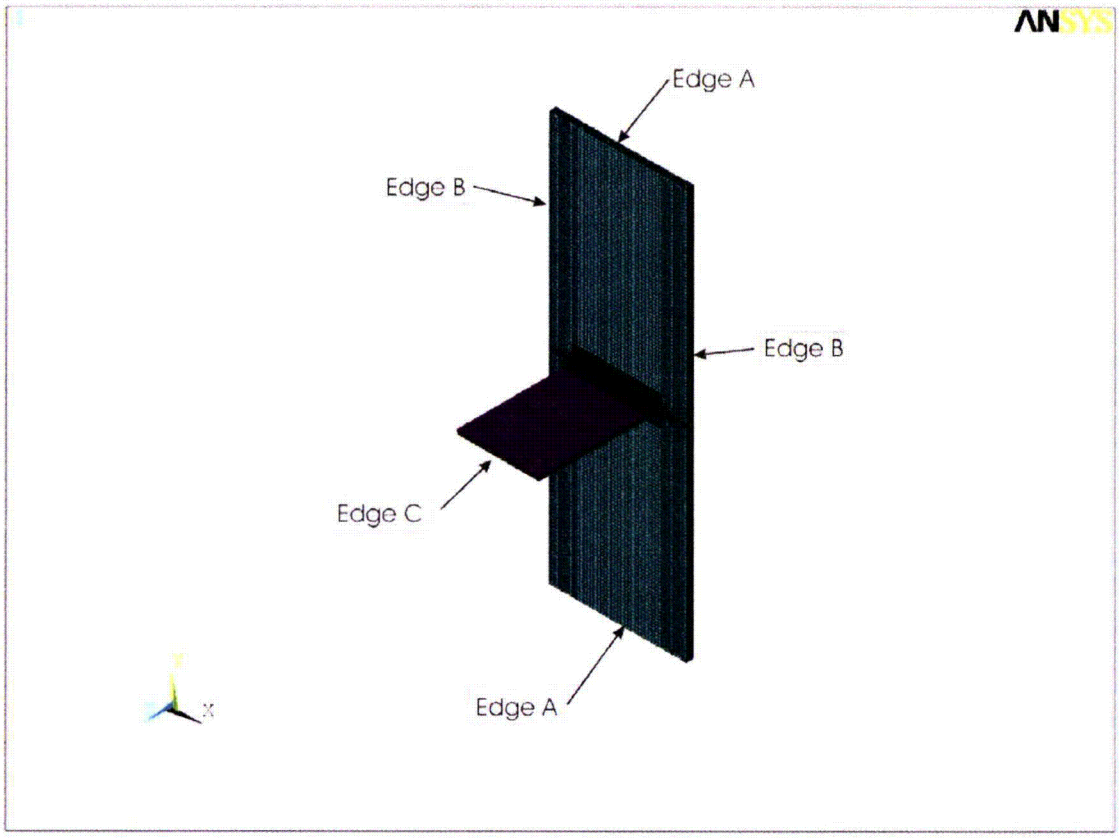

Figure 3-6
Solid Submodel #2

Substructure Analysis Boundary Conditions

Edge A: Applied Displacements

Edge B: Free (i.e., not restrained)

Edge C: Applied Displacements

Submodel Analysis Boundary Conditions

Static Load Cases #1

Edge A: Fixed

Edge B: Free (i.e., not restrained)

Edge C: Applied Displacements

Static Load case #2

Edge A: Fixed

Edge B: Free (i.e., not restrained)

Edge C: Applied Load

Dynamic Load Cases #1

Edge A: Fixed

Edge B: Free (i.e., not restrained)

Edge C: Applied Displacements

Dynamic Load Case #2

Edge A: Fixed

Edge B: Free (i.e., not restrained)

Edge C: Applied Load

3.2 Finite Element Mesh

Shell Finite Element Model

The shell finite element model is modeled using SHELL63 elements. A regular mesh size of 0.25" is used for the shell finite element models. The full shell model consists of approximately 7,800 nodes and 7,600 shell elements. The following Figure 3-7 shows the finite element mesh for the shell finite element models.

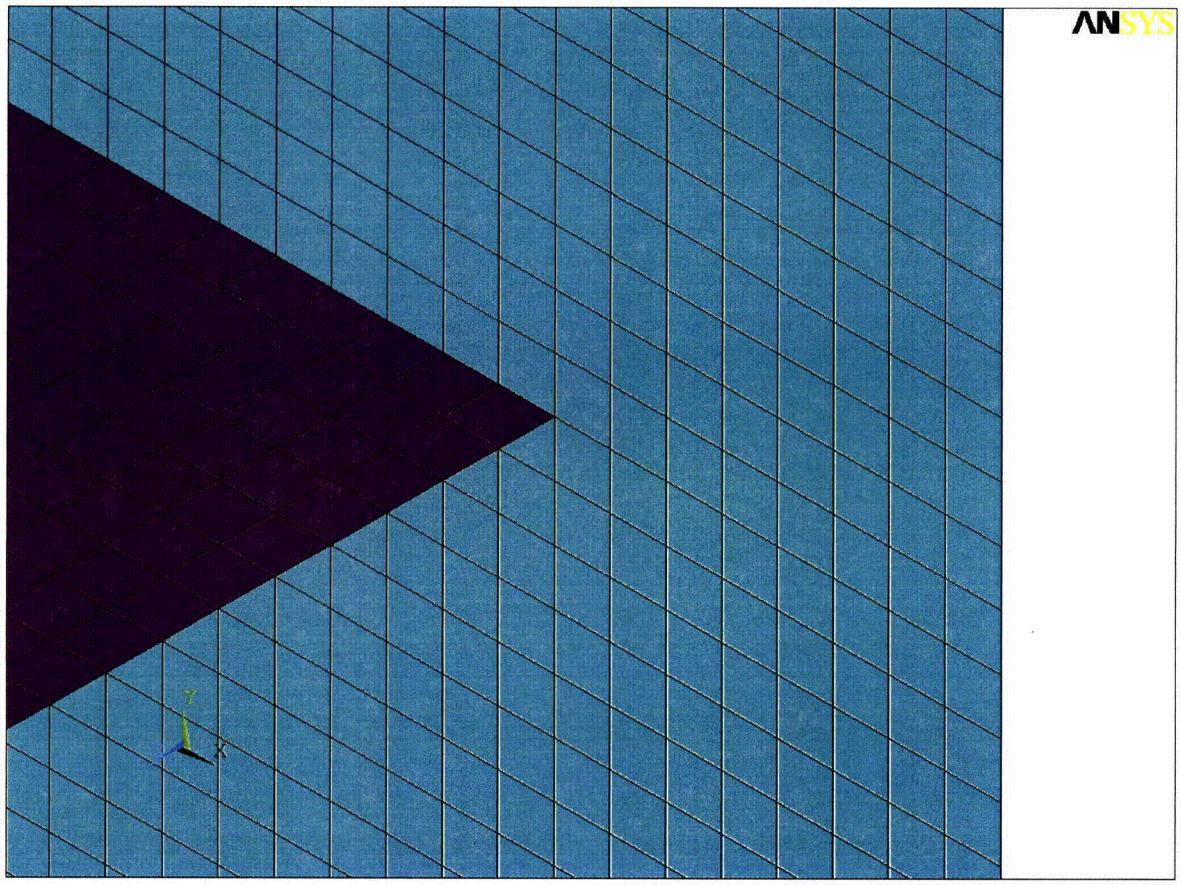

Figure 3-7
Shell Finite Element Model Mesh

Solid Finite Element Model

The solid finite element model is modeled using SOLID45 elements. The solid finite element models generally maintain the same element size of 0.25". In the transition regions around the weld, finer element sizes are used. Six layers of element are modeled across the plate thickness, therefore, providing adequate discretization through the plate thickness to capture the stress variations across the thickness. The entire model consists of approximately 86,000 nodes and 76,000 solid elements. The following Figure 3-8 shows the finite element mesh for the solid finite element models.

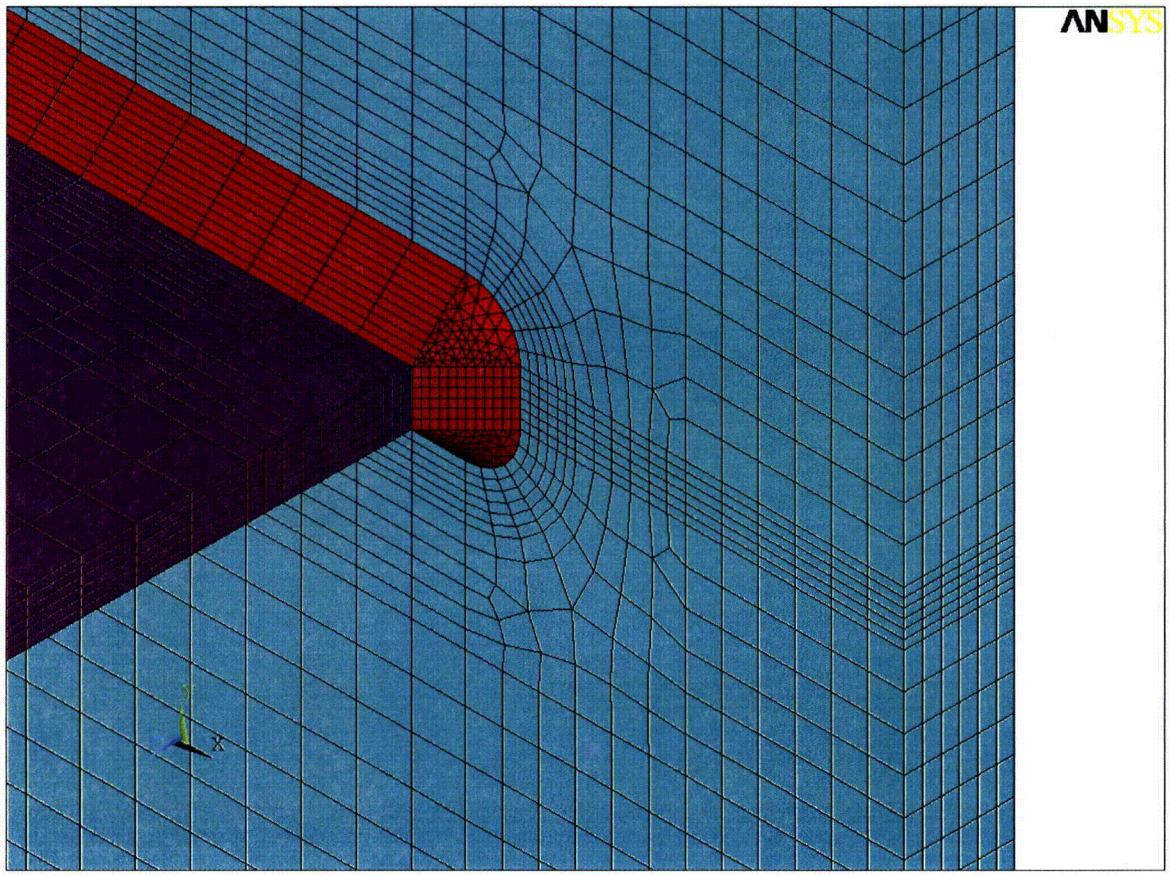

Figure 3-8
Solid Finite Element Model Mesh

3.3 Stress Paths

Linearization stress paths are taken from the weld root to the component surface in the vicinity of the high stress region. In addition, linearization stress paths are also taken from the weld toe to the opposite surface of the connected parts. The stress paths used for the stiffener solid model are shown in the following Figure 3-9 and Figure 3-10.

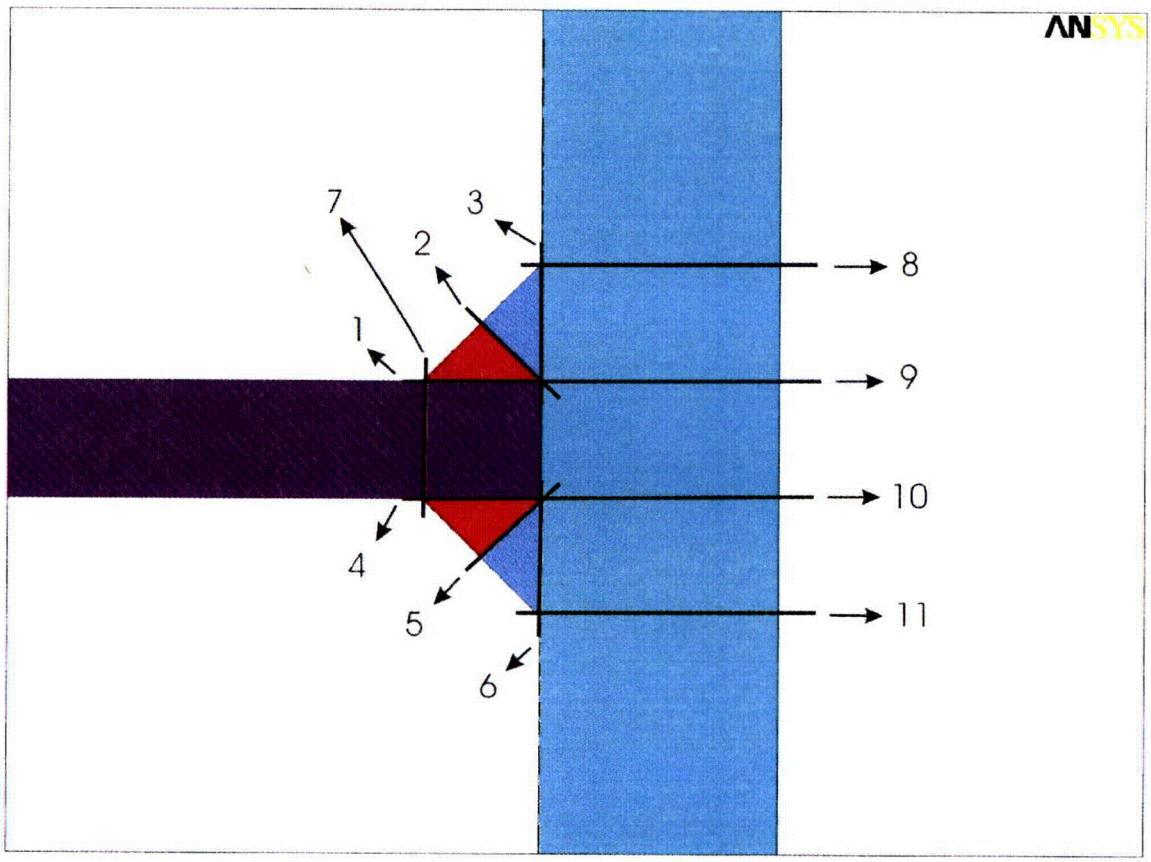

Figure 3-9
Solid Finite Element Model Stress Paths
(Side View)

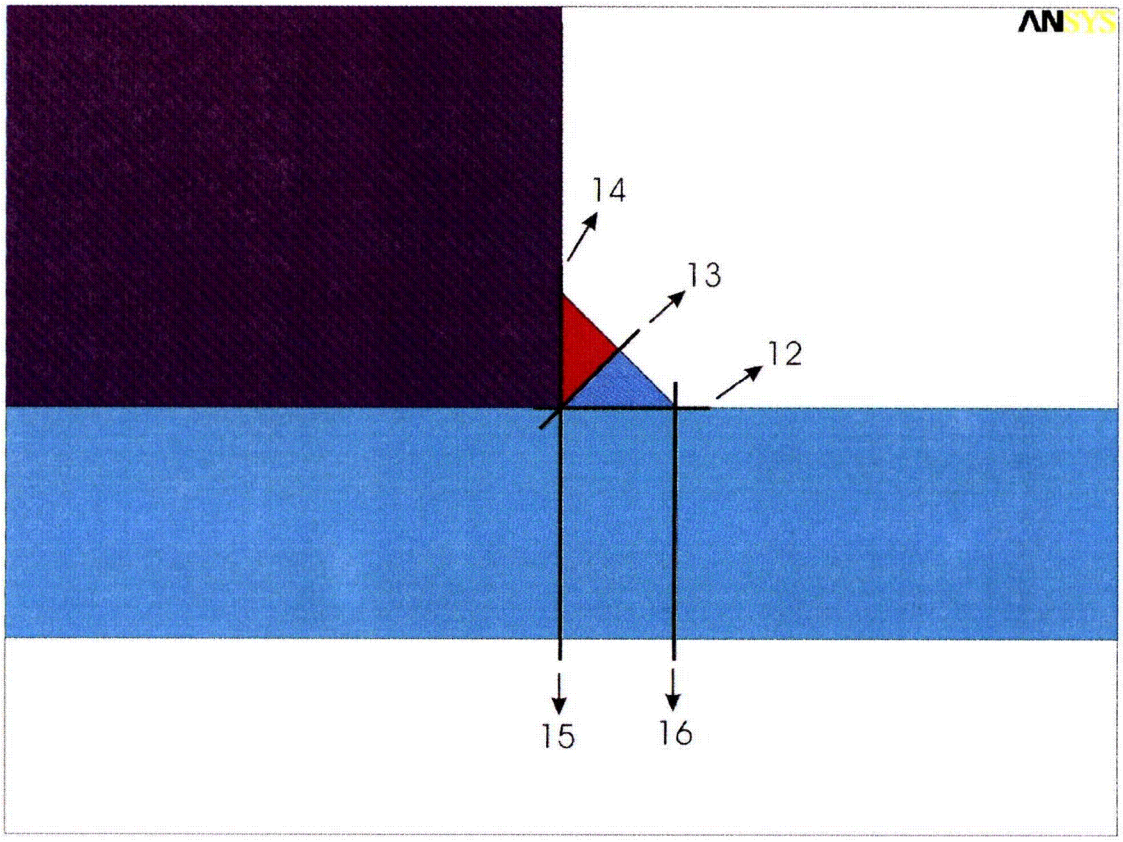

Figure 3-10
Solid Finite Element Model Stress Paths
(Top View)

4.0 LOAD CASES

4.1 Static Analysis Load Cases

Two static load cases are applied:

1. Vertical Load

   A uniform vertical load of 4 lb/in, which amounts to a total load of 24 lb, is applied along Edge C (see Figure 3-1). This load will generate primarily bending stress on the horizontal plate. In the submodel analysis, applied displacements will be used to match the stress intensity along the weld line.

2. Horizontal Load

   A uniform horizontal load of 80 lb/in, which amounts to a total load of 480 lb, is applied along Edge C in the Z direction (see Figure 3-1). This load will generate primarily membrane stress on the horizontal plate. In the submodel analysis, applied loads will be used to match the stress intensity along the weld line.

Static Analysis Objectives

The two static load cases accomplish the following objectives:

1. Applying Displacement in Submodel Analysis

   This is accomplished in the Load Case #1.

2. Applying Load in Submodel Analysis

   This is accomplished in the Load Case #2.

3. Full Solid Finite Element Baseline Analysis

   This analysis provides a direct comparison with the full shell finite elemnt baseline analysis. This analysis removes any inherent approximation and assumption that is associated with the substructure and submodel analyses.

4. Submodel #1 and Submodel #2

   Two submodels are used for substructure and submodel analyses. Submodel #1 is 1/2 the size of the full model, and submodel #2 is 3/4 the size of the full model. This different size will highlight the discrepancies, if any, in the substructure and submodel analyses.

4.2 Dynamic Analysis Load Cases

Two dynamic load cases are applied:

1. Vertical Load

   A harmonic uniform vertical load of 4 lb/in, which amounts to a total load of 24 lb, is applied along Edge C (see Figure 3-1). The freqeuncy of the load is set at 25 Hz. The maximum magnitude of this load is similar to the corresponding static analysis load case.

2. Horizontal Load

   A harmonic uniform horizontal load of 80 lb/in, which amounts to a total load of 480 lb, is applied along Edge C in the Z direction (see Figure 3-1). The frequency of the load is set at 25 Hz. The maximum magnitude of this load is similar to the corresponding static analysis load case.

Dynamic Analysis Objectives

The two dynamic load cases accomplish the following objectives:

1. Applying Displacement in Submodel Analysis

   This is accomplished in the Load Case #1.

2. Applying Load in Submodel Analysis

   This is accomplished in the Load Case #2.

3. Comparing the effectiveness of substructure analysis and submodel analysis.

5.0 STATIC ANALYSIS RESULTS

5.1 Static Load Case #1

5.1.1 Full Shell Finite Element Analysis

Stress Plot

The maximum stress intensity is 5,189 psi, and the stress plot is provided in the following Figure 5-1. This analysis is the full shell model baseline analysis, and the maximum stress intensity of 5,189 psi is used to determine the SRF in the other analyses.

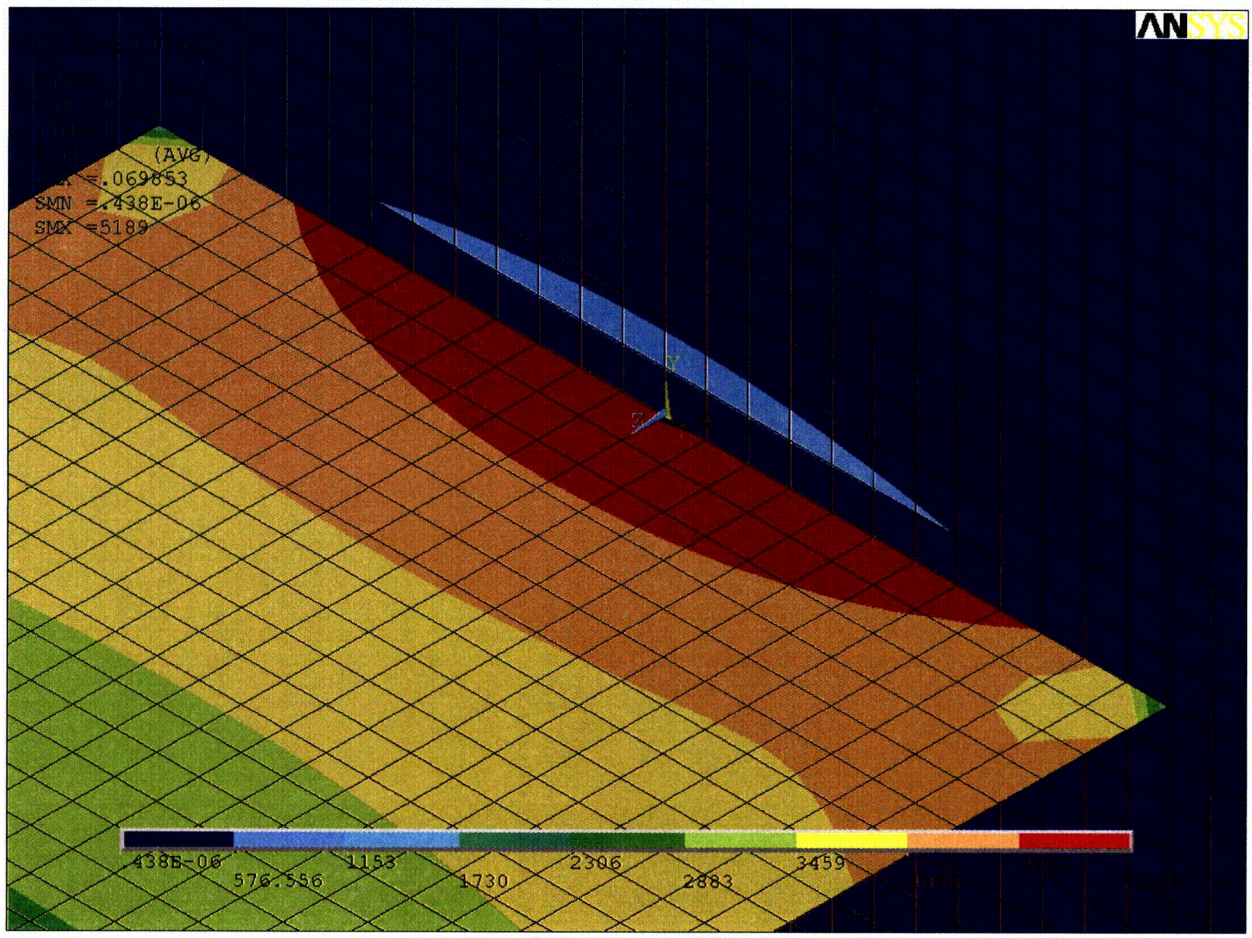

Figure 5-1
Full Shell Model
Stress Plot for Case #1
(Full Shell Model Baseline Analysis)

5.1.2 *Full Solid Finite Element Analysis*

Stress Plot

The maximum non-linearized stress intensity is 5,608 psi, and the stress plot is provided in the following Figure 5-2. This analysis is the full solid model baseline analysis.

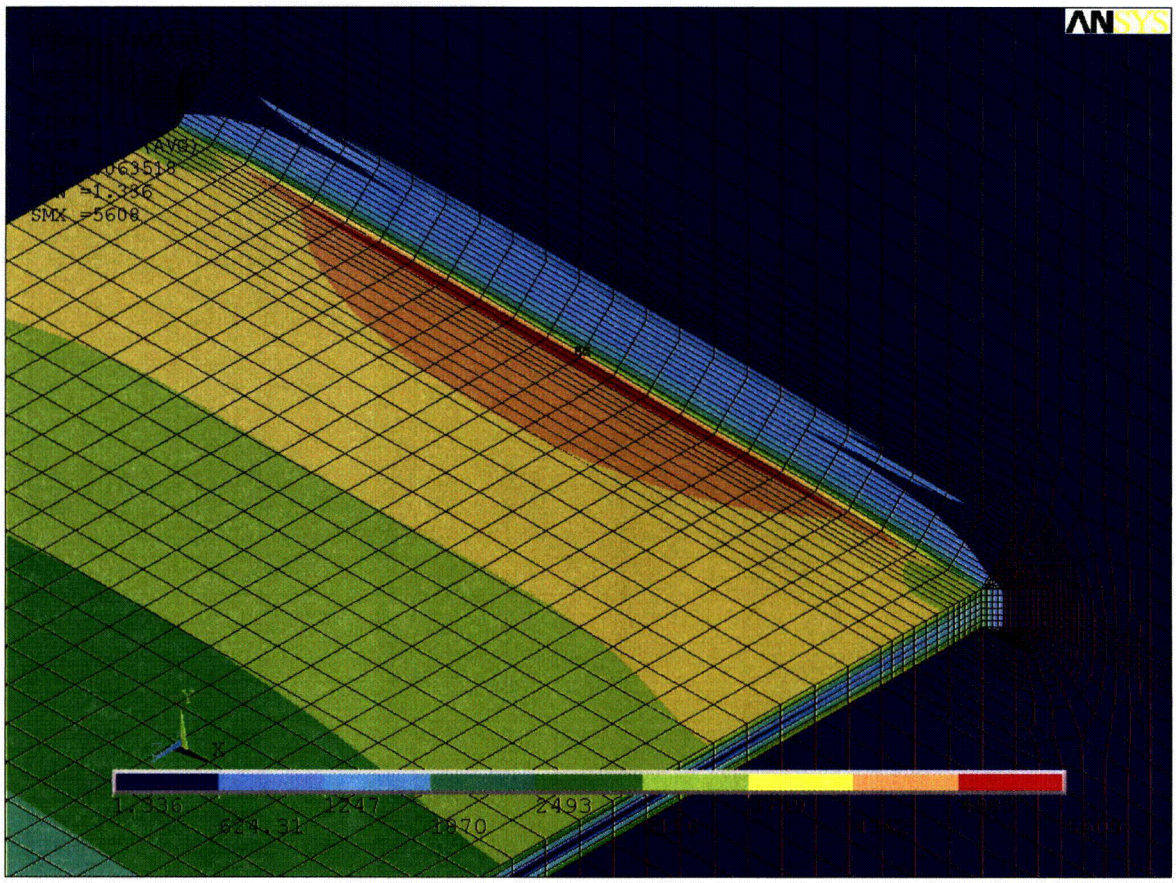

Figure 5-2
Full Solid Model Analysis
Stress Plot for Load Case #1
(Full Solid Model Baseline Analysis)

SRF Table

Table 5-1
Full Solid Model Baseline Analysis SRF
for Static Load Case #1

Path #	Solid (psi)	Shell (psi)	SRF
1	3,043	5,189	0.59
2	1,223		0.24
3	799		0.15
4	3,043		0.59
5	1,223		0.24
6	799		0.15
7	3,020		0.58
8	549		0.11
9	746		0.14
10	746		0.14
11	549		0.11
12	373		0.07
13	417		0.08
14	1,726		0.33
15	364		0.07
16	265		0.05
		Maximum =	**0.59**

5.1.3 Substructure Analysis Using Shell Submodel #1

With reference to Figure 3-3, the displacements along Edges A and C computed in the full shell finite element analysis (Section 5.1.1) are applied onto this shell submodel.

Stress Plot

The maximum stress intensity is 5,198 psi, and the stress plot is provided in the following Figure 5-3.

The maximum stress intensity is the same as the full shell baseline analysis maximum stress intensity, and the stress contours are very similar (see Figure 5-1). This confirms that the shell substructure analysis produces the same stress results as the full shell baseline analysis.

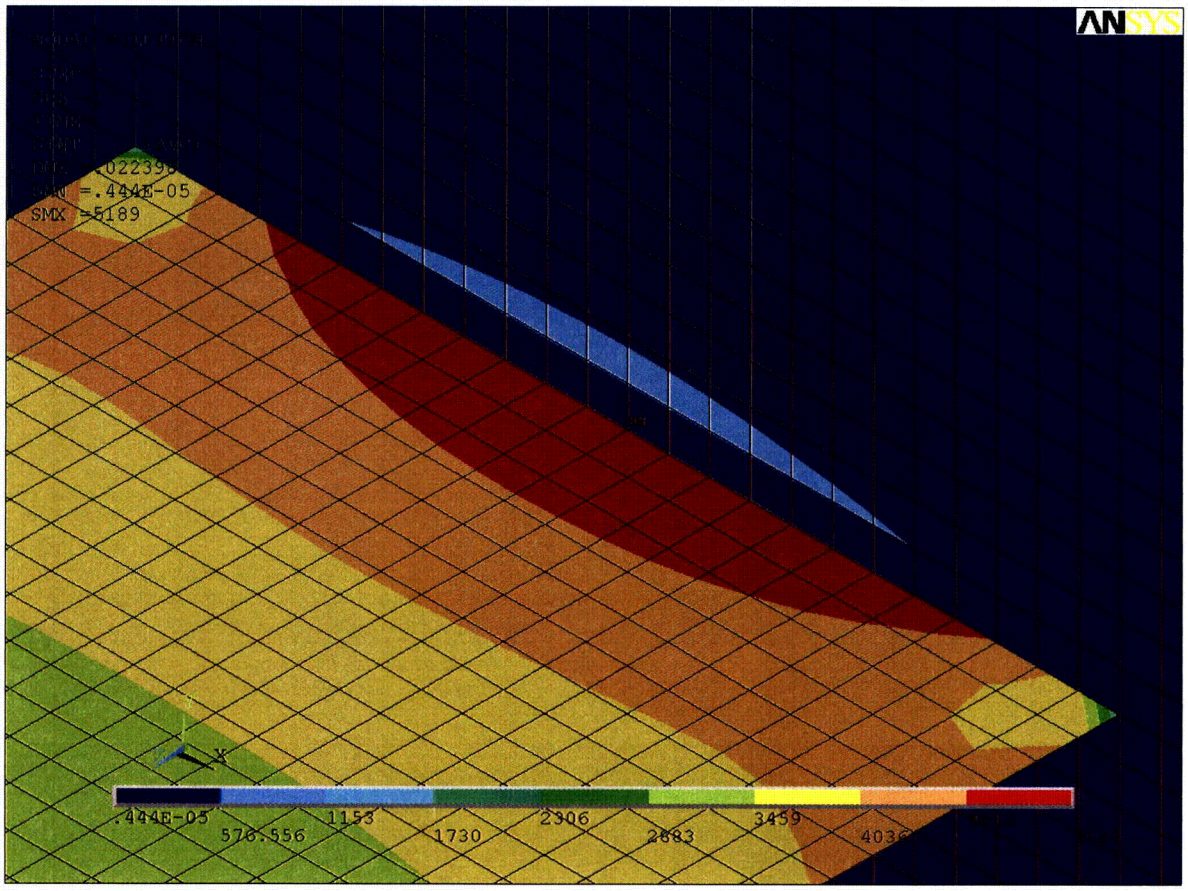

Figure 5-3
Substructure Analysis using Shell Submodel #1
Stress Plot for Load Case #1

5.1.4 Substructure Analysis Using Shell Submodel #2

With reference to Figure 3-5, the displacements along Edges A and C computed in the full shell finite element analysis (Section 5.1.1) are applied onto this shell submodel.

Stress Plot

The maximum stress intensity is 5,198 psi, and the stress plot is provided in the following Figure 5-4.

The maximum stress intensity is the same as the full shell baseline analysis maximum stress intensity, and the stress contours are very similar (see Figure 5-1). This confirms that the shell substructure analysis produces the same stress results as the full shell baseline analysis.

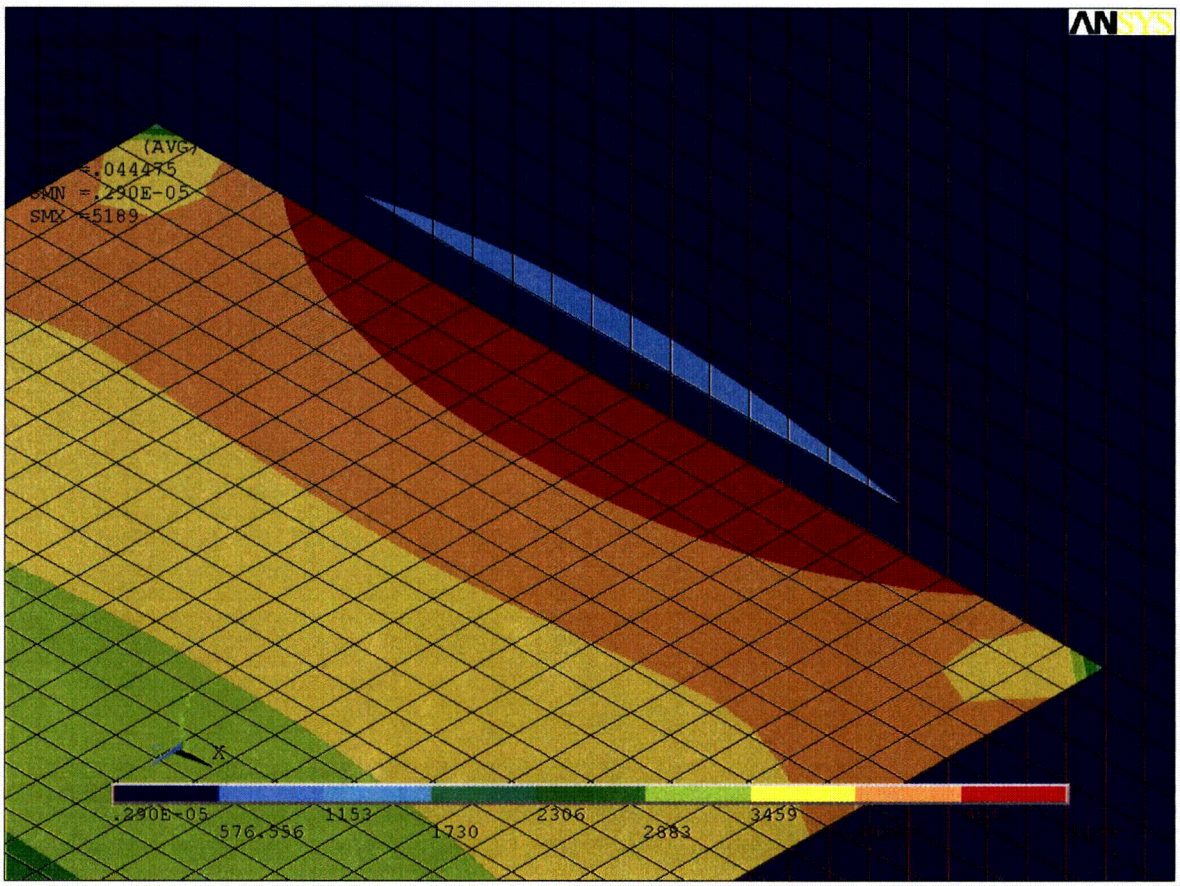

Figure 5-4
Substructure Analysis using Shell Submodel #2
Stress Plot for Load Case #1

5.1.5 Substructure Analysis Using Solid Submodel #1

With reference to Figure 3-4, the displacements along Edges A and C computed in the full shell finite element analysis (Section 5.1.1) are applied onto this solid submodel.

Stress Plot

The maximum non-linearized stress intensity is 7,033 psi, and the stress plot is provided in the following Figure 5-5.

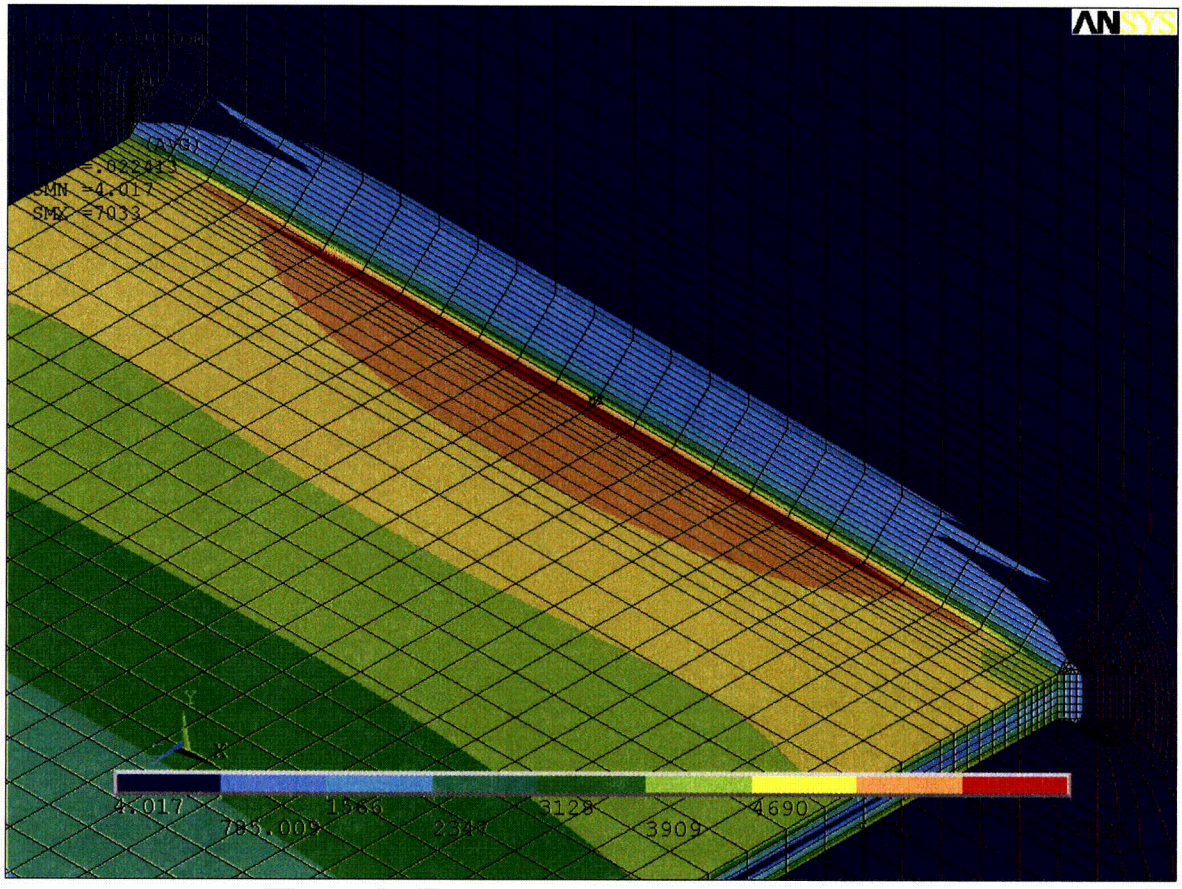

Figure 5-5
Substructure Analysis using Solid Submodel #1
Stress Plot for Load Case #1

SRF Table

Table 5-2
Substructure Analysis (Submodel #1) SRF
for Static Load Case #1

Path #	Solid (psi)	Shell (psi)	SRF
1	3,822	5,189	0.74
2	1,543		0.30
3	1,003		0.19
4	3,822		0.74
5	1,543		0.30
6	1,003		0.19
7	3,785		0.73
8	696		0.13
9	936		0.18
10	936		0.18
11	696		0.13
12	488		0.09
13	546		0.11
14	2,239		0.43
15	477		0.09
16	364		0.07
		Maximum =	**0.74**

5.1.6 Substructure Analysis Using Solid Submodel #2

With reference to Figure 3-6, the displacements along Edges A and C computed in the full shell finite element analysis (Section 5.1.1) are applied onto this solid submodel.

Stress Plot

The maximum non-linearized stress intensity is 6,568 psi, and the stress plot is provided in the following Figure 5-6.

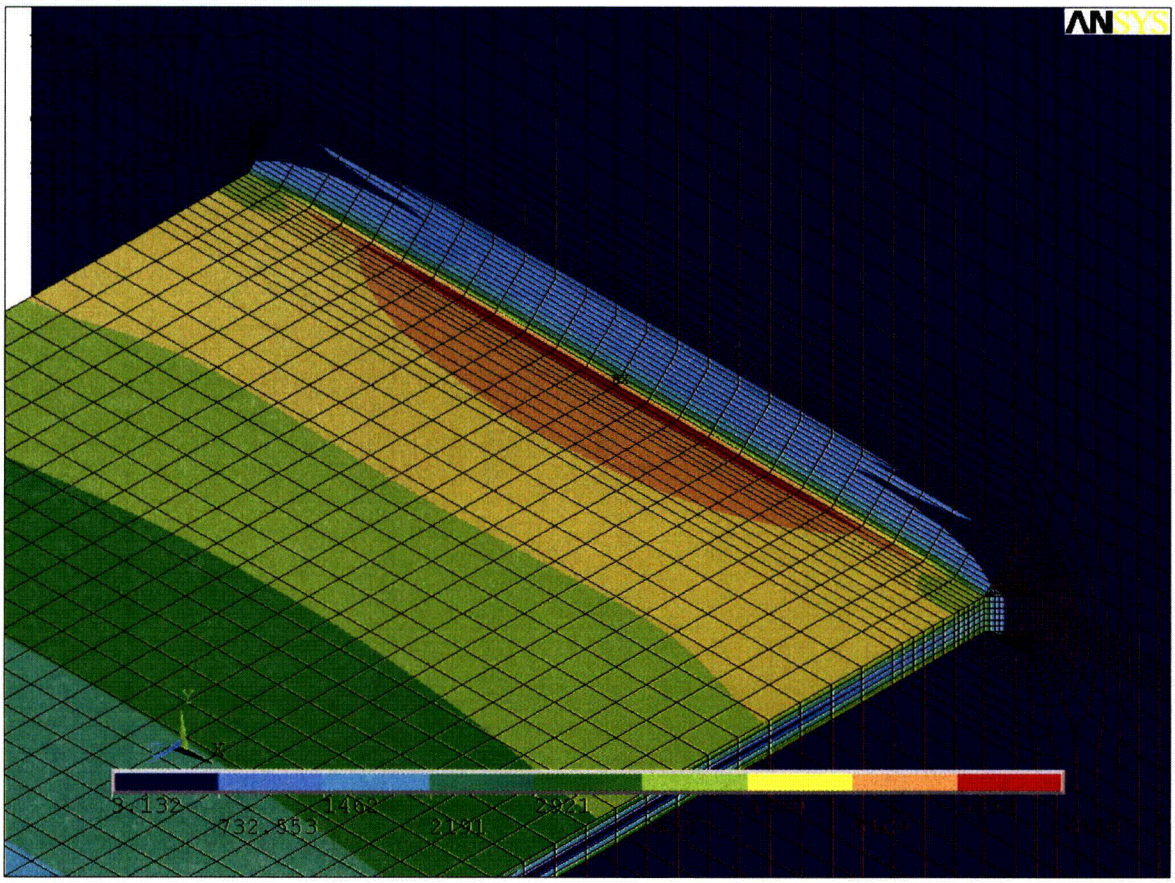

Figure 5-6
Substructure Analysis using Solid Submodel #2
Stress Plot for Load Case #1

SRF Table

Table 5-3
Substructure Analysis (Submodel #2) SRF
for Static Load Case #1

Path #	Solid (psi)	Shell (psi)	SRF
1	3,565	5,189	0.69
2	1,435		0.28
3	936		0.18
4	3,565		0.69
5	1,435		0.28
6	936		0.18
7	3,536		0.68
8	646		0.12
9	874		0.17
10	874		0.17
11	646		0.12
12	445		0.09
13	498		0.10
14	2,051		0.40
15	434		0.08
16	321		0.06
		Maximum =	**0.69**

5.1.7 Submodel Analysis Using Submodel #1

Matching Stress Profile

The stress profile matching is performed along the weld line connecting the vertical plate to the horizontal plate. The matching is accomplished by imposing vertical displacements along the Edge C (see Figure 3-3) of the submodel. Fixed boundary condition is applied to the top and bottom edges. The applied displacements and the comparison of the stress profiles are shown in the following Figure 5-7 and Figure 5-8, respectively.

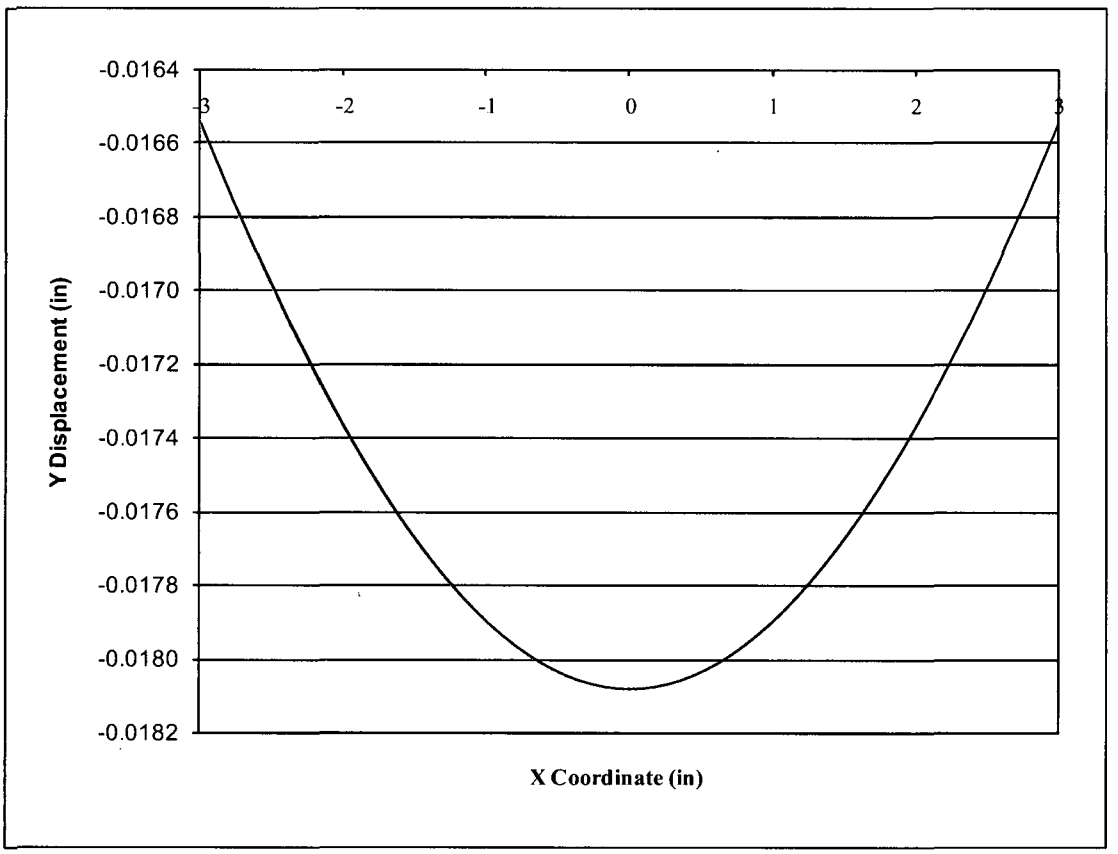

Figure 5-7
Submodel Analysis using Submodel #1
Applied Displacements for Load Case #1

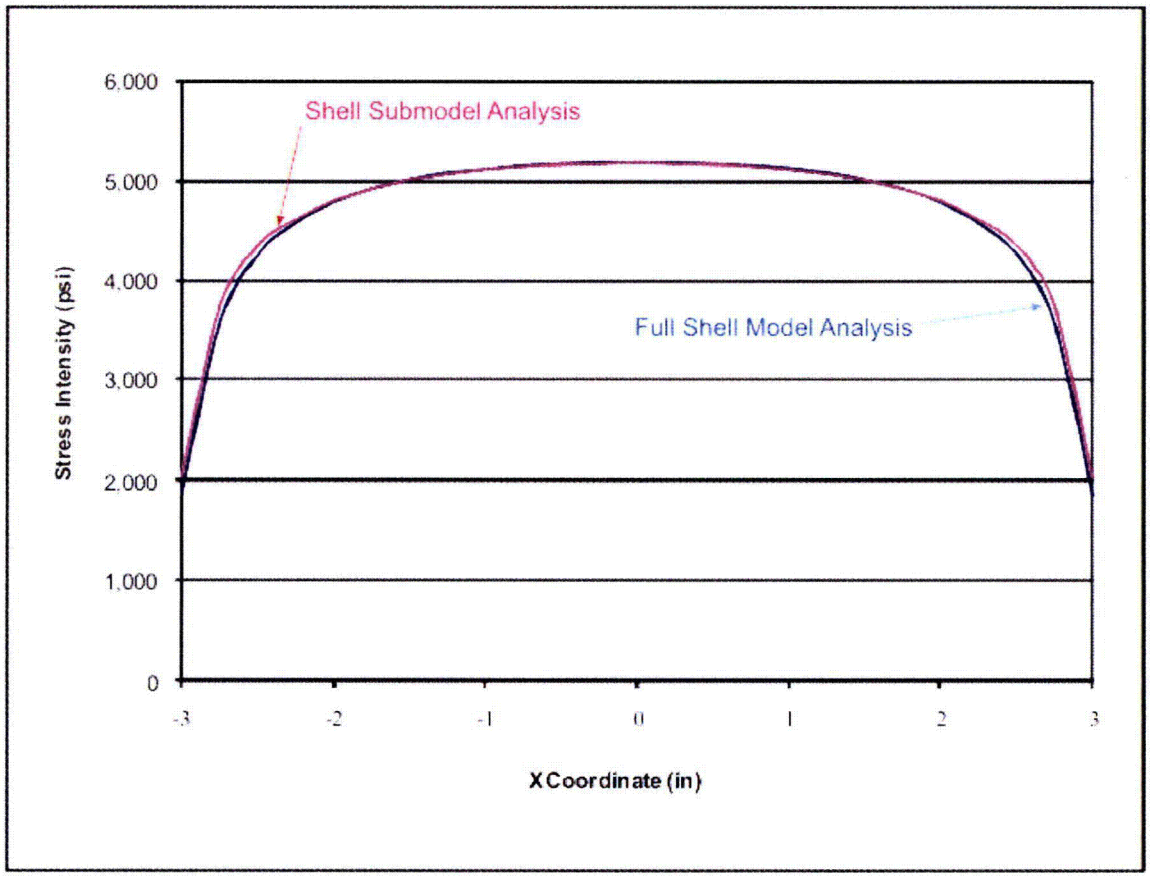

Figure 5-8
Submodel Analysis using Submodel #1
Stress Profile Comparison for Load Case #1

Stress Plot

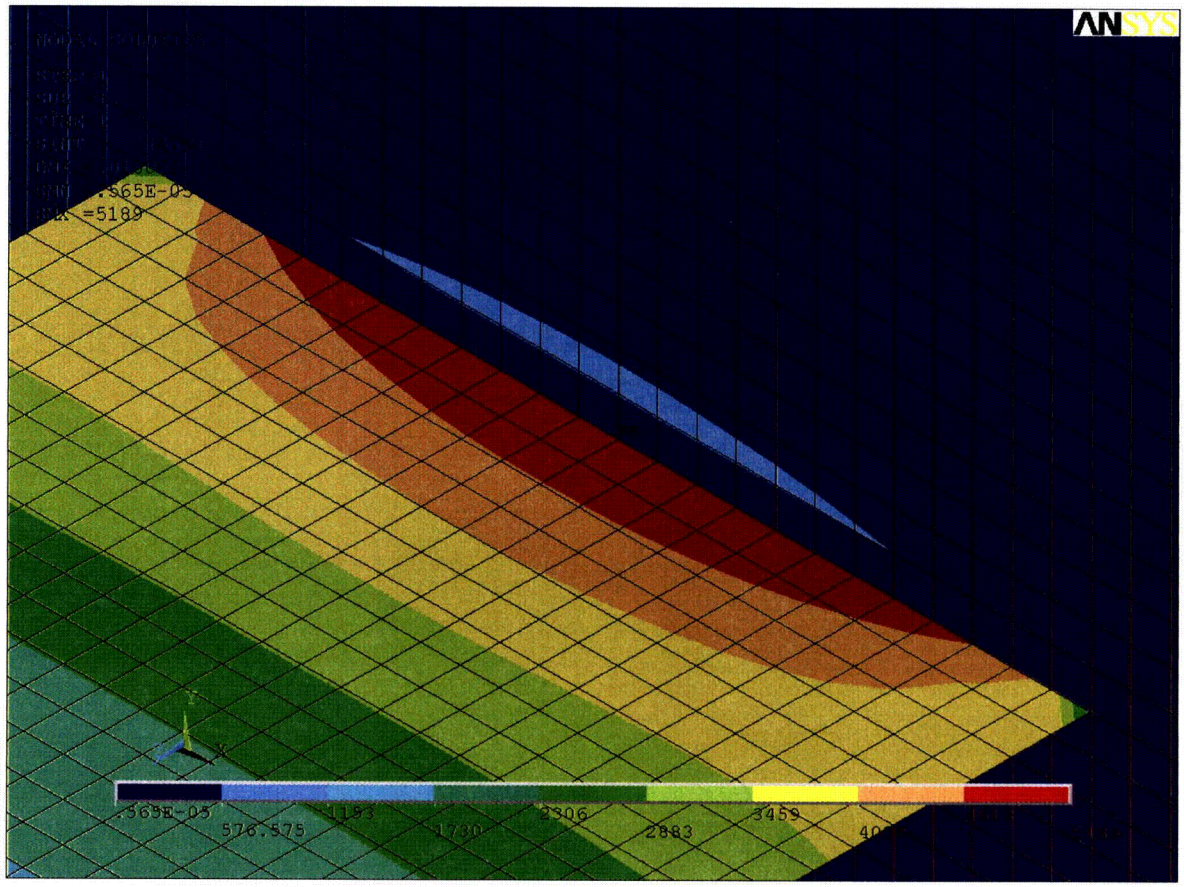

Figure 5-9
Submodel Analysis using Submodel #1
Shell Model Stress Plot for Load Case #1

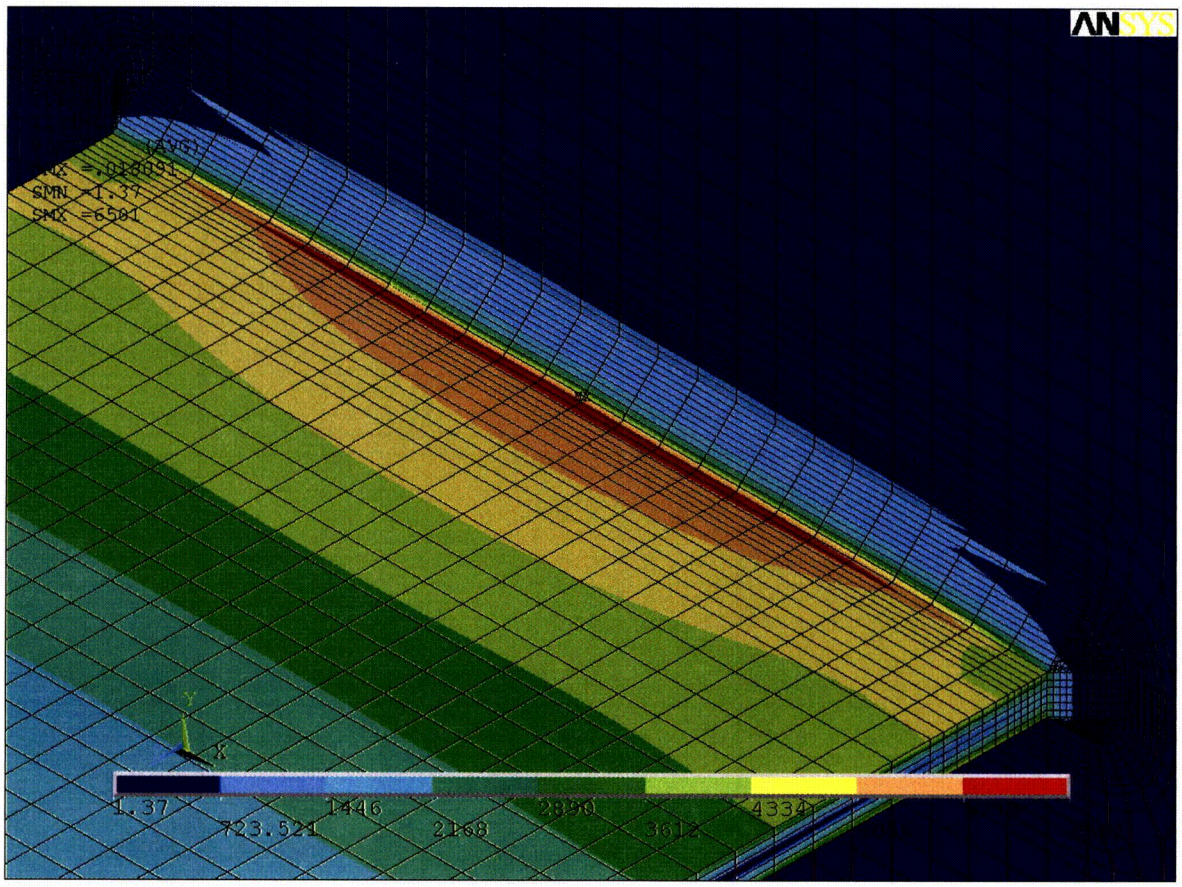

Figure 5-10
Submodel Analysis using Submodel #1
Solid Model Stress Plot for Load Case #1

SRF Table

Table 5-4
Submodel Analysis (Submodel #1) SRF
for Static Load Case #1

Path #	Solid (psi)	Shell (psi)	SRF
1	3,543	5,189	0.68
2	1,443		0.28
3	929		0.18
4	3,543		0.68
5	1,443		0.28
6	929		0.18
7	3,495		0.67
8	645		0.12
9	865		0.17
10	865		0.17
11	645		0.12
12	456		0.09
13	499		0.10
14	2,084		0.40
15	437		0.08
16	367		0.07
		Maximum =	**0.68**

5.1.8 Submodel Analysis Using Submodel #2

Matching Stress Profile

The stress profile matching is performed along the weld line connecting the vertical plate to the horizontal plate. The matching is accomplished by imposing vertical displacements along the Edge C (see Figure 3-5) of the submodel. Fixed boundary condition is applied to the top and bottom edges. The applied displacements and the comparison of the stress profiles are shown in the following Figure 5-11 and Figure 5-12, respectively.

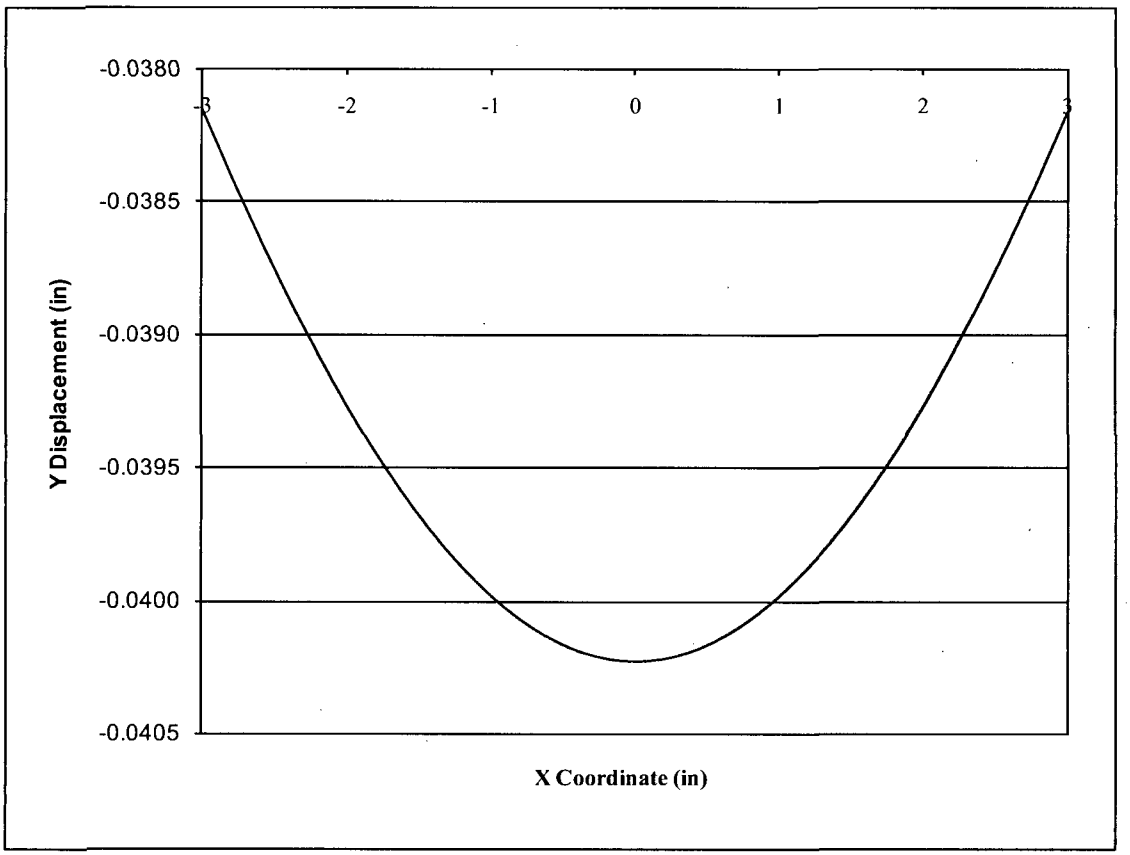

Figure 5-11
Submodel Analysis using Submodel #2
Applied Displacements for Load Case #1

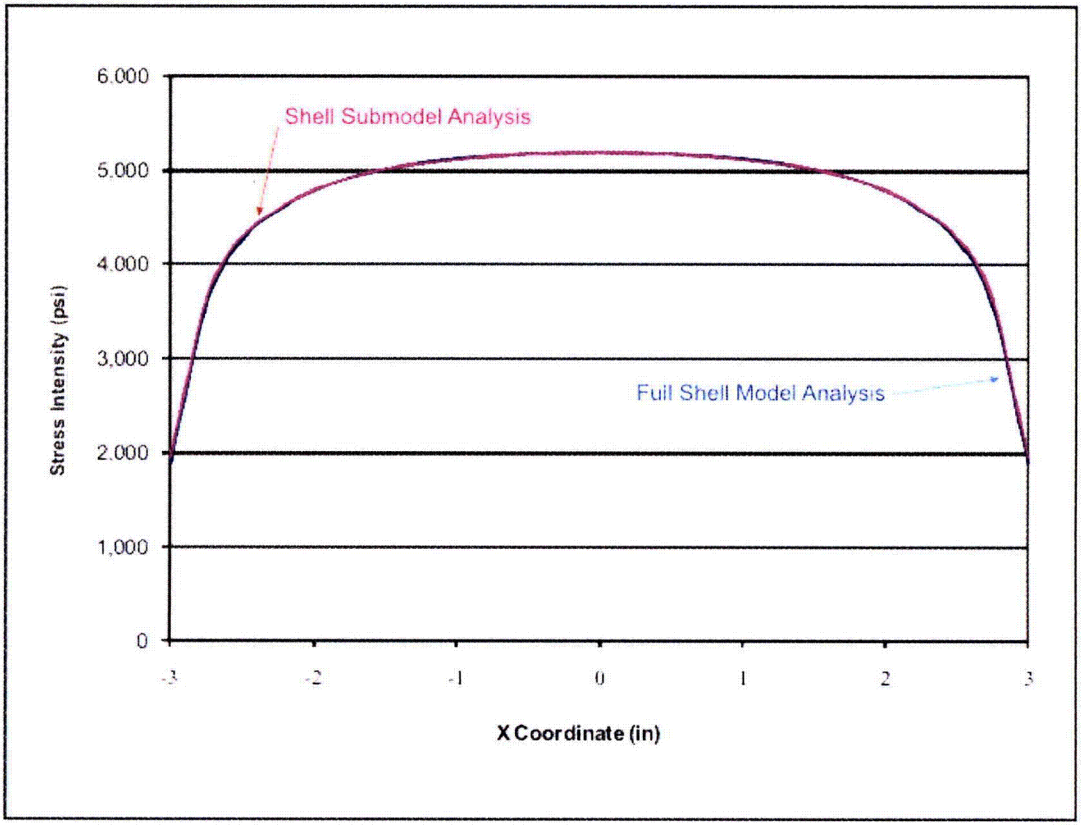

Figure 5-12
Submodel Analysis using Submodel #2
Stress Profile Comparison for Load Case #1

Stress Plot

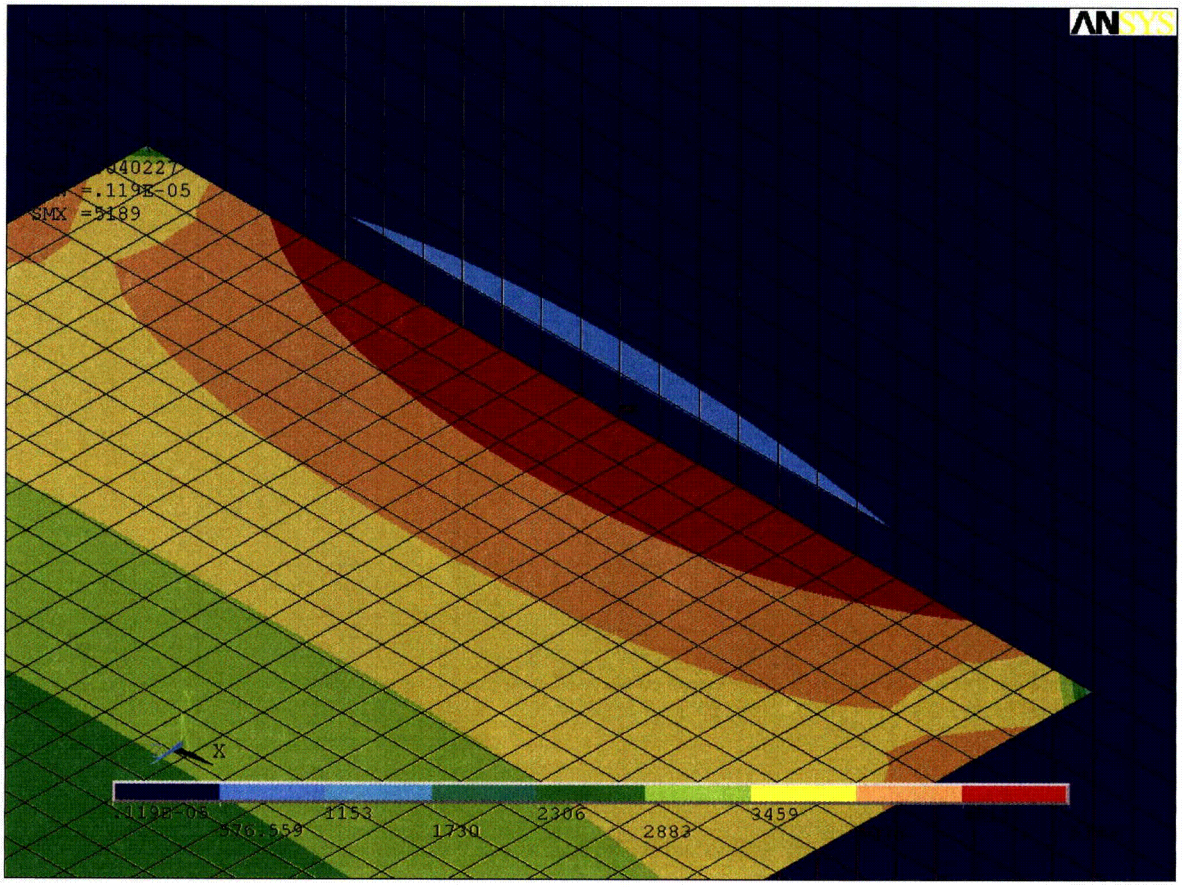

Figure 5-13
Submodel Analysis using Submodel #2
Shell Model Stress Plot for Load Case #1

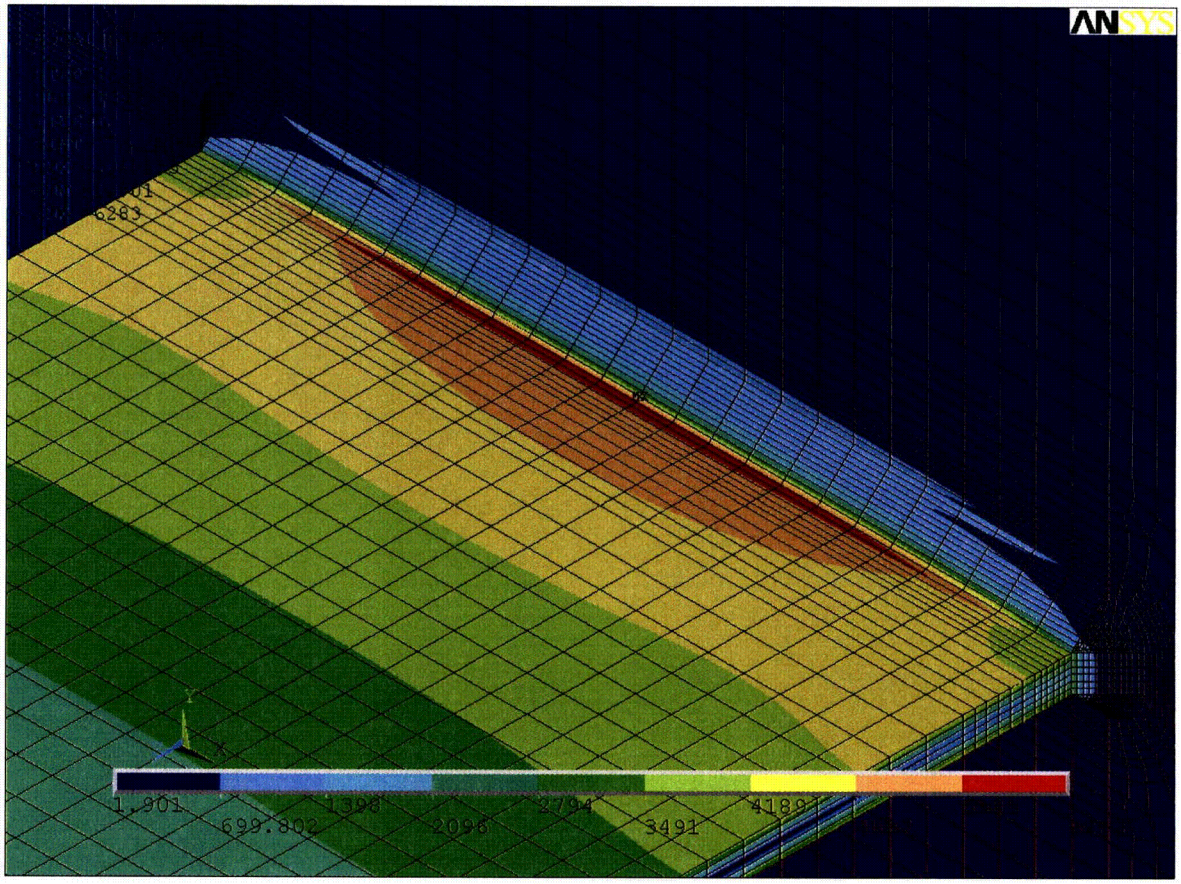

Figure 5-14
Submodel Analysis using Submodel #2
Solid Model Stress Plot for Load Case #1

SRF Table

Table 5-5
Submodel Analysis (Submodel #2) SRF
for Static Load Case #1

Path #	Solid (psi)	Shell (psi)	SRF
1	3,414	5,189	0.66
2	1,378		0.27
3	896		0.17
4	3,414		0.66
5	1,378		0.27
6	896		0.17
7	3,381		0.65
8	618		0.12
9	836		0.16
10	836		0.16
11	618		0.12
12	422		0.08
13	472		0.09
14	1,950		0.38
15	412		0.08
16	318		0.06
		Maximum =	0.66

5.2 Static Load Case #2

5.2.1 Full Shell Finite Element Analysis

Stress Plot

The maximum stress intensity is 6,579 psi, and the stress plot is provided in the following Figure 5-15. This analysis is the full shell model baseline analysis, and the maximum stress intensity of 6,579 psi is used to determine the SRF in the other analyses.

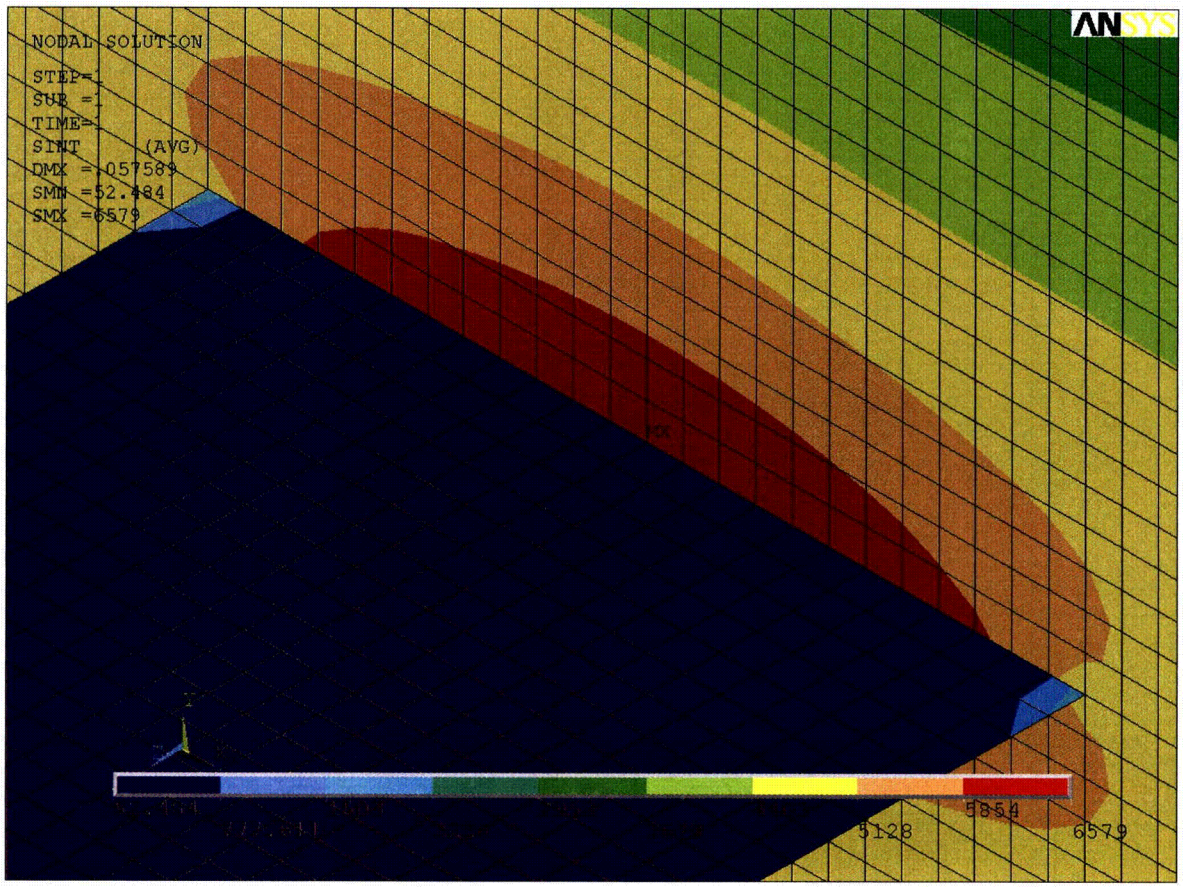

Figure 5-15
Full Shell Model
Stress Plot for Case #2
(Full Shell Model Baseline Analysis)

5.2.2 *Full Solid Finite Element Analysis*

Stress Plot

The maximum non-linearized stress intensity is 10,470 psi, and the stress plot is provided in the following Figure 5-16. This analysis is the full solid model baseline analysis.

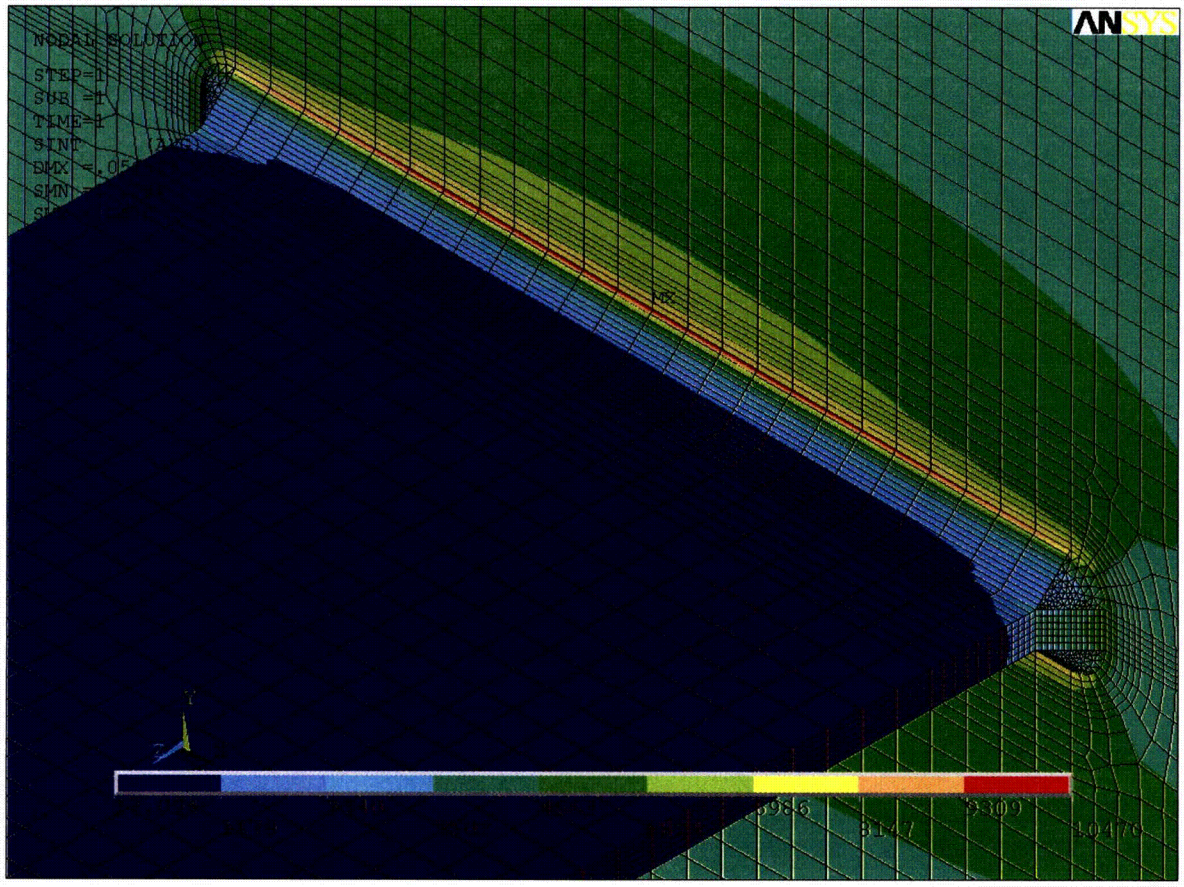

Figure 5-16
Full Solid Model Analysis
Stress Plot for Load Case #2
(Full Solid Model Baseline Analysis)

SRF Table

Table 5-6
Full Solid Model Baseline Analysis SRF
for Static Load Case #2

Path #	Solid (psi)	Shell (psi)	SRF
1	3,760	6,579	0.57
2	3,789		0.58
3	5,733		0.87
4	3,760		0.57
5	3,789		0.58
6	5,733		0.87
7	2,939		0.45
8	5,872		0.89
9	4,731		0.72
10	4,731		0.72
11	5,872		0.89
12	5,042		0.77
13	4,358		0.66
14	3,667		0.56
15	3,720		0.57
16	4,954		0.75
		Maximum =	**0.89**

5.2.3 *Substructure Analysis Using Shell Submodel #1*

With reference to Figure 3-3, the displacements along Edges A and C computed in the full shell finite element analysis (Section 5.2.1) are applied onto this solid submodel.

Stress Plot

The maximum stress intensity is 6,579 psi, and the stress plot is provided in the following Figure 5-17.

The maximum stress intensity is the same as the full shell baseline analysis maximum stress intensity, and the stress contours are very similar (see Figure 5-15). This confirms that the shell substructure analysis produces the same stress results as the full shell baseline analysis.

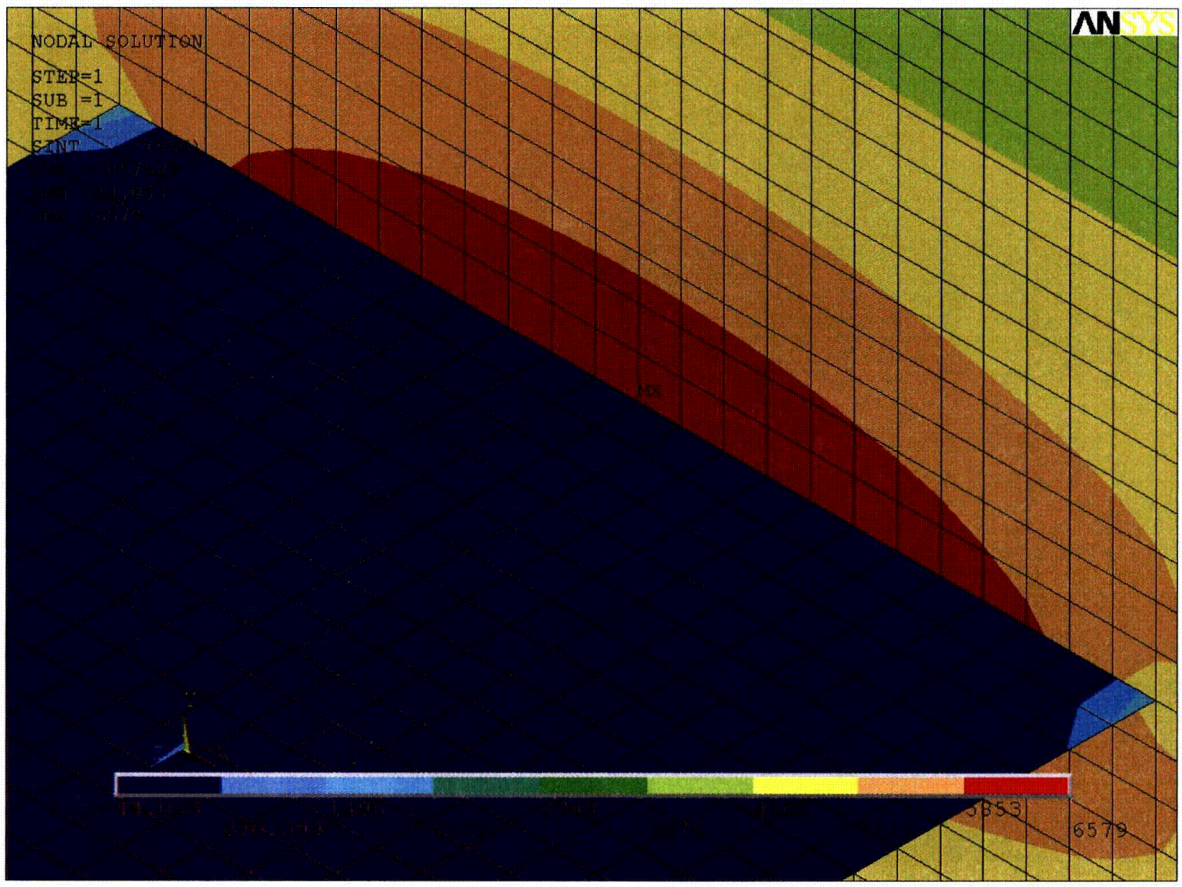

Figure 5-17
Substructure Analysis using Shell Submodel #1
Stress Plot for Load Case #2

5.2.4 Substructure Analysis Using Shell Submodel #2

With reference to Figure 3-5, the displacements along Edges A and C computed in the full shell finite element analysis (Section 5.2.1) are applied onto this solid submodel.

Stress Plot

The maximum stress intensity is 6,579 psi, and the stress plot is provided in the following Figure 5-18.

The maximum stress intensity is the same as the full shell baseline analysis maximum stress intensity, and the stress contours are very similar (see Figure 5-15). This confirms that the shell substructure analysis produces the same stress results as the full shell baseline analysis.

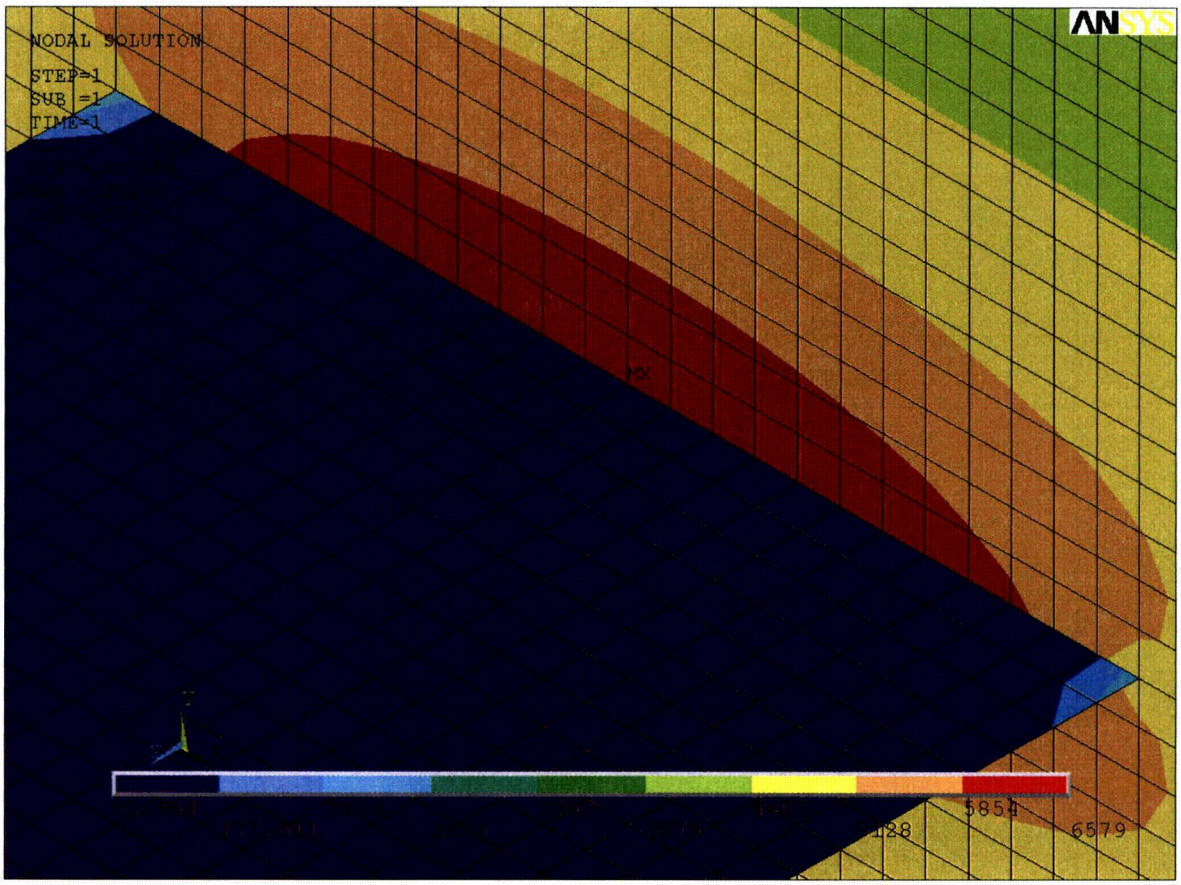

Figure 5-18
Substructure Analysis using Shell Submodel #2
Stress Plot for Load Case #2

5.2.5 *Substructure Analysis Using Solid Submodel #1*

With reference to Figure 3-3, the displacements along Edges A and C computed in the full shell finite element analysis (Section 5.2.1) are applied onto this solid submodel.

Stress Plot

The maximum non-linearized stress intensity is 10,789 psi, and the stress plot is provided in the following Figure 5-19.

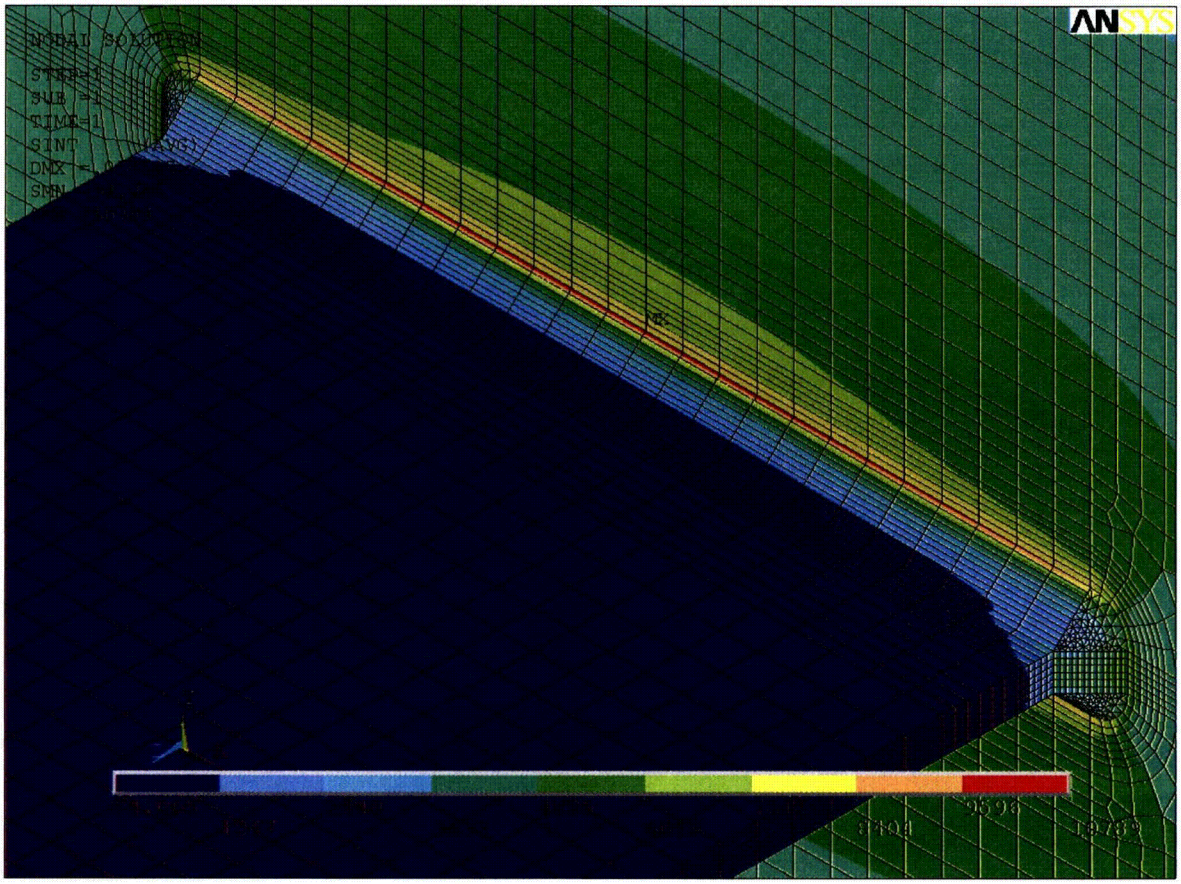

Figure 5-19
Substructure Analysis using Solid Submodel #1
Stress Plot for Load Case #2

SRF Table

Table 5-7
Substructure Analysis (Submodel #1) SRF
for Static Load Case #2

Path #	Solid (psi)	Shell (psi)	SRF
1	3,874	6,579	0.59
2	3,904		0.59
3	5,909		0.90
4	3,874		0.59
5	3,904		0.59
6	5,909		0.90
7	2,965		0.45
8	6,036		0.92
9	4,861		0.74
10	4,861		0.74
11	6,036		0.92
12	5,207		0.79
13	4,456		0.68
14	3,768		0.57
15	3,825		0.58
16	5,109		0.78
		Maximum =	**0.92**

5.2.6 *Substructure Analysis Using Solid Submodel #2*

With reference to Figure 3-3, the displacements along Edges A and C computed in the full shell finite element analysis (Section 5.2.1) are applied onto this solid submodel.

Stress Plot

The maximum non-linearized stress intensity is 10,673 psi, and the stress plot is provided in the following Figure 5-20.

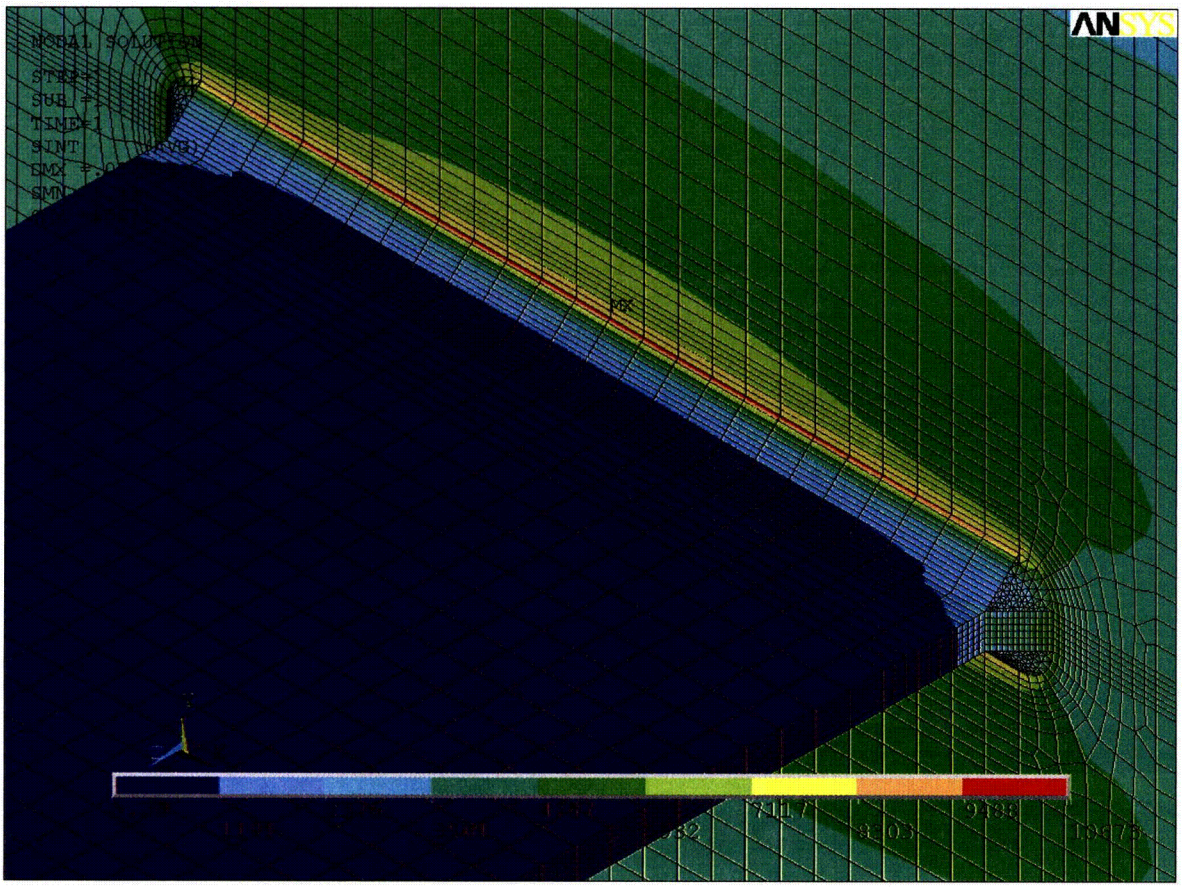

Figure 5-20
Substructure Analysis using Solid Submodel #2
Stress Plot for Load Case #2

SRF Table

Table 5-8
Substructure Analysis (Submodel #2) SRF
for Static Load Case #2

Path #	Solid (psi)	Shell (psi)	SRF
1	3,833	6,579	0.58
2	3,863		0.59
3	5,845		0.89
4	3,833		0.58
5	3,863		0.59
6	5,845		0.89
7	2,981		0.45
8	5,981		0.91
9	4,818		0.73
10	4,818		0.73
11	5,981		0.91
12	5,142		0.78
13	4,434		0.67
14	3,736		0.57
15	3,791		0.58
16	5,051		0.77
		Maximum =	**0.91**

5.2.7 Submodel Analysis Using Submodel #1

Matching Stress Profile

The stress profile matching is performed along the weld line connecting the vertical plate to the horizontal plate. The matching is accomplished by applying a horizontal (Z) load along the Edge C (see Figure 3-3) of the submodel. The nodes at the top and bottom edges are restrained in X and Z translations. The applied loads and the comparison of the stress profiles are shown in the following Figure 5-21 and Figure 5-22, respectively.

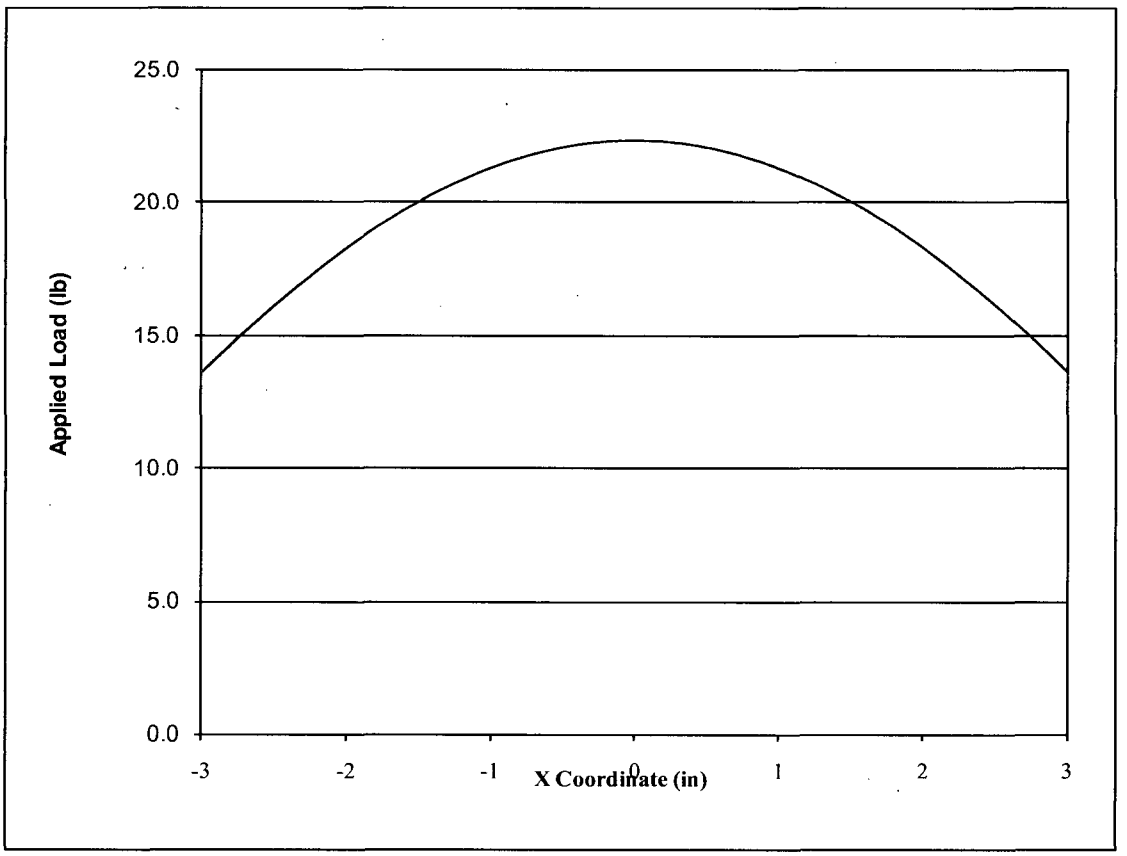

Figure 5-21
Submodel Analysis using Submodel #1
Applied Loads for Load Case #2

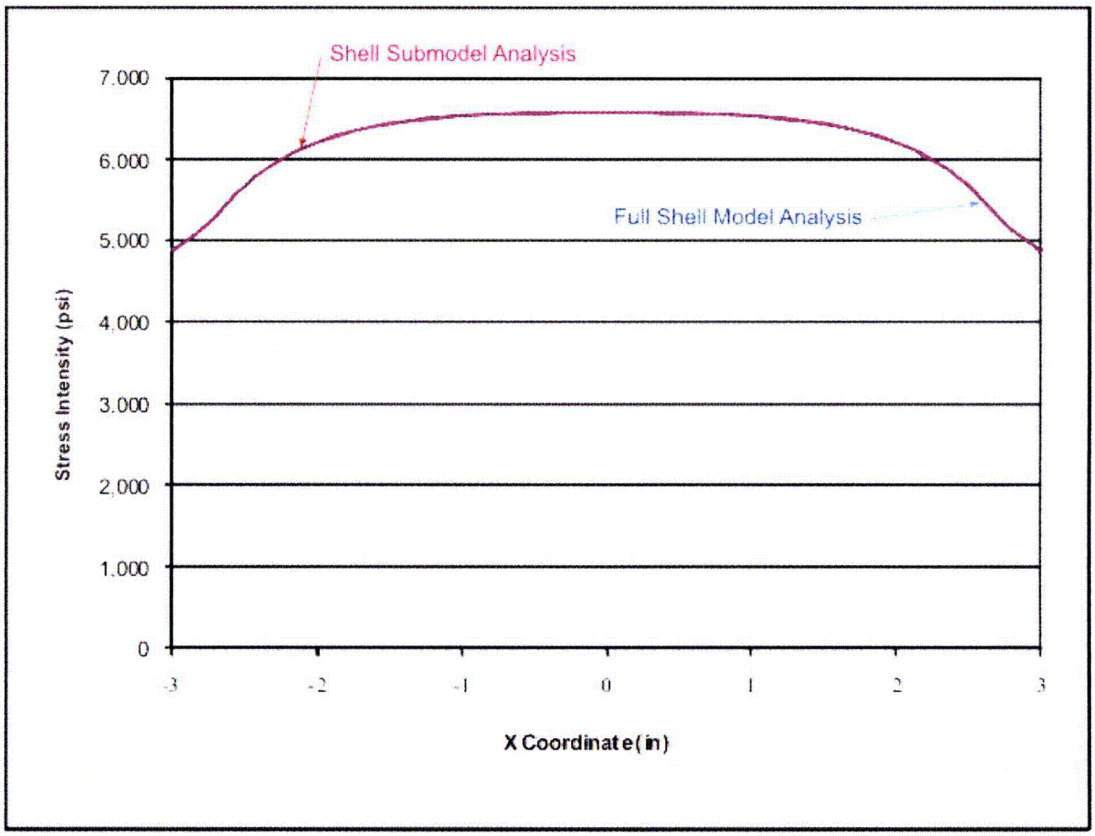

Figure 5-22
Submodel Analysis using Submodel #1
Stress Profile Comparison for Load Case #2

Stress Plot

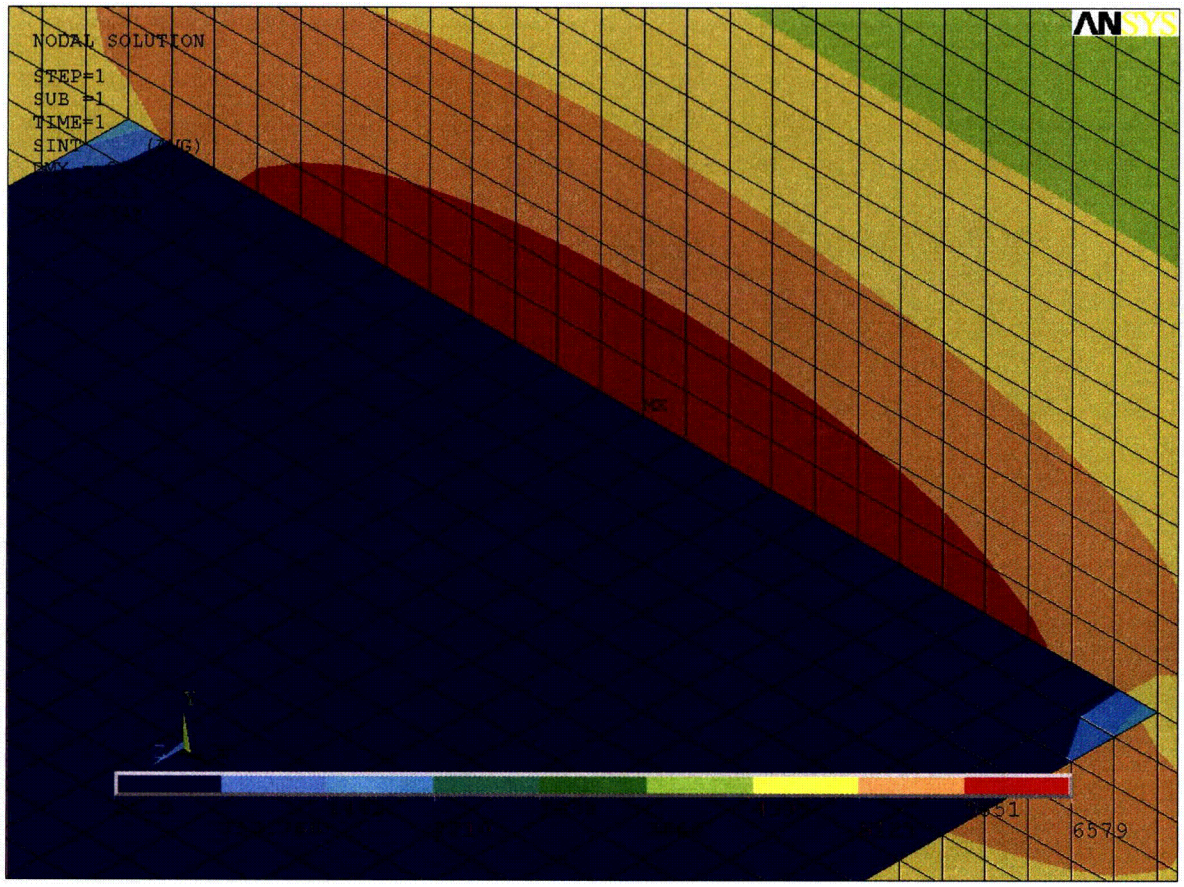

Figure 5-23
Submodel Analysis using Submodel #1
Shell Model Stress Plot for Load Case #2

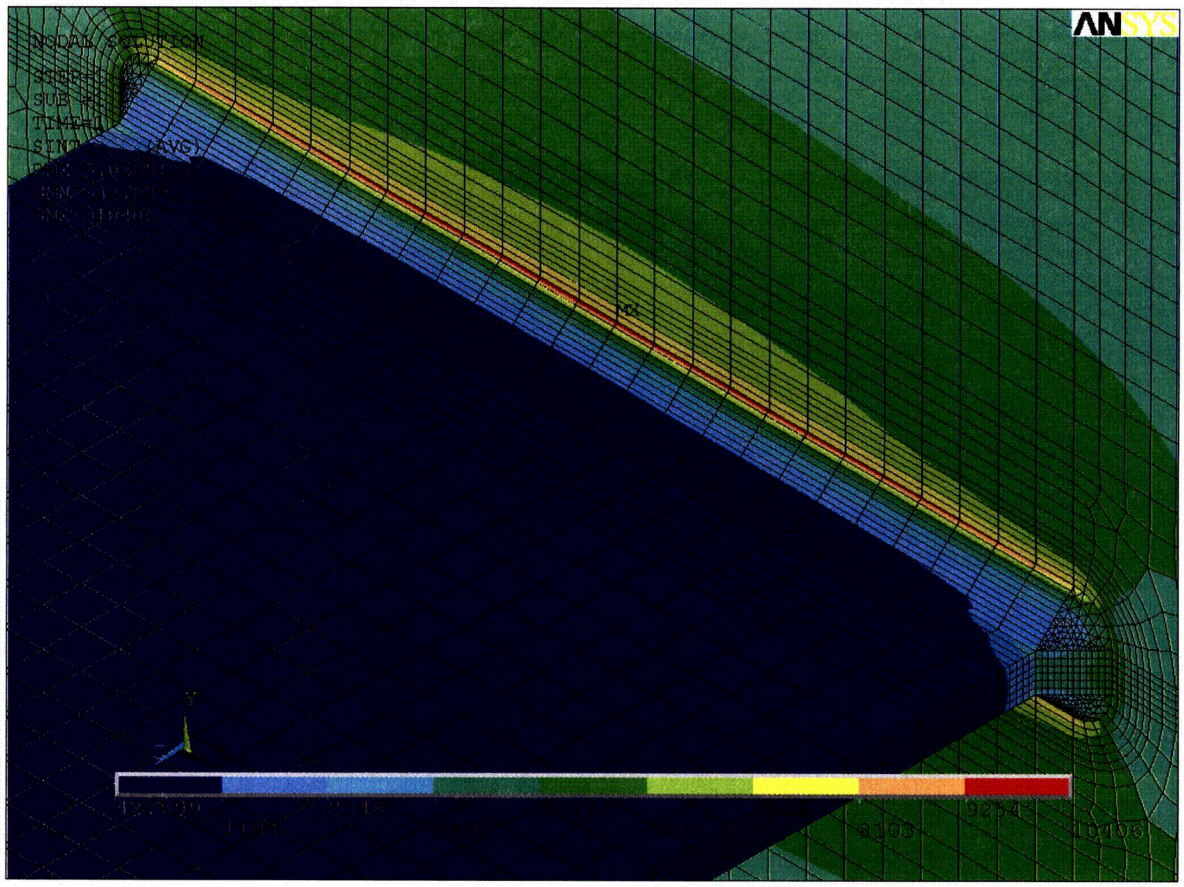

Figure 5-24
Submodel Analysis using Submodel #1
Solid Model Stress Plot for Load Case #2

SRF Table

Table 5-9
Submodel Analysis (Submodel #1) SRF
for Static Load Case #2

Path #	Solid (psi)	Shell (psi)	SRF
1	3,737	6,579	0.57
2	3,765		0.57
3	5,697		0.87
4	3,737		0.57
5	3,765		0.57
6	5,697		0.87
7	2,911		0.44
8	5,849		0.89
9	4,715		0.72
10	4,715		0.72
11	5,849		0.89
12	5,014		0.76
13	4,326		0.66
14	3,644		0.55
15	3,697		0.56
16	4,924		0.75
		Maximum =	**0.89**

5.2.8 *Submodel Analysis Using Submodel #2*

Matching Stress Profile

The stress profile matching is performed along the weld line connecting the vertical plate to the horizontal plate. The matching is accomplished by applying a horizontal (Z) load along the Edge C (see Figure 3-5) of the submodel. The nodes at the top and bottom edges (i.e., Edge A) are fixed. The applied loads and the comparison of the stress profiles are shown in the following Figure 5-25 and Figure 5-26, respectively.

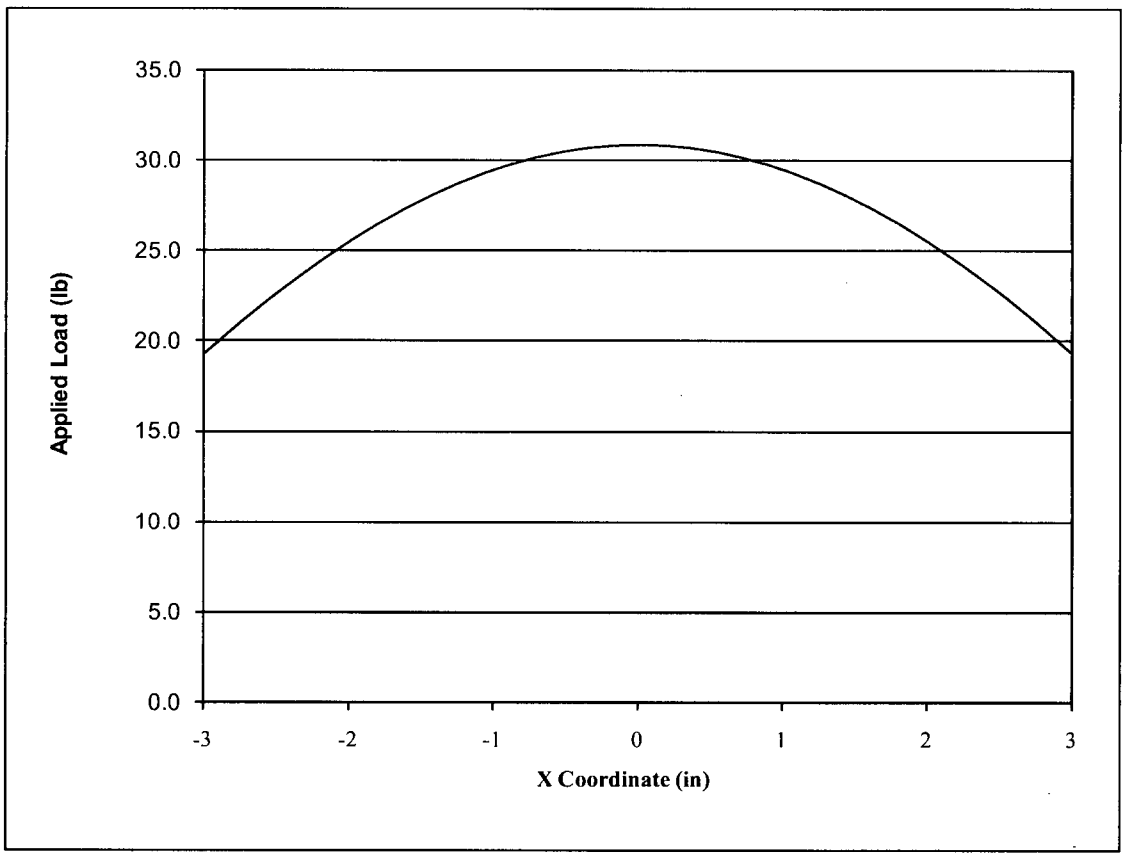

Figure 5-25
Submodel Analysis using Submodel #2
Applied Loads for Load Case #2

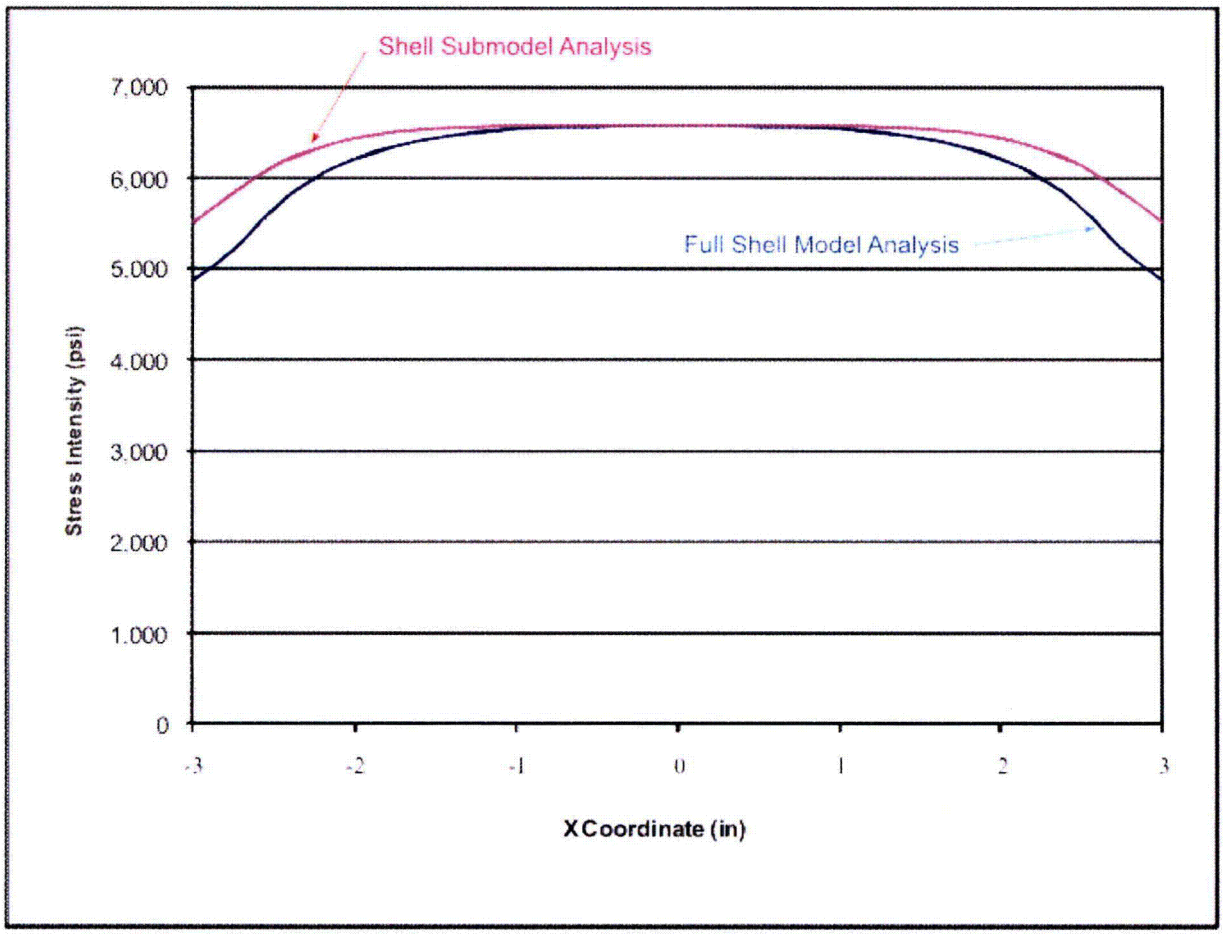

Figure 5-26
Submodel Analysis using Submodel #2
Stress Profile Comparison for Load Case #2

Stress Plot

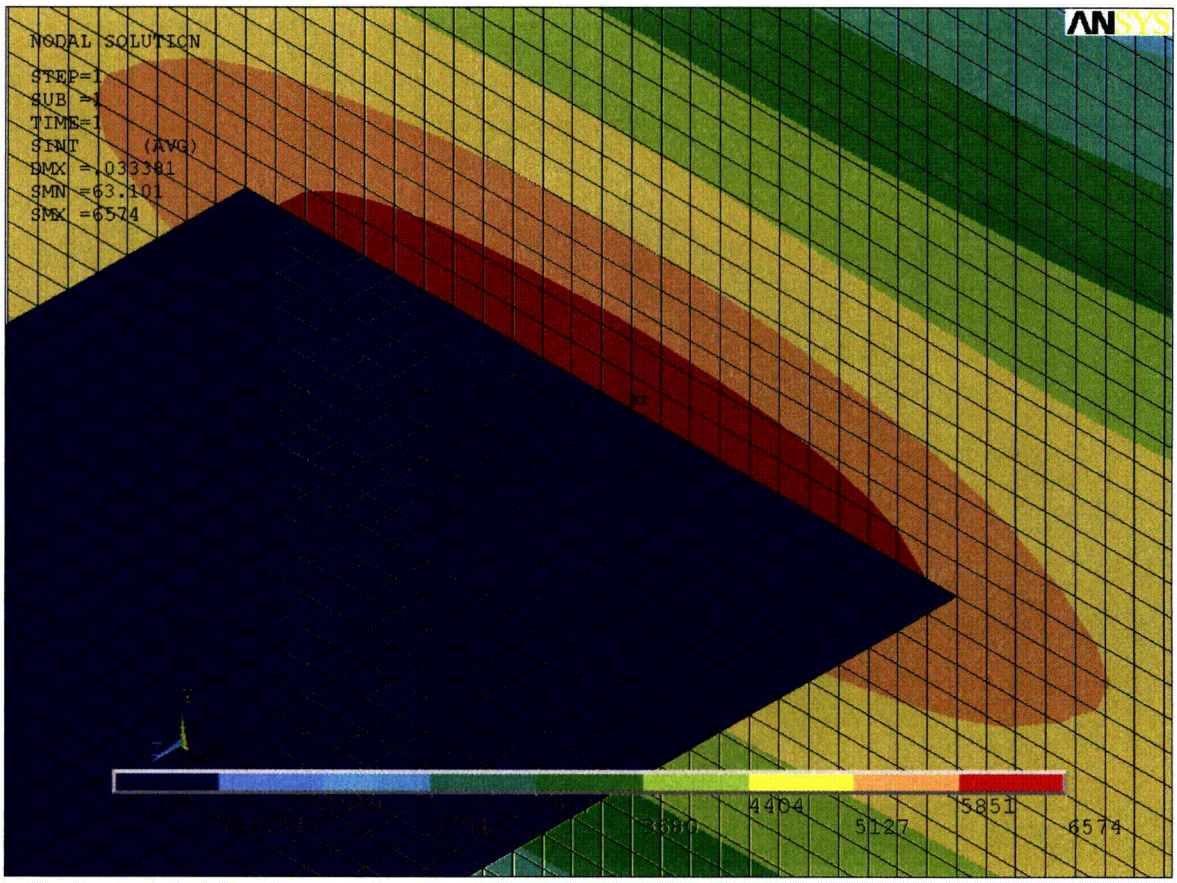

Figure 5-27
Submodel Analysis using Submodel #2
Shell Model Stress Plot for Load Case #2

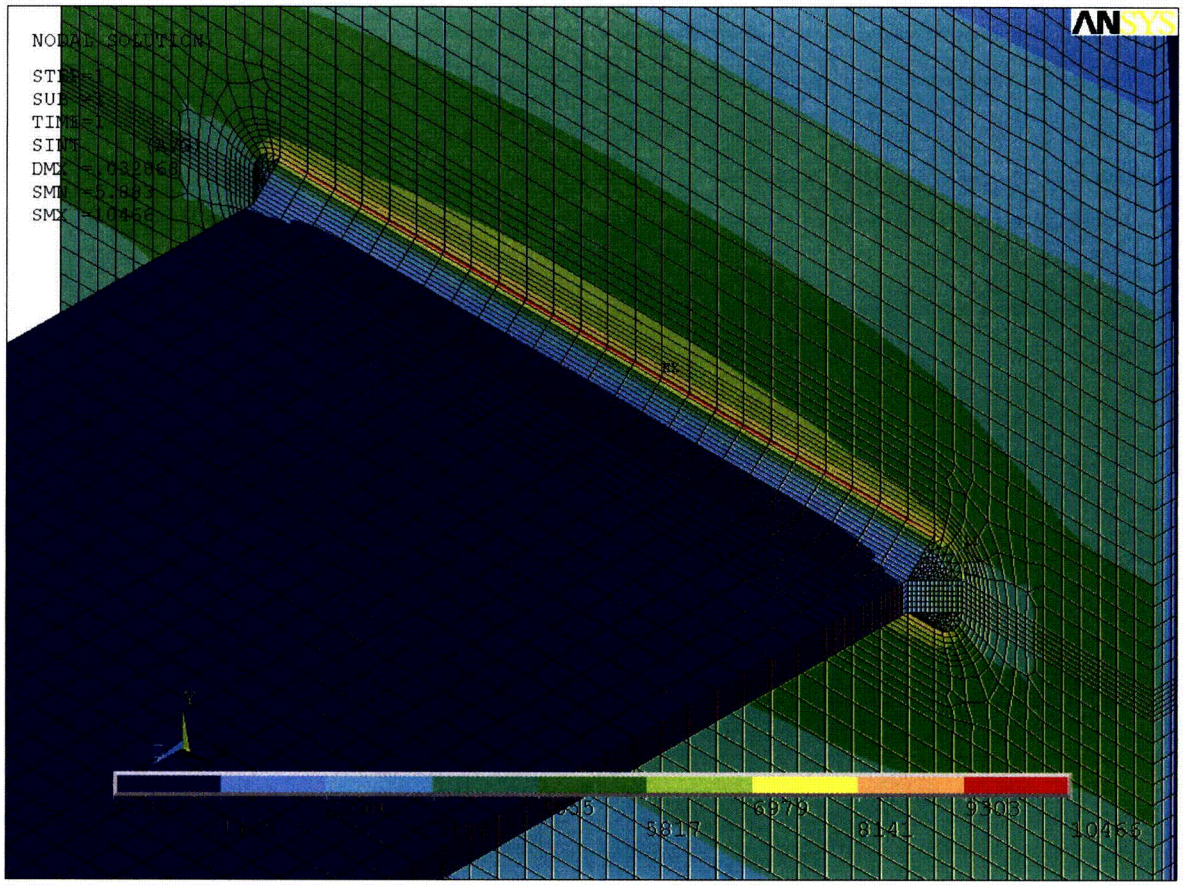

Figure 5-28
Submodel Analysis using Submodel #2
Solid Model Stress Plot for Load Case #2

SRF Table

Table 5-10
Submodel Analysis (Submodel #2) SRF
for Static Load Case #2

Path #	Solid (psi)	Shell (psi)	SRF
1	3,755	6,579	0.57
2	3,784		0.58
3	5,736		0.87
4	3,755		0.57
5	3,784		0.58
6	5,736		0.87
7	1,763		0.27
8	5,851		0.89
9	4,719		0.72
10	4,719		0.72
11	5,851		0.89
12	5,482		0.83
13	3,706		0.56
14	3,504		0.53
15	3,608		0.55
16	5,143		0.78
		Maximum =	**0.89**

6.0 DYNAMIC ANALYSIS RESULTS

The dynamic analyses consist of the following:

1. Full Shell Finite Element Time History Analysis

   This is the shell baseline time history analysis. The results of the substructure and submodel analyses are compared to the result of the shell baseline analysis to calculate the Stress Reduction Factors. The analyses are documented in Sections 6.4.1 and 6.5.1 for Load Cases #1 and #2, respectively.

2. Solid Finite Element Time History Analysis

   This is the solid baseline time history analysis. This analysis provides a direct comparison with the full shell baseline time history analysis. This comparison removes any inherent approximation and assumption that are associated with the substructure and submodel analyses. The analyses are documented in Sections 6.4.2 and 6.5.2 for Load Cases #1 and #2, respectively.

   By symmetry, only half of the solid model is used in the analysis. Symmetric boundary conditions are imposed at the plane of half symmetry. Using the half solid model saves significant execution time without compromising accuracy.

3. Substructure Time History Analysis using Shell Submodel #2

   This time history analysis uses the full shell analysis displacements along the submodel boundaries for all the time steps calculated in the full shell finite element time history analysis as input into the shell submodel #2. The analyses are documented in Sections 6.4.3 and 6.5.3 for Load Cases #1 and #2, respectively.

4. Substructure Time History Analysis using Solid Submodel #2

   This time history analysis uses the full shell analysis displacements along the submodel boundaries for all the time steps calculated in the full shell finite element time history analysis as input into the solid submodel #2. The analyses are documented in Sections 6.4.4 and 6.5.4 for Load Cases #1 and #2, respectively.

5. Submodel Analysis using Shell and Solid Submodel #2

   This static analysis uses submodel analysis approach of matching the submodel stress intensity profile to the full shell stress intensity profile at the time step that corresponds to the maximum stress intensity along the welded connection. The analyses are documented in Sections 6.4.5 and 6.5.5 for Load Cases #1 and #2, respectively.

6.1 Structural Modal Analysis

6.1.1 Shell Model Modal Frequencies

Modal analysis of the shell structure is performed to determine the fundamental frequencies of the system. The following Table 6-1 and Table 6-2 summarize the major frequencies in the vertical (Y direction) and the horizontal (Z direction) directions, which correspond to the directions of the Load Cases #1 and #2, respectively.

Table 6-1
Shell Model Structural Vertical (Y direction) Modal Frequencies

Mode # (1)	Frequency (Hz)	Period (s)	Participation Factor	Cumulative Mass Fraction
1	51.82	0.019	0.090	0.759
4	170.90	0.006	0.003	0.760
7	329.64	0.003	-0.051	1.000

Note: (1) Insignificant modes have been excluded from the table.

Table 6-2
Shell Model Structural Horizontal (Z direction) Modal Frequencies

Mode # (1)	Frequency (Hz)	Period (s)	Participation Factor	Cumulative Mass Fraction
2	55.51	0.018	0.336	0.848
6	310.60	0.003	0.142	1.000

Note: (1) Insignificant modes have been excluded from the table.

6.1.2 Solid Model Modal Frequencies

Modal analysis of the solid structure is also performed to determine the fundamental frequencies of the system. The following Table 6-3 and Table 6-4 summarize the major frequencies in the vertical (Y direction) and the horizontal (Z direction) directions, which correspond to the directions of the Load Cases #1 and #2, respectively.

Table 6-3
Solid Model Structural Vertical (Y direction) Modal Frequencies

Mode # (1)	Frequency (Hz)	Period (s)	Participation Factor	Cumulative Mass Fraction
1	55.14	0.018	0.089	0.758
4	170.72	0.006	-0.003	0.759
7	349.84	0.003	-0.050	1.000

Note: (1) Insignificant modes have been excluded from the table.

Table 6-4
Solid Model Structural Horizontal (Z direction) Modal Frequencies

Mode # (1)	Frequency (Hz)	Period (s)	Participation Factor	Cumulative Mass Fraction
2	55.72	0.018	0.336	0.848
6	311.31	0.003	0.142	1.000

Note: (1) Insignificant modes have been excluded from the table.

Observation

By introducing the weld into the solid model, the fundamental frequencies have increased slightly as follows:

- Vertical Y-Direction: From 51.82 Hz to 55.14 Hz (an increase of 6%).
- Horizontal Z-Direction: From 55.51 Hz to 55.72 Hz (an increase of 0.4%).

6.2 Structural Damping Values

The structural critical damping value is 1% (Reference 6).

The damping used in the dynamic transient analysis is the Alpha and Beta damping, also known as the Rayleigh damping and is defined by Rayleigh damping constants α and β. The damping matrix, C, is calculated by using these constants to multiply the mass matrix, M, and the stiffness matrix, K:

$$C = \alpha M + \beta K$$

The values of α and β are calculated from modal damping ratio, ξ_i, which is the ratio of actual damping to critical damping for a particular mode of vibration, i. If ω_i is the natural frequency of the mode i, α and β satisfy the relation:

$$\xi_i = \alpha/2\omega_i + \beta\omega_i/2$$ (Reference 4, Structural Analysis Guide, Section 5.9.3)

Therefore, given ξ and a frequency range between ω_i and ω_j, two simultaneous equations can be solved for α and β.

In this analysis, the frequency range is 52 Hz and 350 Hz, which cover the frequency range from mode #1 to mode #7 (see Table 6-1 through Table 6-3). The calculated values are:

α = 5.689

β = 7.918E-6

The calculations of α and β are documented in the spreadsheet *Damping(Rev1).xls* (described in Appendix A).

6.3 Time History Analysis Integration Time Step

The accuracy of the transient dynamic solution depends on the integration time step. For the Newmark time integration used herein, it is recommended that using approximately twenty points per cycle of the highest frequency of interest results in a reasonably accurate solution. That is, if f is the frequency (in Hz), the integration time step (ITS) is given by:

ITS = $1/(20f)$ (Reference 4, Structural Analysis Guide, Section 5.9.1)

The modal analysis shows that the highest major mode is 349.84 Hz, in the vertical direction (see Table 6-1). The applied harmonic load frequency is set at 25 Hz (see Section 4.2). Therefore, use 350 Hz as the highest frequency of interest.

ITS = 1/(20*350)

= 0.000143 seconds

6.4 Dynamic Load Case #1

6.4.1 Full Shell Finite Element Time History Analysis

Transient Displacement Plot

The maximum vertical displacement occurs at the corner nodes along the load application line. The following Figure 6-1 shows a plot of the nodal transient displacements.

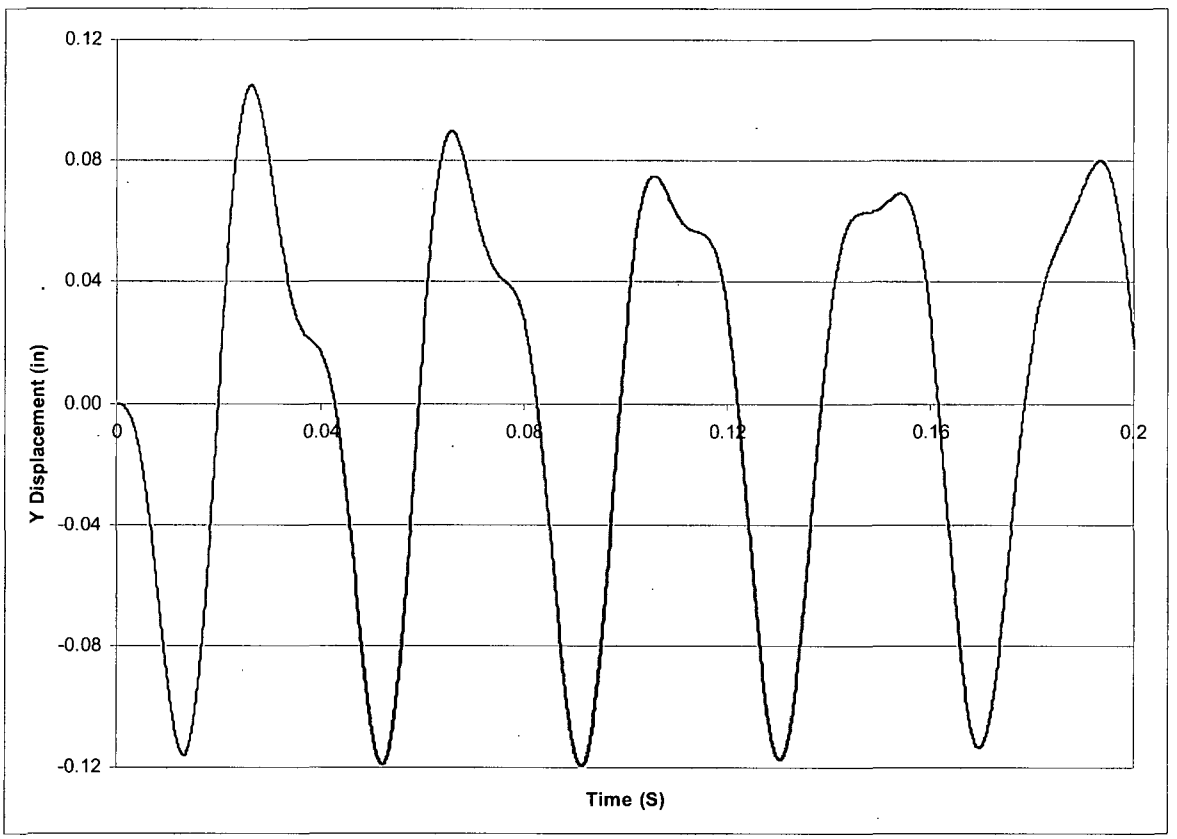

Figure 6-1
Full Shell Model Time History Analysis
Vertical Transient Displacements for Load Case #1

Transient Stress Intensity Plot

The maximum stress intensity occurs at one of the weld line nodes. The following Figure 6-2 shows a plot of the nodal transient stress intensities. The maximum stress intensity is 9,468 psi, which occurs at 0.052143 seconds time step.

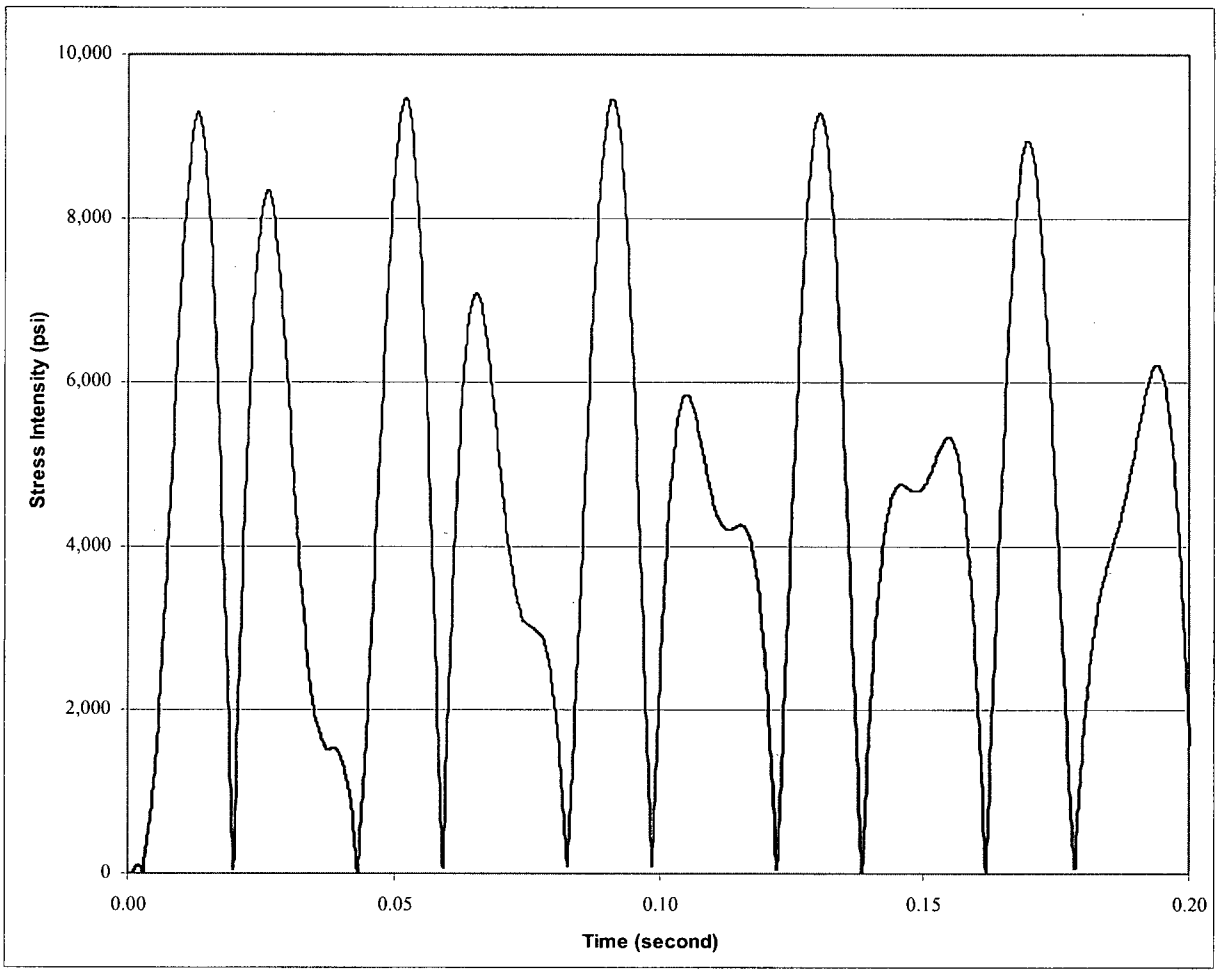

Figure 6-2
Full Shell Model Time History Analysis
Nodal Stress Intensity for Load Case #1

Vertical Displacement Plot

The following Figure 6-3 shows the vertical displacements at 0.052143 seconds time step, when the maximum stress intensity occurs.

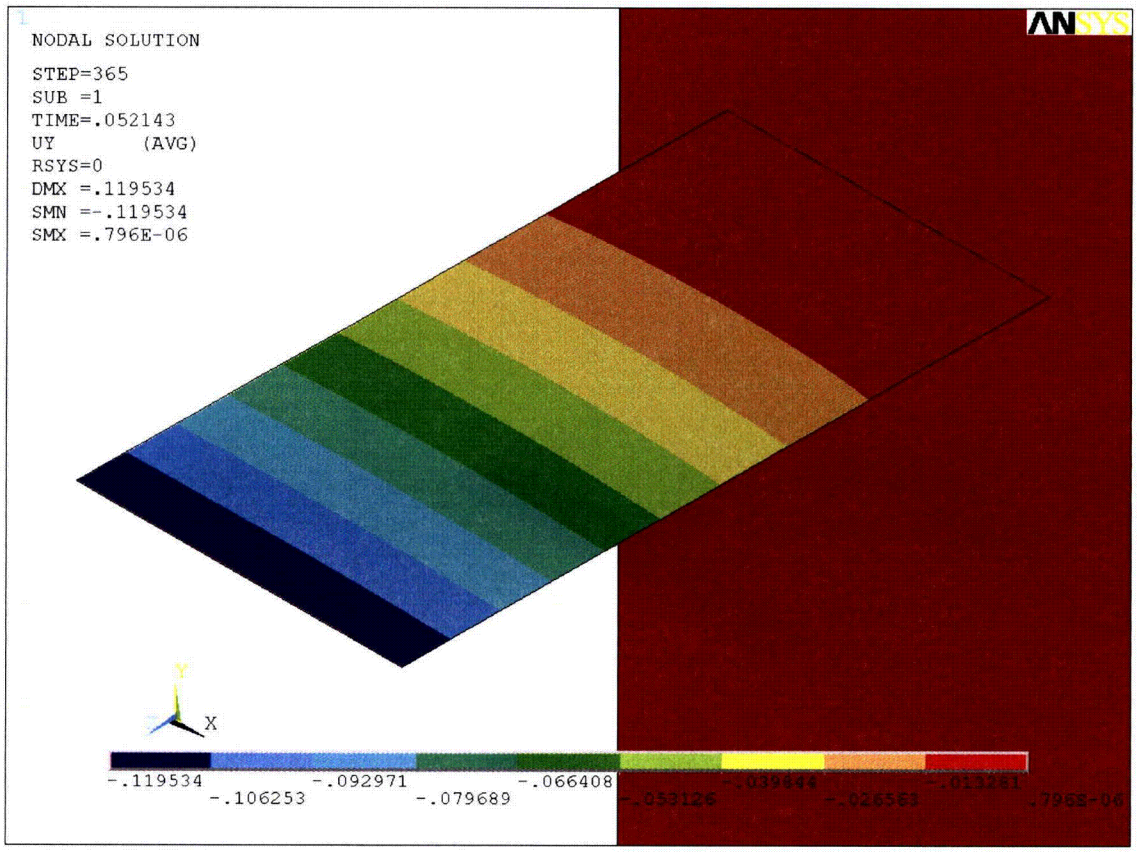

Figure 6-3
Full Shell Model Time History Analysis
Vertical Displacement Plot for Load Case #1
(Full Shell Model Baseline Analysis)

Maximum Stress Plot

The maximum stress intensity is 9,468 psi, which occurs at 0.052143 seconds time step. The stress plot at that time step is provided in the following Figure 6-4. This analysis is the full shell model baseline analysis, and the maximum stress intensity of 9,468 psi is used to determine the SRF in other analyses.

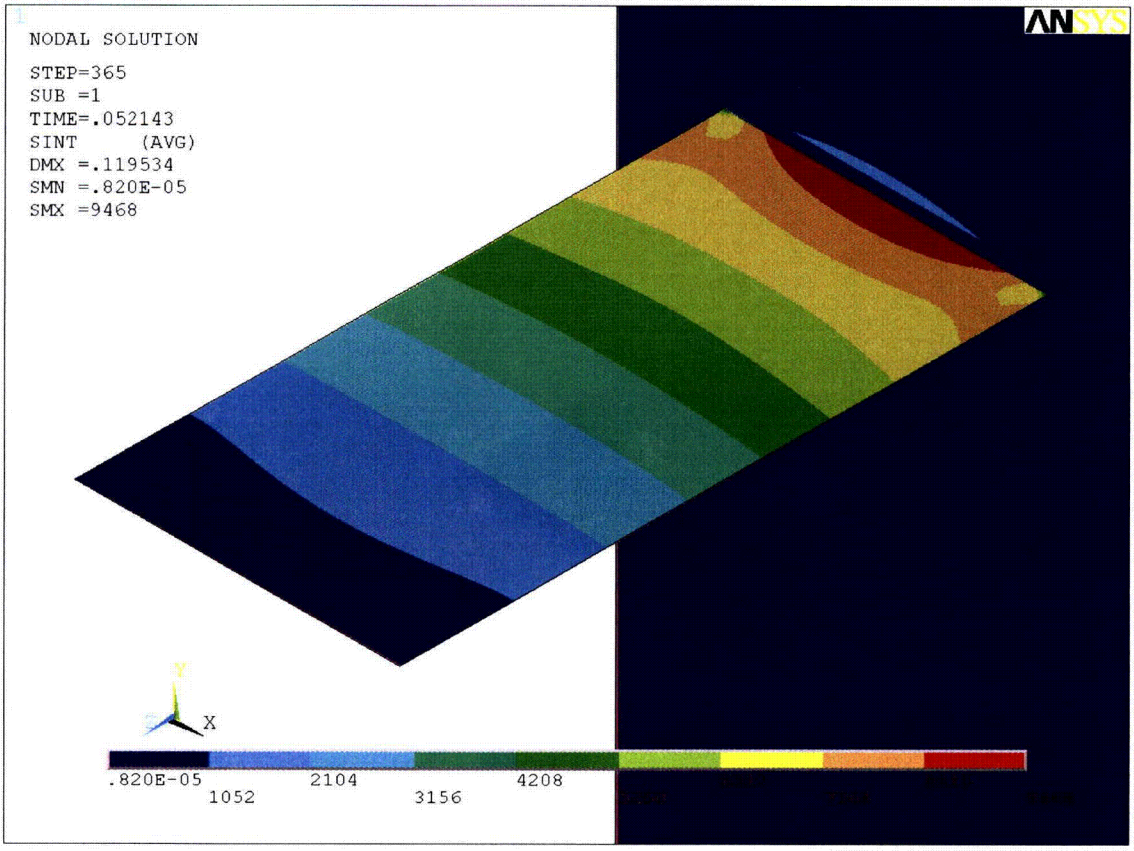

Figure 6-4
Full Shell Model Time History Analysis
Maximum Stress Intensity Plot for Load Case #1
(Full Shell Model Baseline Analysis)

6.4.2 *Full Solid Finite Element Time History Analysis*

By symmetry, only half of the solid model is used in the time history analysis. Symmetric boundary conditions are imposed at the plane of half symmetry. Using half the solid model saves significant execution time without compromising accuracy.

Transient Displacement Plot

The maximum vertical displacement occurs at the corner nodes along the load application line. The following Figure 6-5 shows a plot of the nodal transient displacements for both the shell and solid models.

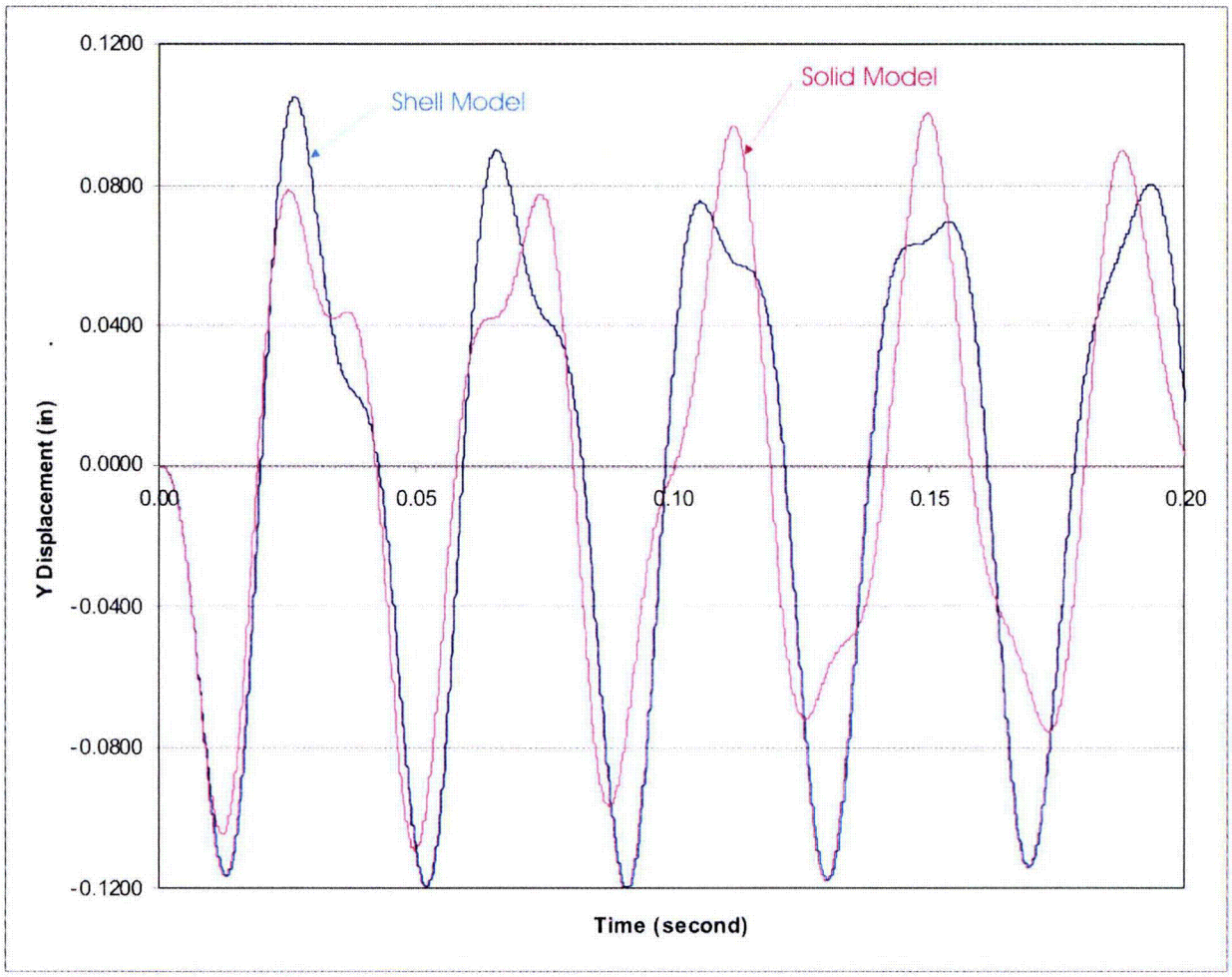

Figure 6-5
Shell and Solid Model Time History Analysis
Vertical Transient Displacement for Load Case #1

Transient Stress Intensity Plot

The maximum stress intensity occurs at one of the weld line nodes. The following Figure 6-6 shows a plot of the transient stress intensities for both the shell and solid models.

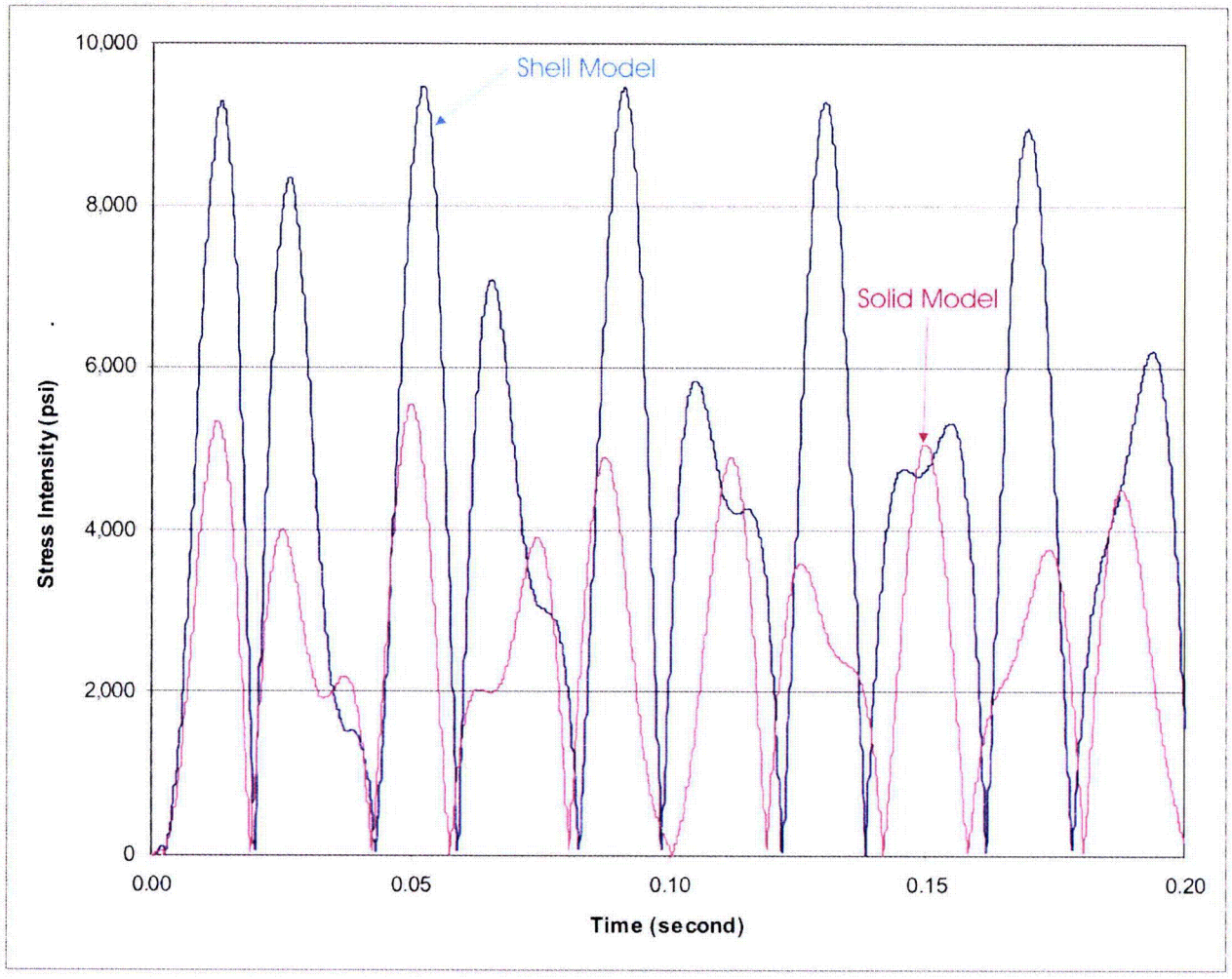

Figure 6-6
Shell and Solid Model Time History Analysis
Stress Intensity for Load Case #1

Note that the shell model stress intensity corresponds to the maximum nodal stress intensity while the solid model stress intensity corresponds to the maximum linearized stress intensity.

Vertical Displacement Plot

The following Figure 6-7 shows the vertical displacements at 0.05000 seconds time step, when the maximum linearized stress intensity occurs.

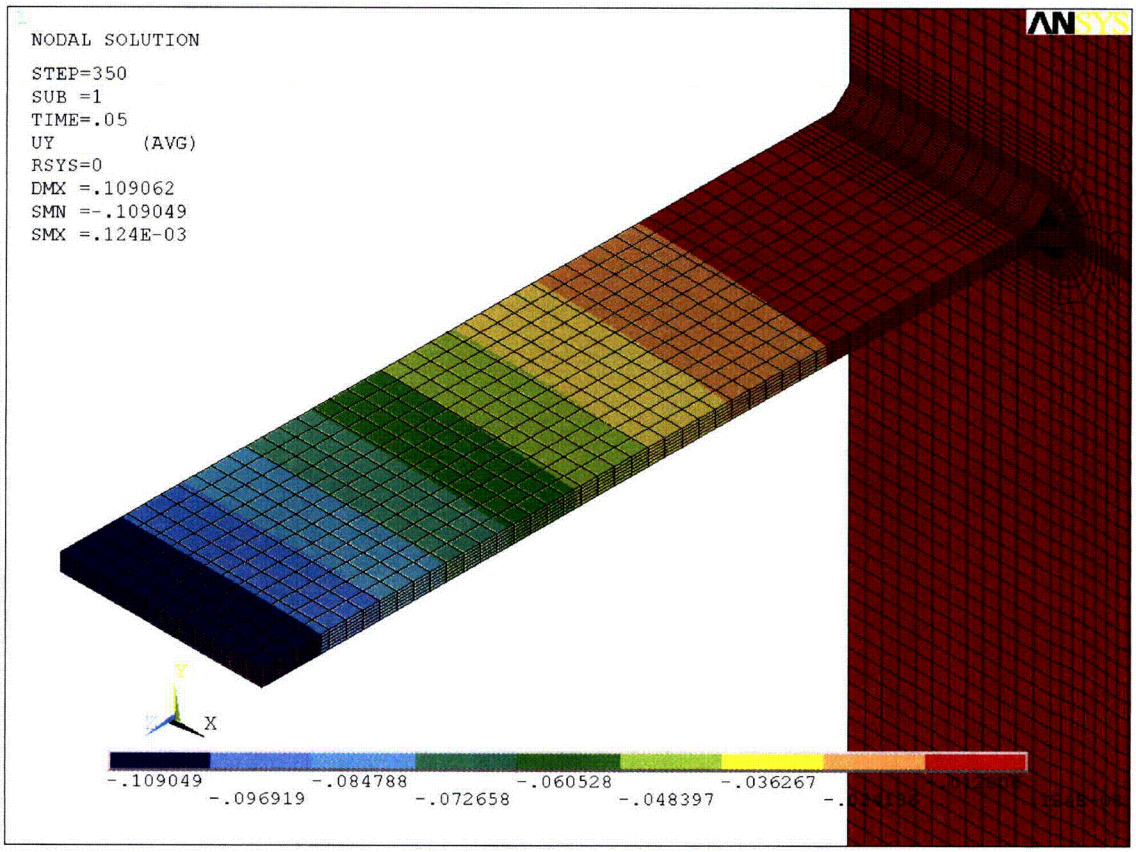

Figure 6-7
Full Solid Model Time History Analysis
Vertical Displacement Plot for Load Case #1
(Full Solid Model Baseline Analysis)

Maximum Stress Plot

The maximum linearized stress intensity is 5,546 psi (see Figure 6-6), which occurs at 0.05000 seconds time step. The non-linearized stress intensity plot at that time step is provided in the following Figure 6-8.

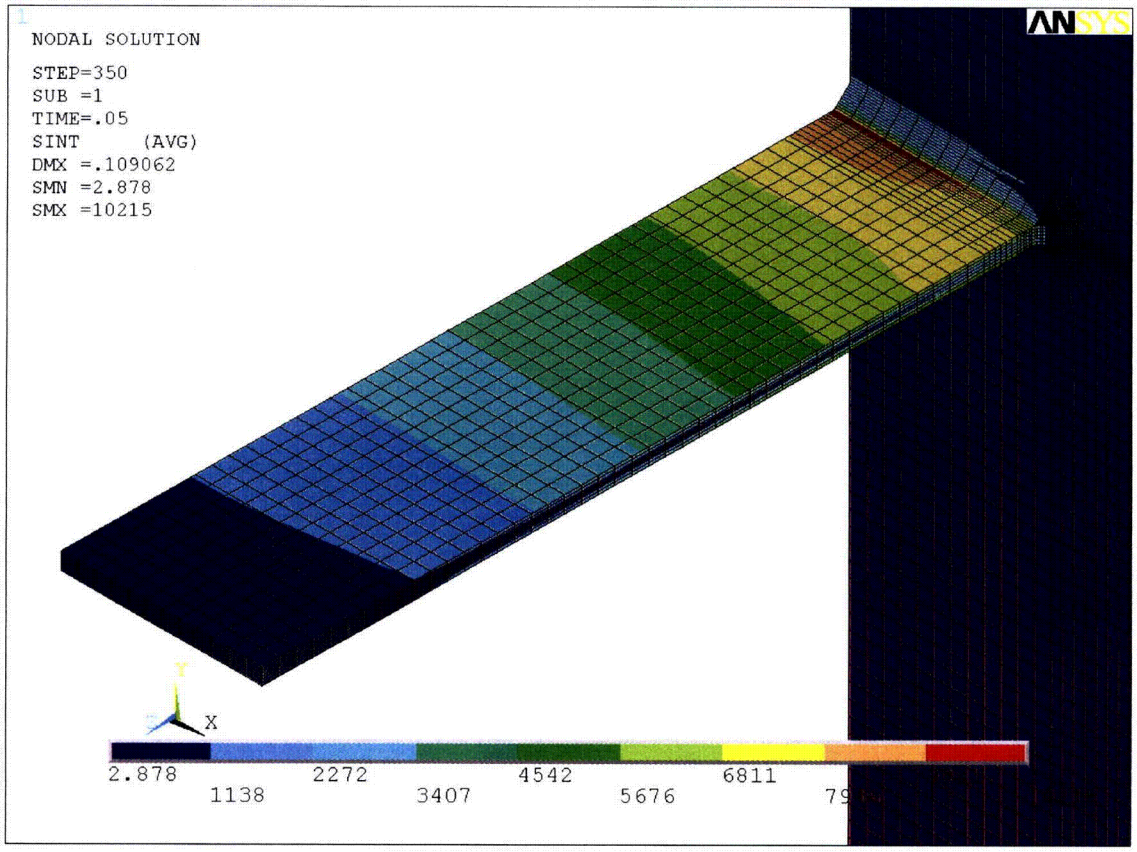

Figure 6-8
Full Solid Model Time History Analysis
Maximum Stress Intensity Plot for Load Case #1
(Full Solid Model Baseline Analysis)

SRF Table

Table 6-5
Full Solid Model Time History Analysis SRF
for Dynamic Load Case #1

Path #	Solid (psi)	Shell (psi)	SRF
1	5,546	9,468	0.59
2	2,233		0.24
3	1,457		0.15
4	5,546		0.59
5	2,233		0.24
6	1,457		0.15
7	5,500		0.58
8	1,008		0.11
9	1,359		0.14
10	1,359		0.14
11	1,008		0.11
12	694		0.07
13	775		0.08
14	3,190		0.34
15	677		0.07
16	497		0.05
		Maximum =	**0.59**

6.4.3 *Substructure Time History Analysis Using Shell Submodel #2*

With reference to Figure 3-5, the displacements along Edges A and C computed in the full shell finite element time history analysis, at each of the 1,400 time steps, (Section 6.4.1) are applied onto this shell submodel #2 in a time history analysis. The time history stress intensities calculated in this analysis are plotted and compared with the results of the full shell time history analysis.

Transient Stress Intensity Plot

The maximum stress intensity occurs at one of the weld line nodes. The following Figure 6-9 shows a plot of the nodal transient stress intensities.

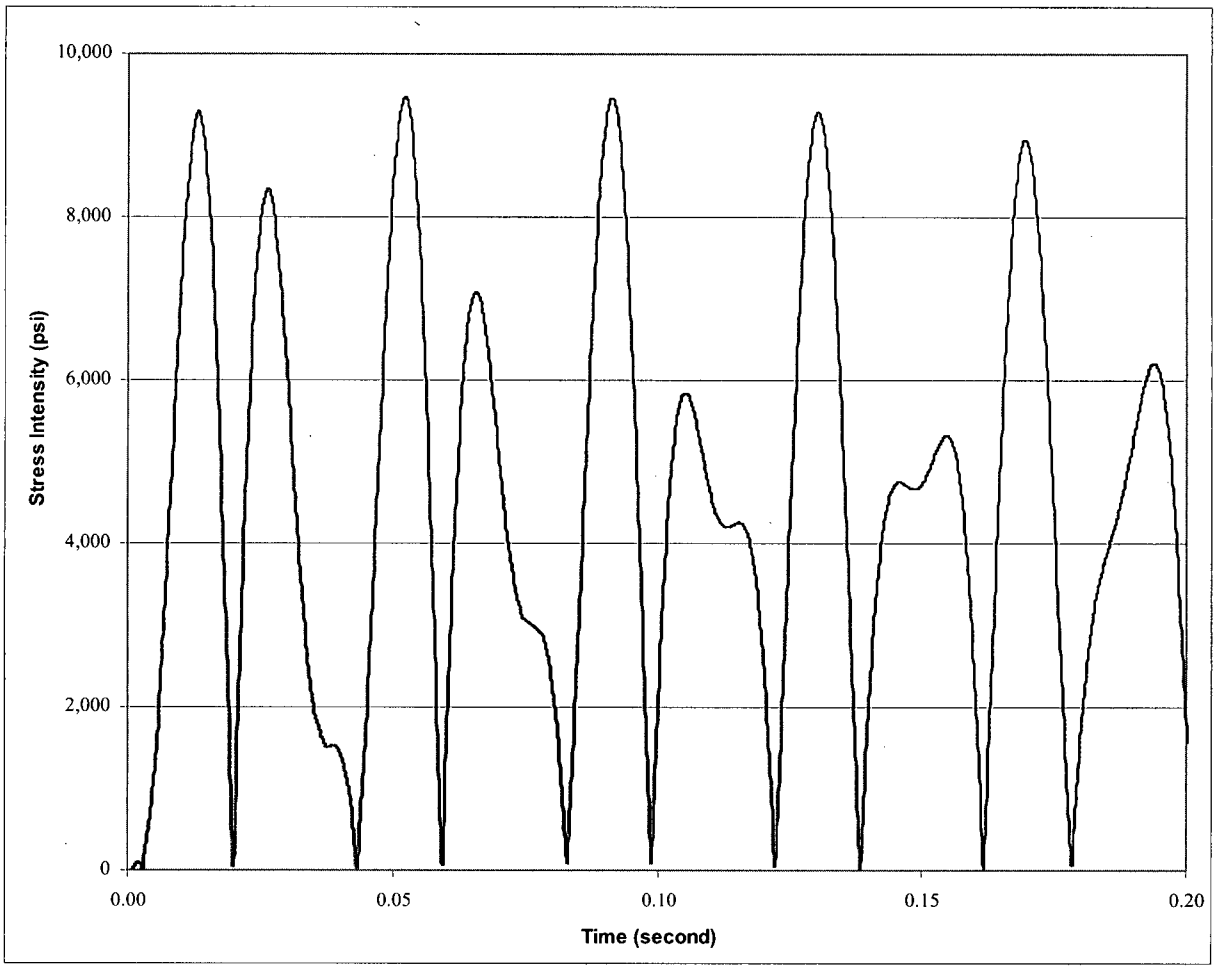

Figure 6-9
Substructure Time History Analysis using Shell Submodel #2
Nodal Stress Intensity for Load Case #1

Vertical Displacement Plot

The following Figure 6-10 shows the vertical displacements at 0.052143 seconds time step, when the maximum stress intensity occurs.

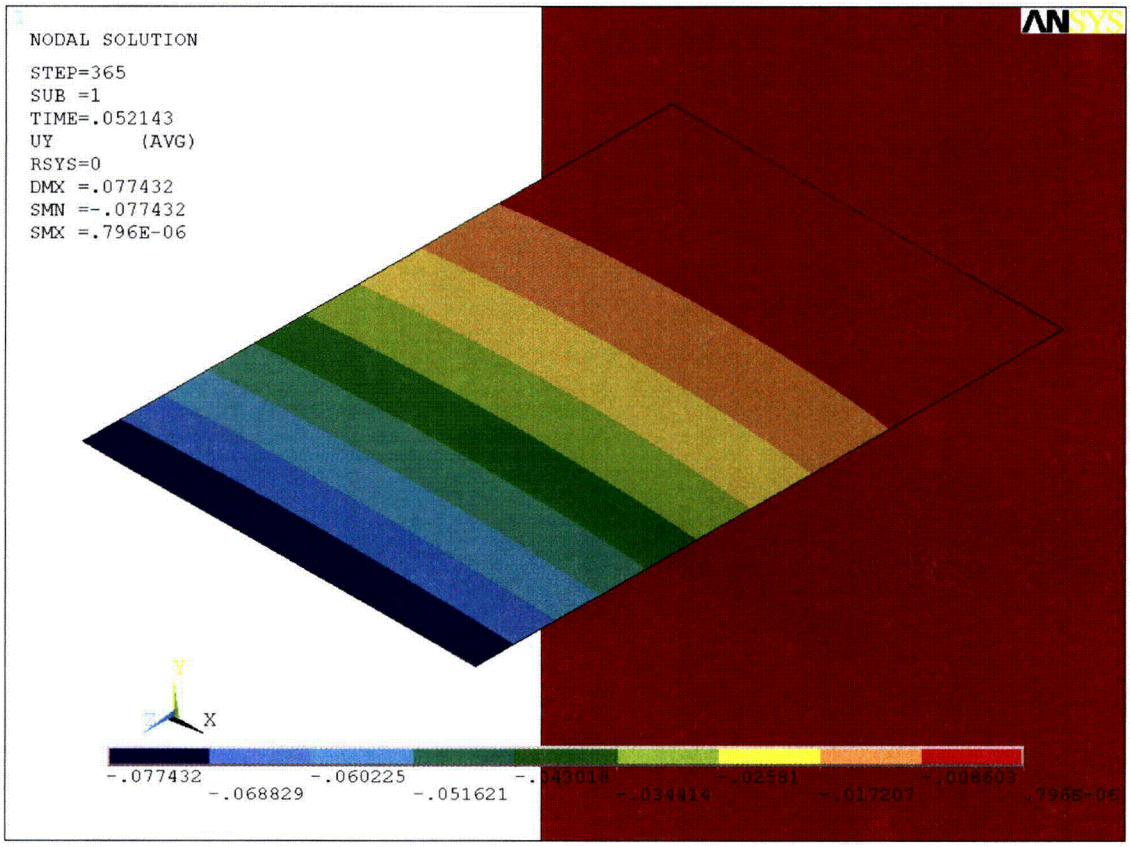

Figure 6-10
Substructure Time History Analysis using Shell Submodel #2
Vertical Displacement Plot for Load Case #1

Maximum Stress Plot

The maximum stress intensity is 9,468 psi, which occurs at 0.052143 seconds time step. The stress plot at that time step is provided in the following Figure 6-11.

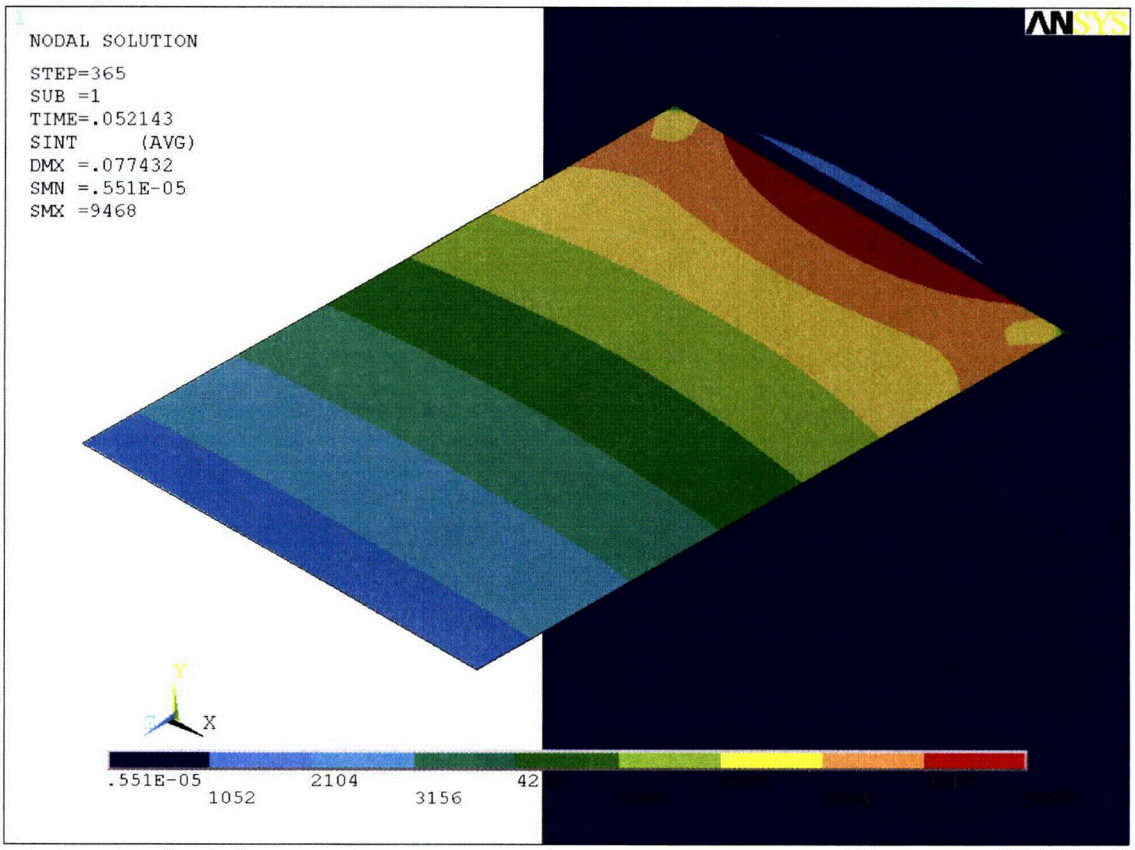

Figure 6-11
Substructure Time History Analysis using Shell Submodel #2
Maximum Stress Intensity Plot for Load Case #1

Comparison

The stress intensity plots shown in Figure 6-2 and Figure 6-9 show that the shapes of the plots are the same. The maximum stress intensities for both analyses are 9,468 psi, and they both occur at the time step of 0.052143 seconds. The comparisons show that the substructure time history analysis using shell submodel produces the same results as the full shell time history analysis.

6.4.4 *Substructure Time History Analysis Using Solid Submodel #2*

With reference to Figure 3-5, the displacements along Edges A and C computed in the full shell finite element time history analysis, at each of the 1,400 time steps, (Section 6.4.1) are applied onto this solid submodel #2 in a time history analysis.

By symmetry, only half of the solid submodel #2 is used in the time history analysis. Symmetric boundary conditions are imposed at the plane of half symmetry. Using half the solid model saves significant execution time without compromising accuracy.

Stress Plot

The stress plot is provided in the following Figure 6-12, which shows the maximum non-linearized stress intensity of 11,909 psi at the time step of 0.052143 seconds.

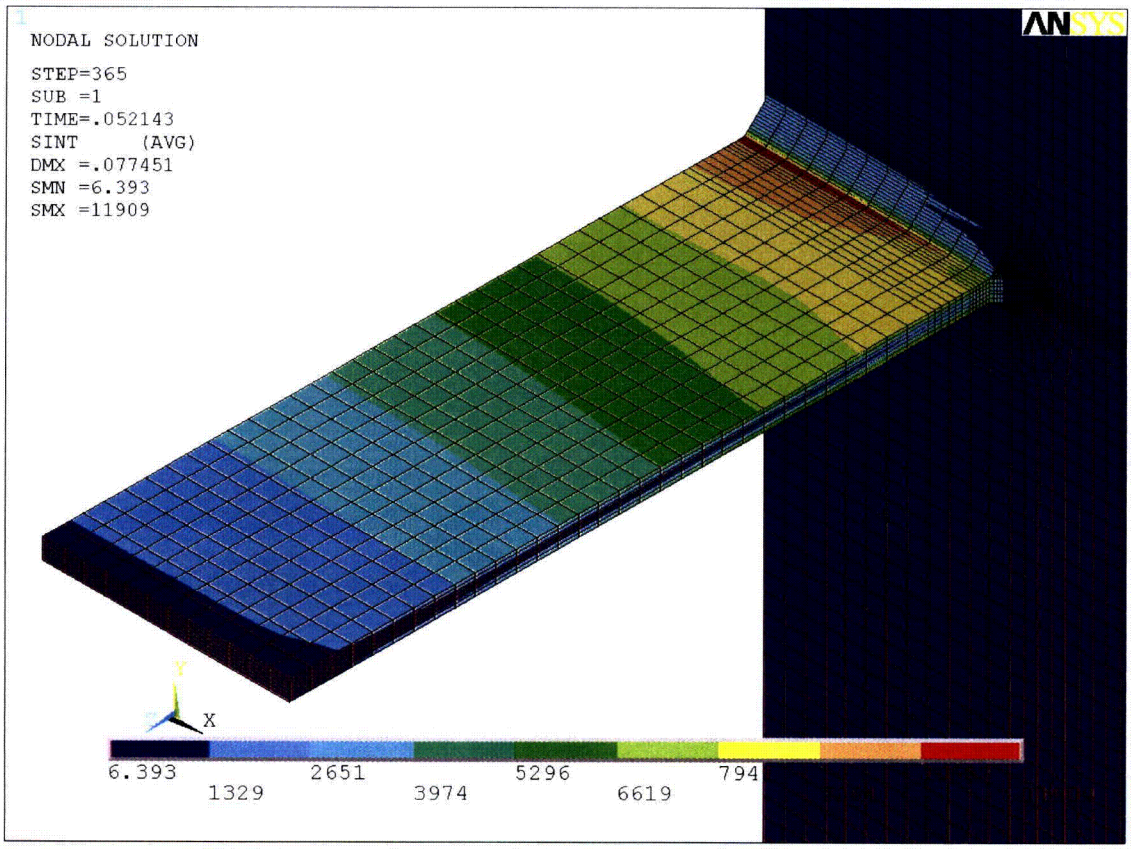

Figure 6-12
Substructure Time History Analysis using Solid Submodel #2
Maximum Stress Intensity Plot for Load Case #1

SRF Table

Table 6-6
Substructure Time History Analysis using Solid Submodel #2 SRF for Dynamic Load Case #1

Path #	Solid (psi)	Shell (psi)	SRF
1	6,468	9,468	0.68
2	2,608		0.28
3	1,699		0.18
4	6,468		0.68
5	2,608		0.28
6	1,699		0.18
7	6,411		0.68
8	1,179		0.12
9	1,585		0.17
10	1,585		0.17
11	1,179		0.12
12	822		0.09
13	919		0.10
14	3,770		0.40
15	802		0.08
16	598		0.06
		Maximum =	**0.68**

6.4.5 *Submodel Analysis Using Submodel #2*

Matching Stress Profile

The stress profile matching is performed along the weld line connecting the vertical plate to the horizontal plate. The matching is accomplished by imposing vertical displacements along the Edge C (see Figure 3-3) of the submodel. Fixed boundary condition is applied to the top and bottom edges. The applied displacements and the comparison of the stress profiles are shown in the following Figure 6-13 and Figure 6-14, respectively.

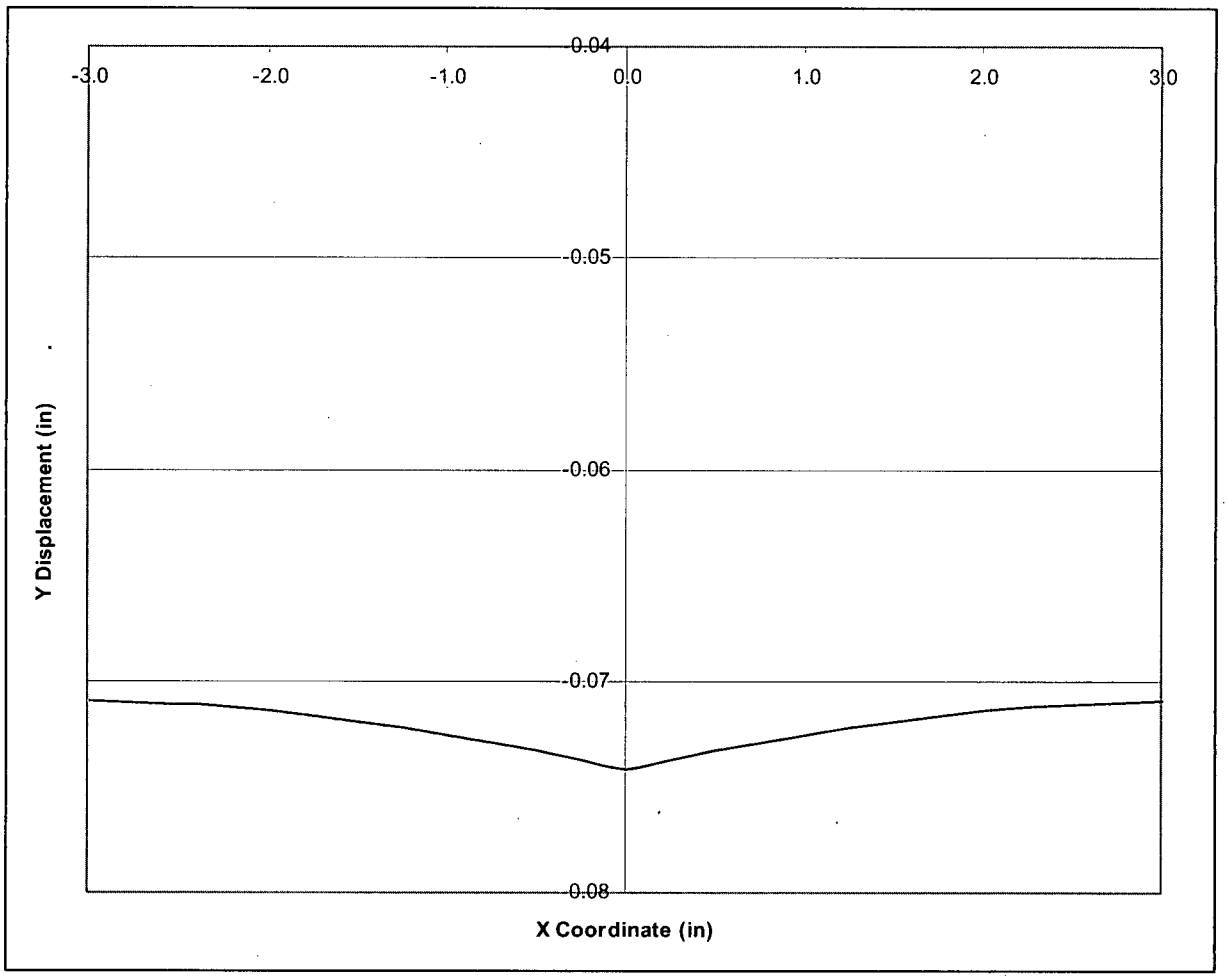

Figure 6-13
Submodel Analysis using Submodel #2
Applied Displacements for Load Case #1

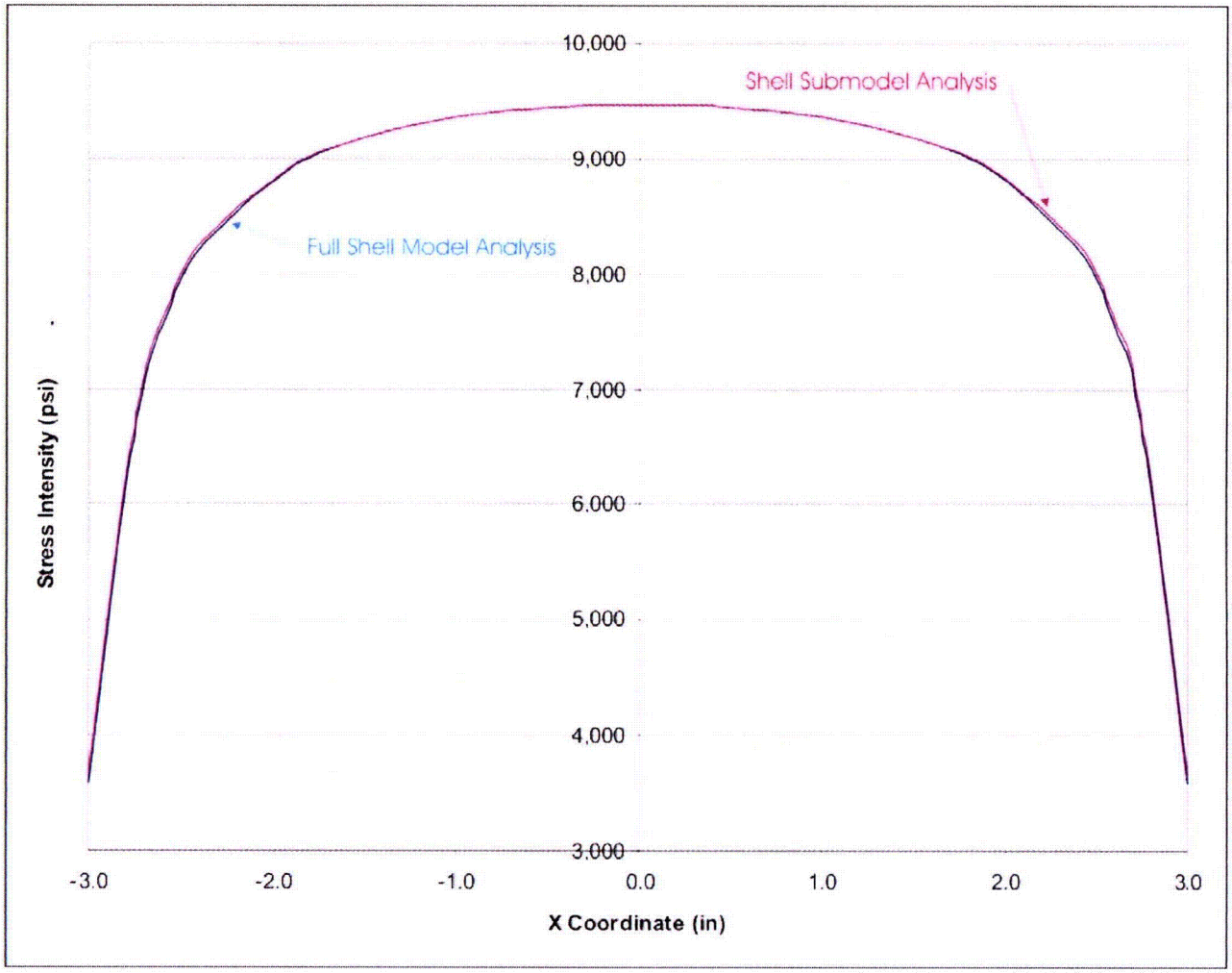

Figure 6-14
Submodel Analysis using Submodel #2
Stress Profile Comparison for Load Case #1

Stress Plot

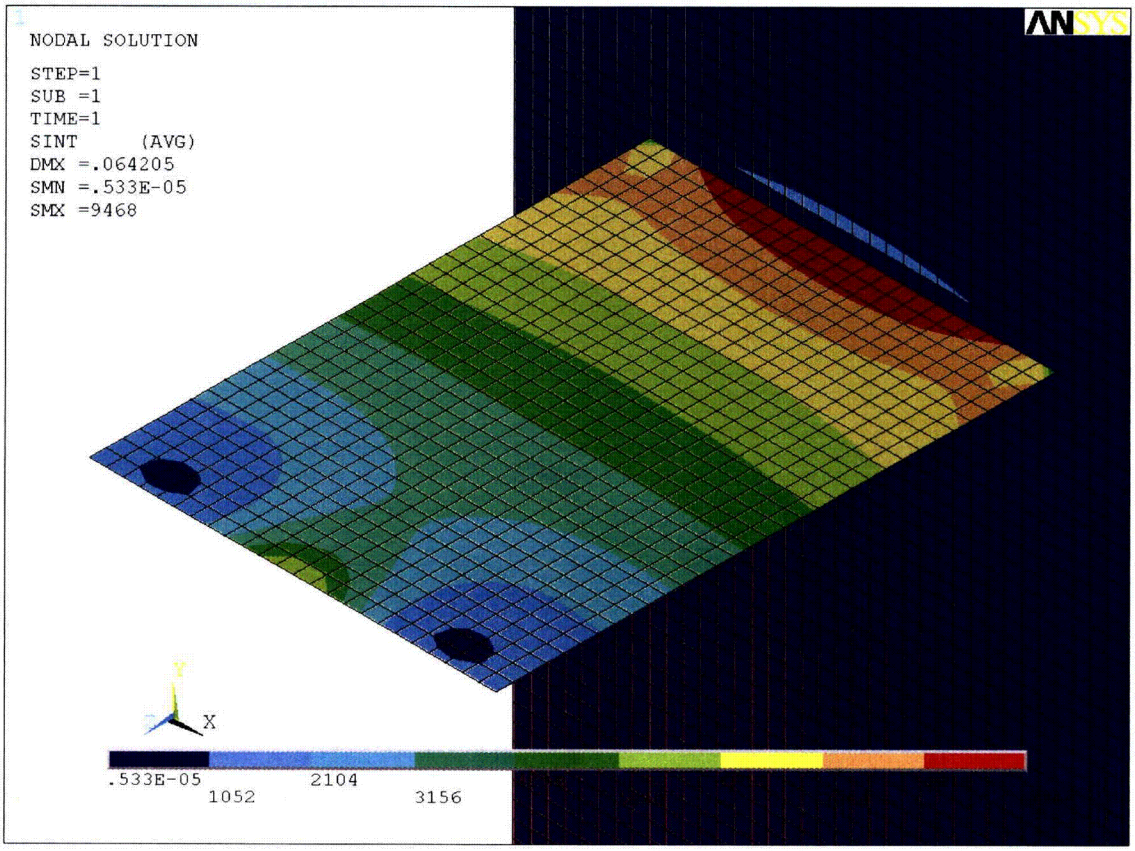

Figure 6-15
Submodel Analysis using Submodel #2
Shell Model Maximum Stress Intensity Plot for Load Case #1

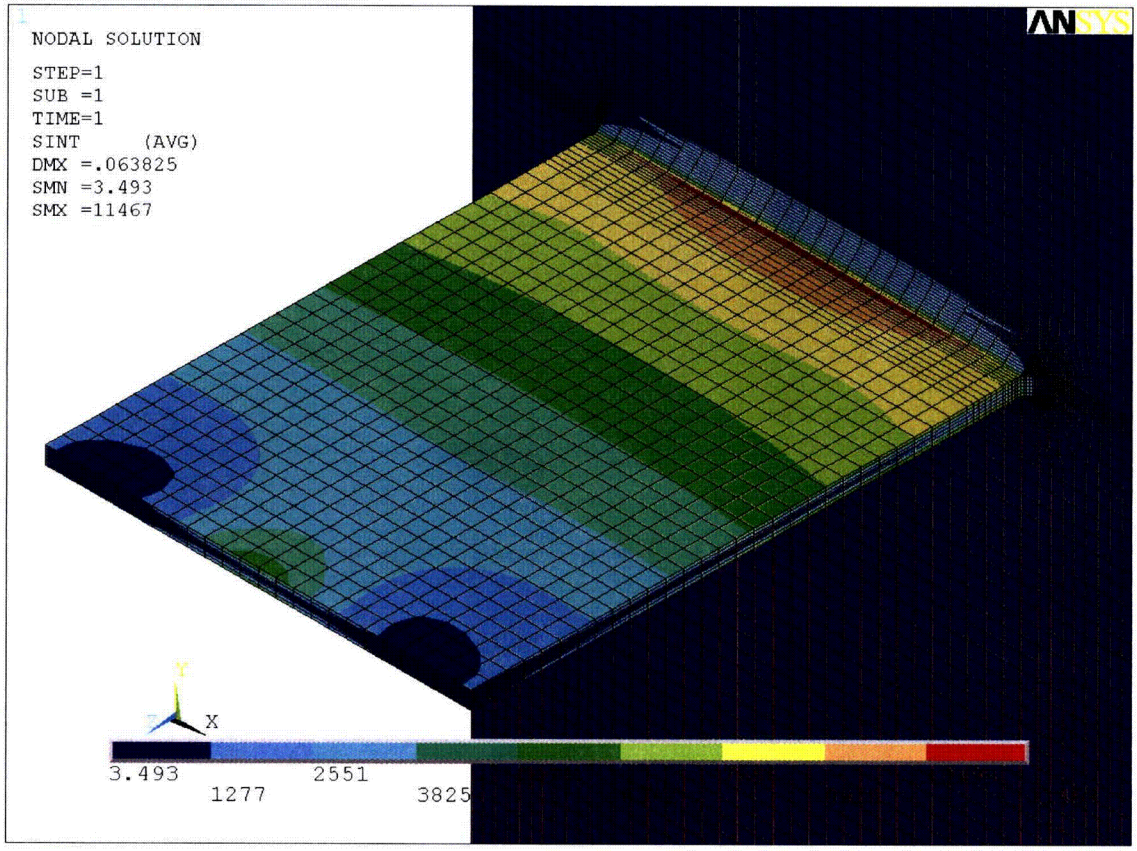

Figure 6-16
Submodel Analysis using Submodel #2
Solid Model Maximum Stress Intensity Plot for Load Case #1

SRF Table

Table 6-7
Submodel Analysis (Submodel #2) SRF
for Dynamic Load Case #1

Path #	Solid (psi)	Shell (psi)	SRF
1	6,229	9,468	0.66
2	2,512		0.27
3	1,635		0.17
4	6,229		0.66
5	2,512		0.27
6	1,635		0.17
7	6,172		0.65
8	1,128		0.12
9	1,525		0.16
10	1,525		0.16
11	1,128		0.12
12	784		0.08
13	876		0.09
14	3,611		0.38
15	765		0.08
16	589		0.06
		Maximum =	**0.66**

6.5 Dynamic Load Case #2

6.5.1 Full Shell Finite Element Time History Analysis

Transient Displacement Plot

The maximum horizontal displacement in the applied load Z direction occurs at the edge node of the load application line. The following Figure 6-17 shows a plot of the nodal transient displacements.

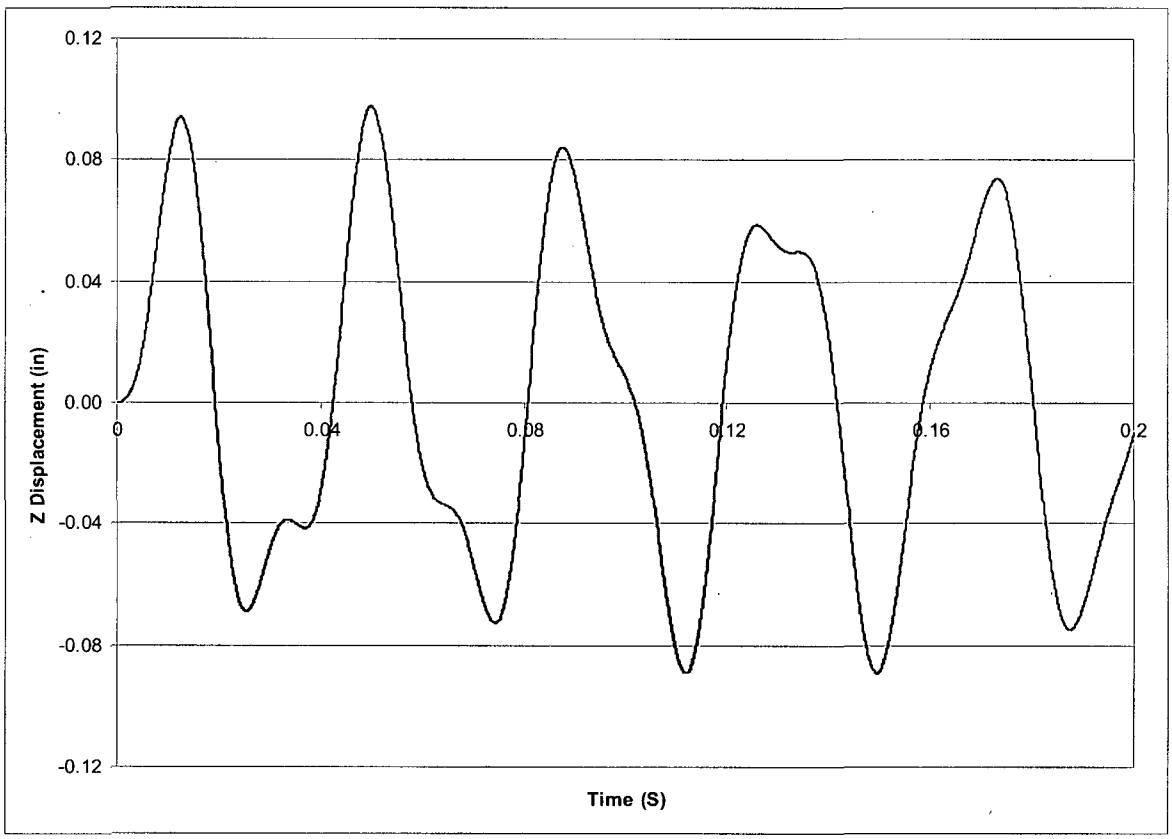

Figure 6-17
Full Shell Model Time History Analysis
Horizontal Transient Displacement for Load Case #2

Transient Stress Intensity Plot

The maximum stress intensity occurs at the one of the weld line nodes. The following Figure 6-18 shows a plot of the nodal transient stress intensities. The maximum stress intensity is 10,328 psi, which occurs at 0.049857 seconds time step.

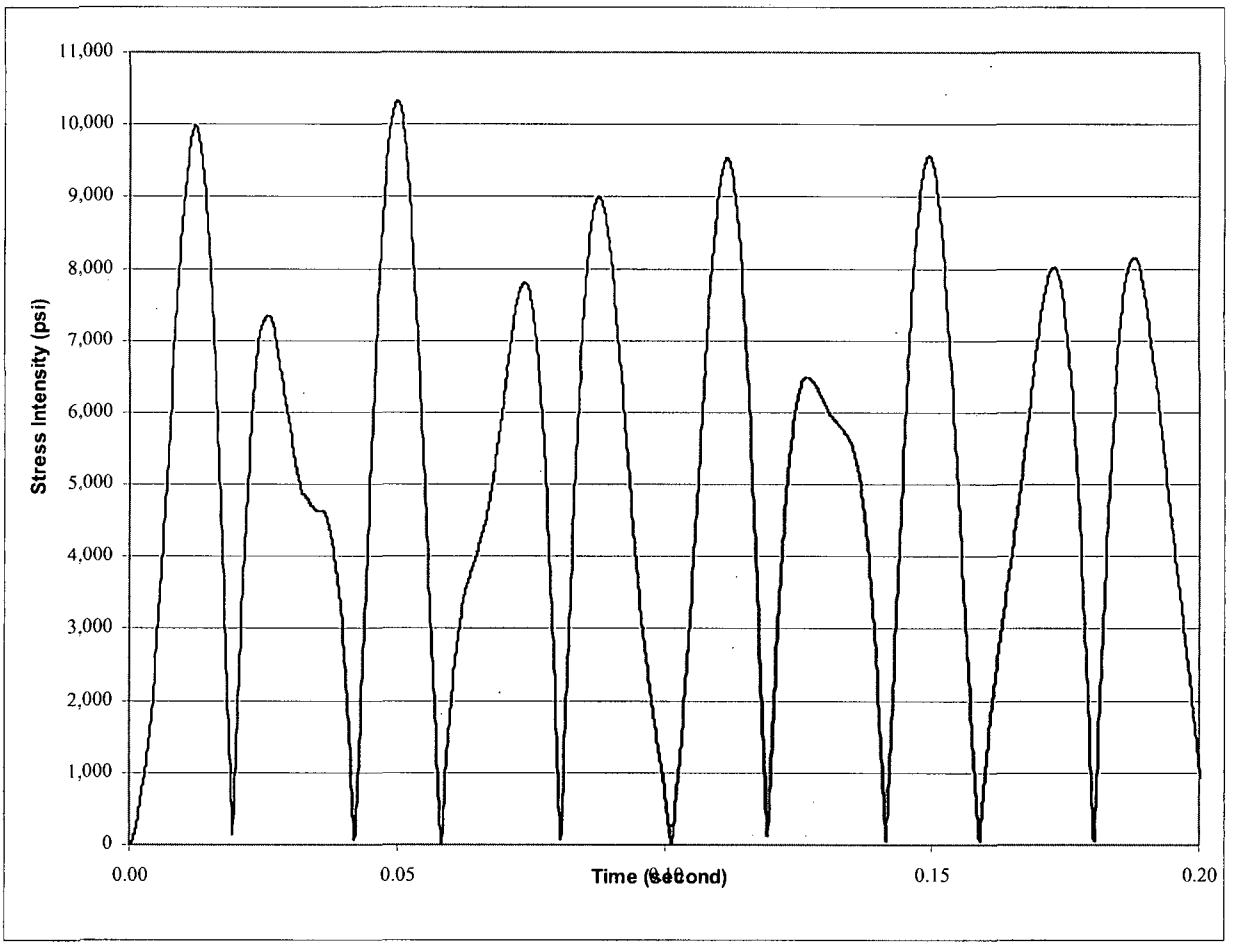

Figure 6-18
Full Shell Model Time History Analysis
Nodal Stress Intensity for Load Case #2

Horizontal Displacement Plot

The following Figure 6-19 shows the horizontal Z displacements at 0.049857 seconds time step, when the maximum stress intensity occurs.

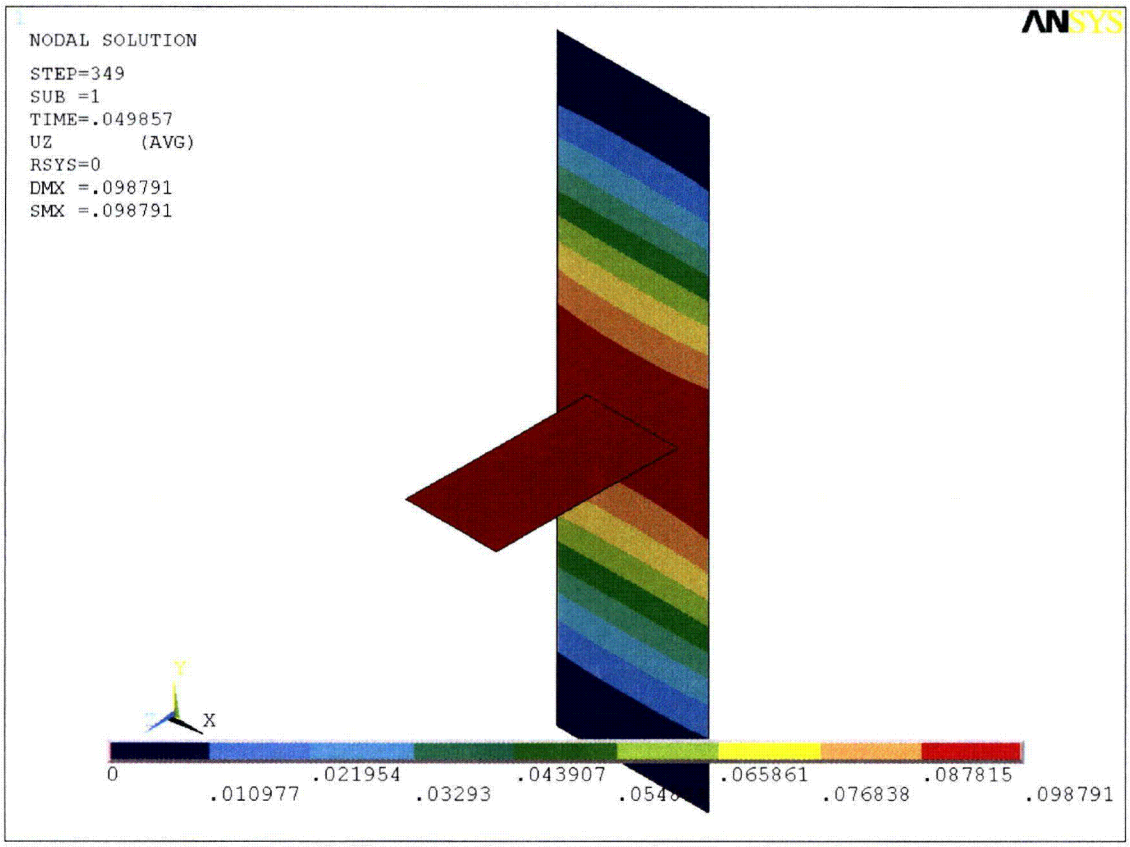

Figure 6-19
Full Shell Model Time History Analysis
Horizontal Displacement Plot for Load Case #2
(Full Shell Model Baseline Analysis)

Maximum Stress Plot

The maximum stress intensity is 10,328 psi, which occurs at 0.049857 seconds time step. The stress plot at that time step is provided in the following Figure 6-20. This analysis is the full shell model baseline analysis, and the maximum stress intensity of 10,328 psi is used to determine the SRF in other analyses.

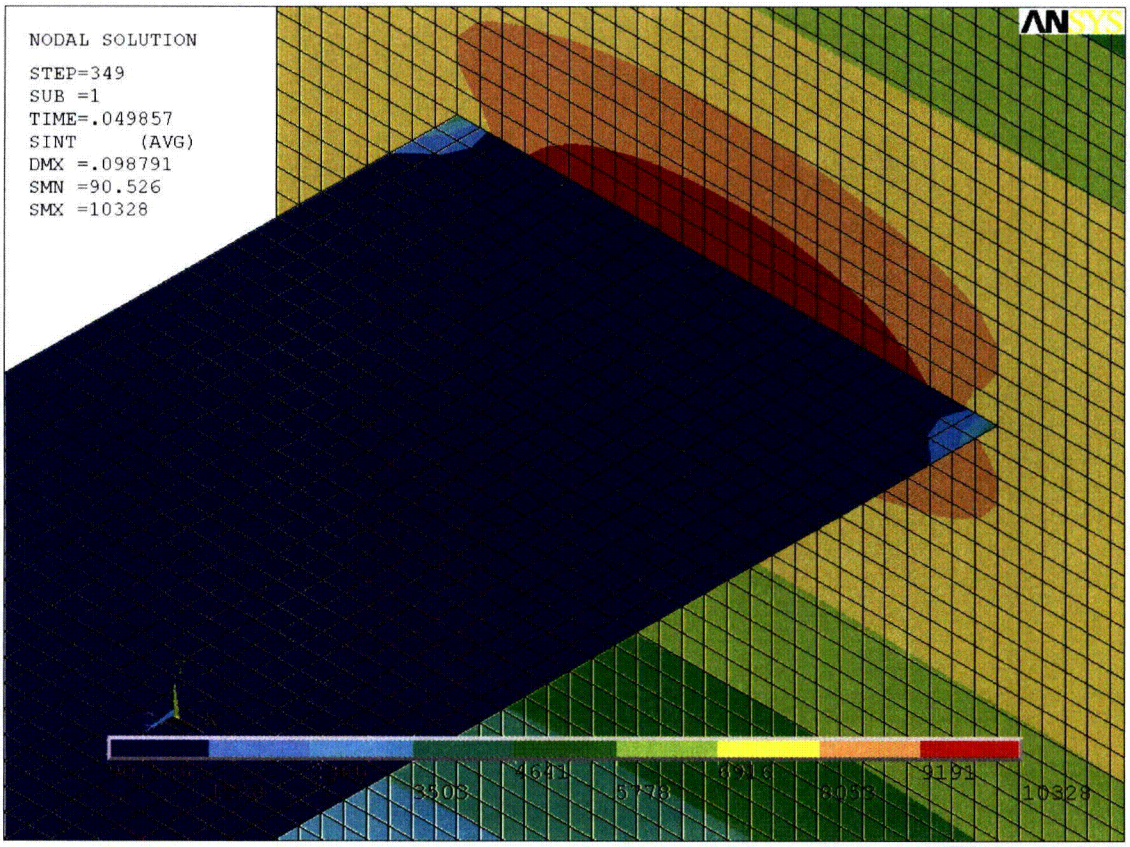

Figure 6-20
Full Shell Model Time History Analysis
Maximum Stress Intensity Plot for Load Case #2
(Full Shell Model Baseline Analysis)

6.5.2 *Full Solid Finite Element Time History Analysis*

By symmetry, only half of the solid model is used in the time history analysis. Symmetric boundary conditions are imposed at the plane of half symmetry. Using half the solid model saves significant execution time without compromising accuracy.

Transient Displacement Plot

The maximum horizontal displacement occurs at the nodes along the load application line. The following Figure 6-21 shows a plot of the nodal transient displacements for both the shell and solid models.

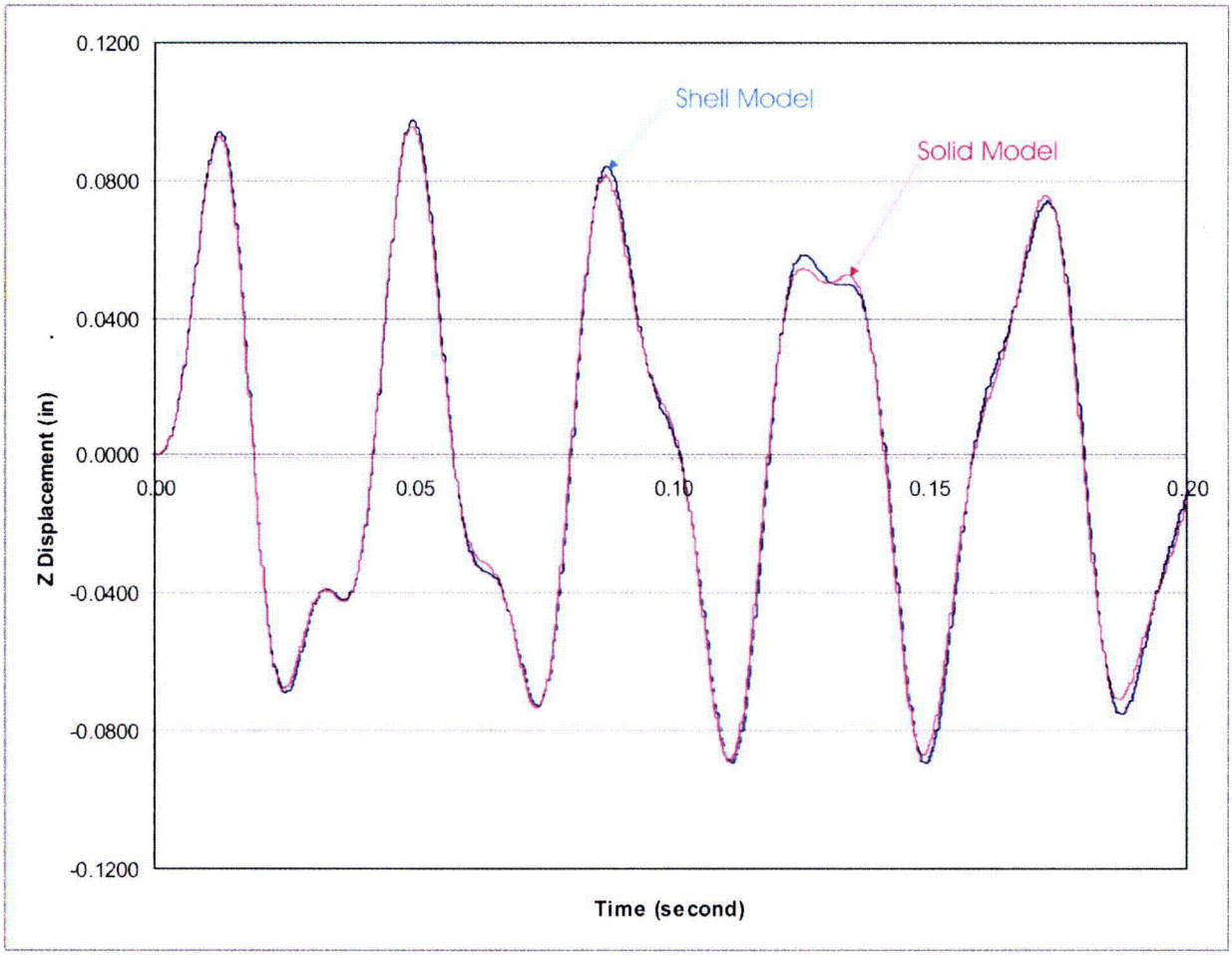

Figure 6-21
Shell and Solid Model Time History Analysis
Horizontal Transient Displacement for Load Case #2

Transient Stress Intensity Plot

The maximum stress intensity occurs at one of the weld line nodes. The following Figure 6-22 shows a plot of the transient stress intensities for both the shell and solid models.

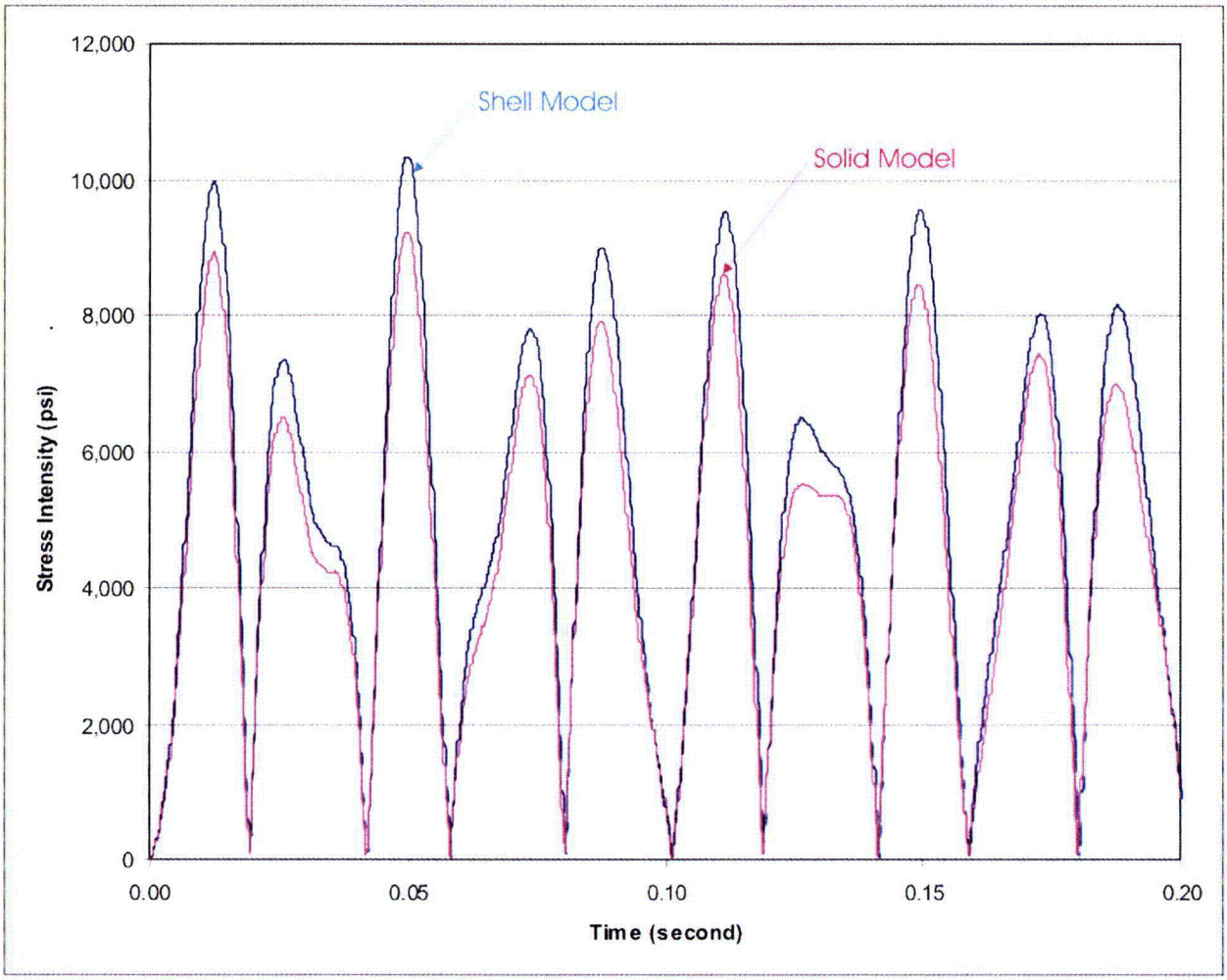

Figure 6-22
Shell and Solid Model Time History Analysis
Stress Intensity for Load Case #2

Note that the shell model stress intensity corresponds to the maximum nodal stress intensity while the solid model stress intensity corresponds to the maximum linearized stress intensity.

Horizontal Displacement Plot

The following Figure 6-23 shows the Z-horizontal displacements at 0.049714 seconds time step, when the maximum stress intensity occurs.

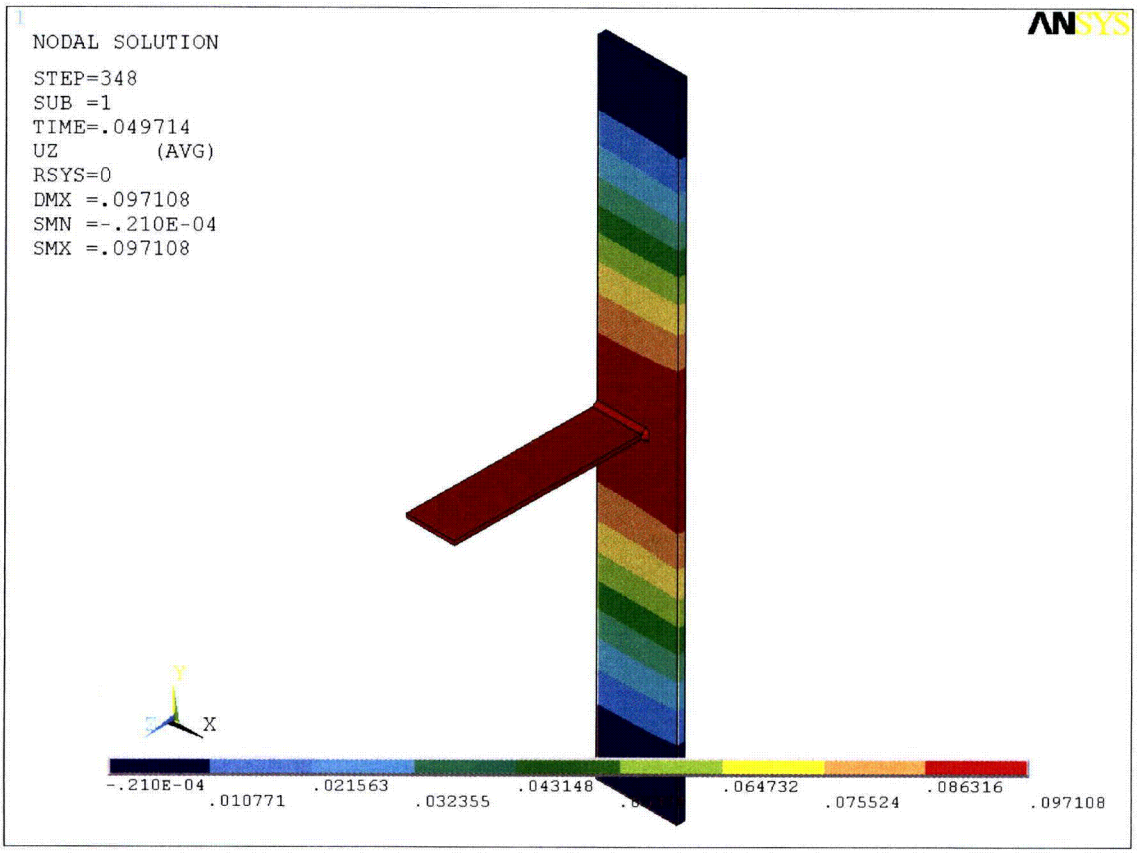

Figure 6-23
Full Solid Model Time History Analysis
Horizontal Displacement Plot for Load Case #2
(Full Solid Model Baseline Analysis)

Maximum Stress Plot

The maximum linearized stress intensity is 9,219 psi (see Section6.5.1). This occurs at 0.049714 seconds time step. The non-linearized stress intensity plot at that time step is provided in the following Figure 6-24.

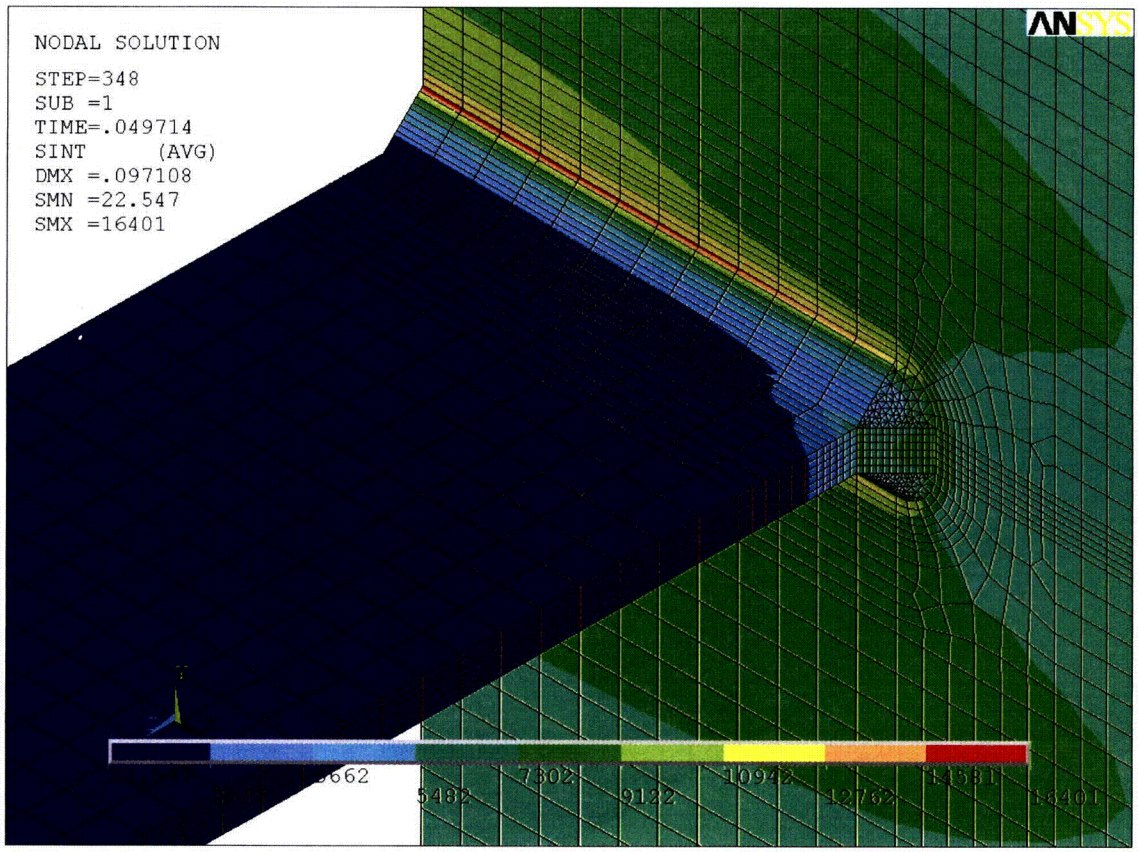

Figure 6-24
Full Solid Model Time History Analysis
Maximum Stress Intensity Plot for Load Case #2
(Full Solid Model Baseline Analysis)

SRF Table

Table 6-8
Full Solid Model Time History Analysis SRF
for Dynamic Load Case #2

Path #	Solid (psi)	Shell (psi)	SRF
1	5,920	10,328	0.57
2	5,964		0.58
3	8,976		0.87
4	5,920		0.57
5	5,964		0.58
6	8,976		0.87
7	5,765		0.56
8	9,219		0.89
9	7,421		0.72
10	7,421		0.72
11	9,219		0.89
12	7,928		0.77
13	7,450		0.72
14	5,955		0.58
15	6,005		0.58
16	8,089		0.78
		Maximum =	**0.89**

6.5.3 Substructure Time History Analysis Using Shell Submodel #2

With reference to Figure 3-5, the displacements along Edges A and C computed in the full shell finite element time history analysis, at each of the 1,400 time steps, (Section 6.5.1) are applied onto this shell submodel #2 in a time history analysis. The time history stress intensities calculated in this analysis are plotted and compared with the results of the full shell time history analysis.

Transient Stress Intensity Plot

The maximum stress intensity occurs at one of the weld line nodes. The following Figure 6-25 shows a plot of the nodal transient stress intensities.

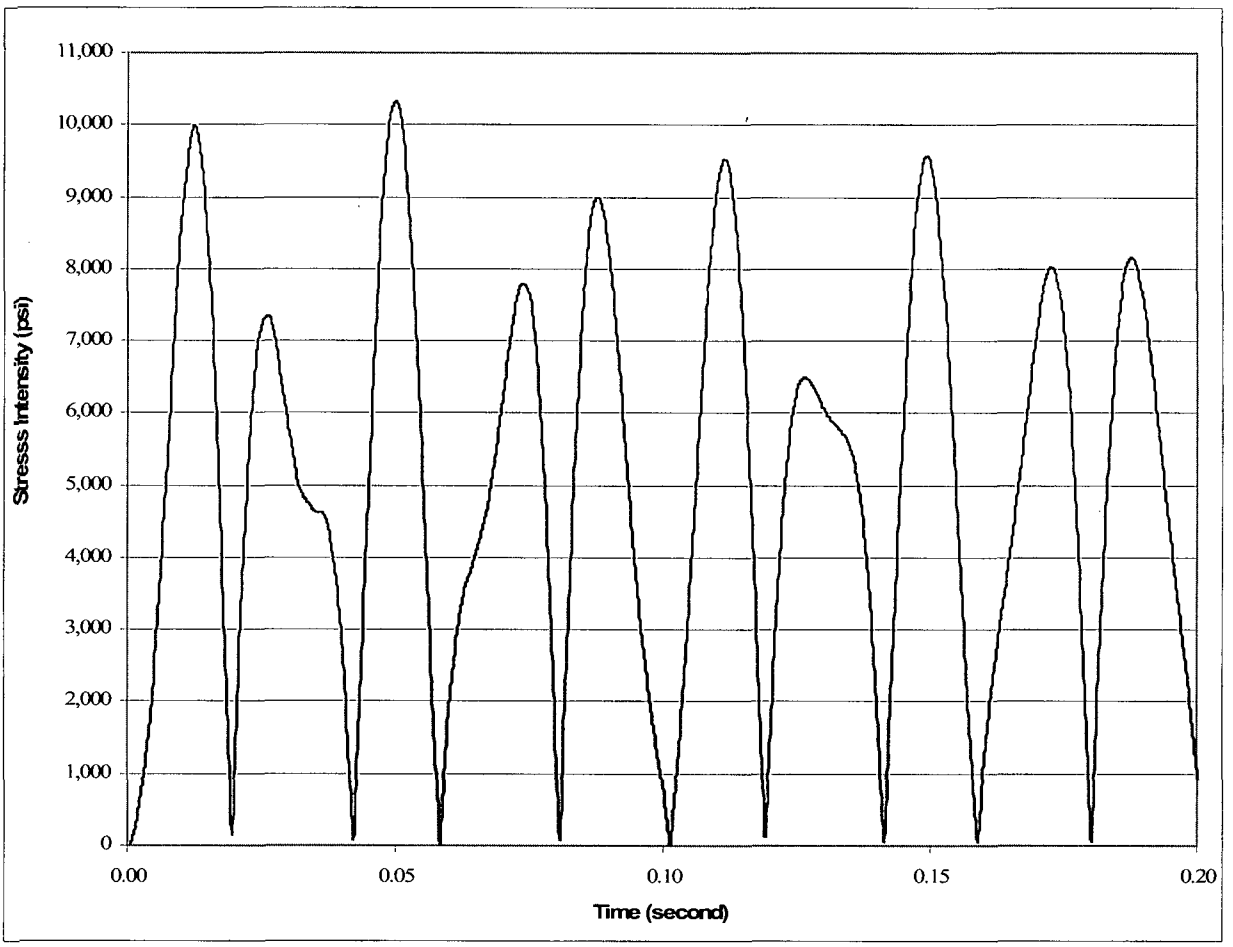

Figure 6-25
Substructure Time History Analysis using Shell Submodel #2
Nodal Stress Intensity for Load Case #2

Vertical Displacement Plot

The following Figure 6-26 shows the vertical displacements at 0.049857 seconds time step, when the maximum stress intensity occurs.

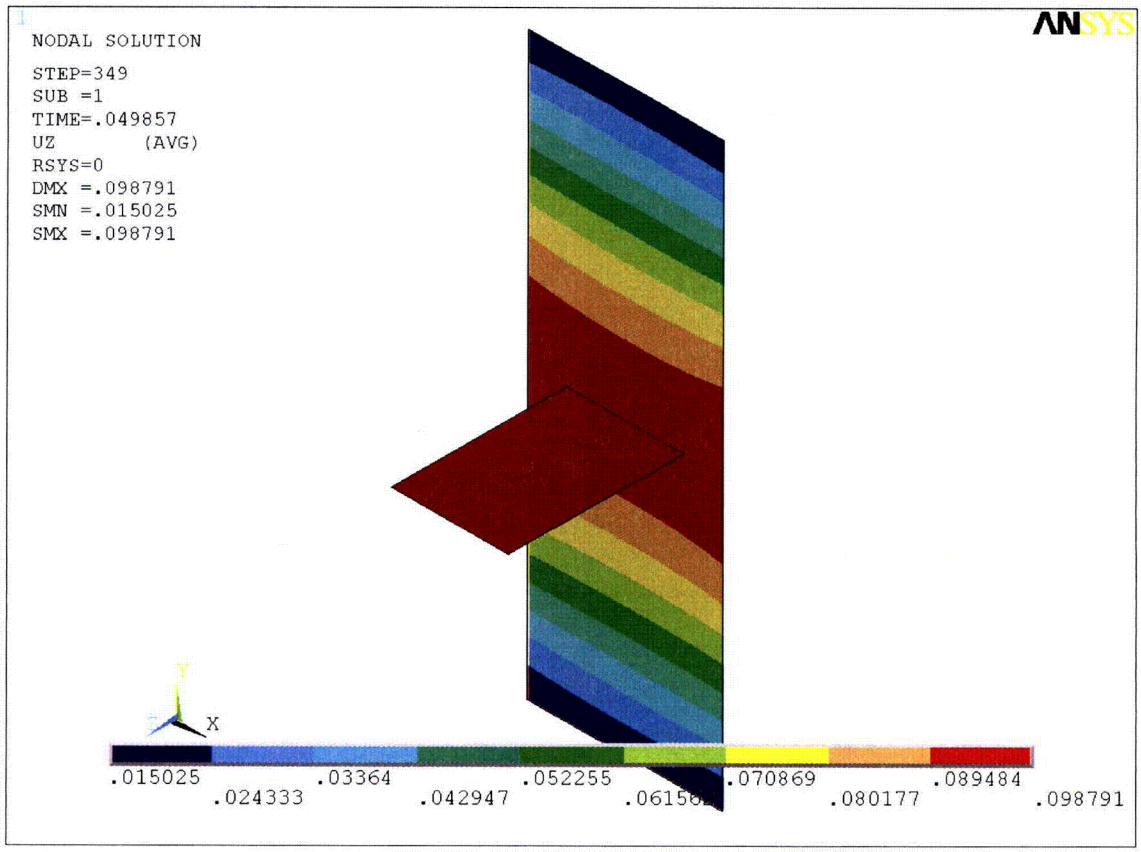

Figure 6-26
Substructure Time History Analysis using Shell Submodel #2
Horizontal Displacement Plot for Load Case #2

Maximum Stress Plot

The maximum stress intensity is 10,328 psi, which occurs at 0.049857 seconds time step. The stress plot at that time step is provided in the following Figure 6-27.

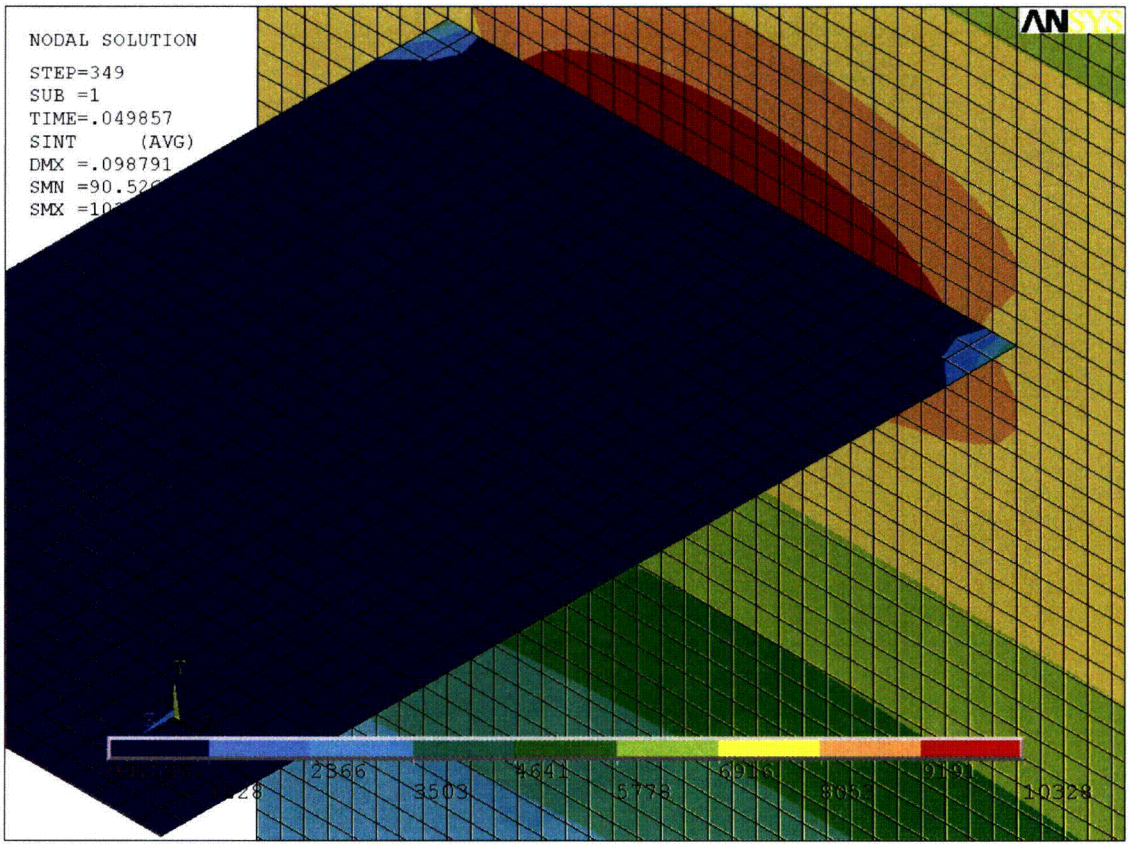

Figure 6-27
Substructure Time History Analysis using Shell Submodel #2
Maximum Stress Intensity Plot for Load Case #2

Comparison

The stress intensity plots shown in Figure 6-20 and Figure 6-27 show that the shapes of the plots are the same. The maximum stress intensities for both analyses are 10,328 psi, and they both occur at the time step of 0.049857 seconds. The comparisons show that the substructure time history analysis using shell submodel produces the same results as the full shell time history analysis.

6.5.4 Substructure Time History Analysis Using Solid Submodel #2

With reference to Figure 3-5, the displacements along Edges A and C computed in the full shell finite element time history analysis, at each of the 1,400 time steps, (Section 6.5.1) are applied onto this solid submodel #2 in a time history analysis.

By symmetry, only half of the solid submodel #2 is used in the time history analysis. Using half the solid model saves significant execution time without compromising accuracy.

Stress Plot

The maximum non-linearized stress intensity is 16,787 psi, and the stress plot is provided in the following Figure 6-28.

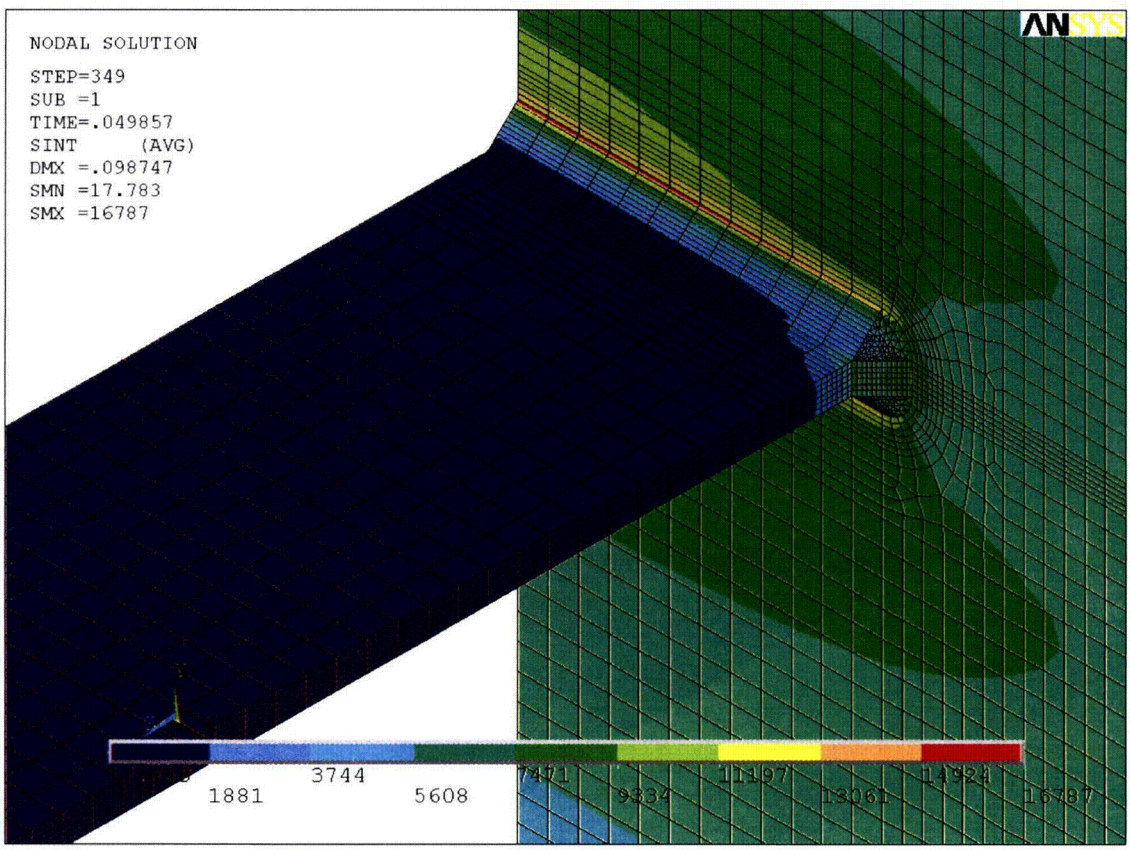

Figure 6-28
Substructure Time History Analysis using Solid Submodel #2
Maximum Stress Intensity Plot for Load Case #2

SRF Table

Table 6-9
Substructure Time History Analysis using Solid Submodel #2 SRF for Dynamic Load Case #2

Path #	Solid (psi)	Shell (psi)	SRF
1	6,058	10,328	0.59
2	6,104		0.59
3	9,188		0.89
4	6,058		0.59
5	6,104		0.59
6	9,188		0.89
7	5,864		0.57
8	9,429		0.91
9	7,589		0.73
10	7,589		0.73
11	9,429		0.91
12	8,100		0.78
13	7,606		0.74
14	6,089		0.59
15	6,142		0.59
16	8,267		0.80
		Maximum =	**0.91**

6.5.5 *Submodel Analysis Using Submodel #2*

Matching Stress Profile

The stress profile matching is performed along the weld line connecting the vertical plate to the horizontal plate. The matching is accomplished by imposing horizontal forces along the Edge B (see Figure 3-3) of the submodel. The nodes at the top and bottom edges (i.e. Edge A) are fuuly restrained. The applied loads and the comparison of the stress profiles are shown in the following Figure 6-29 and Figure 6-30, respectively.

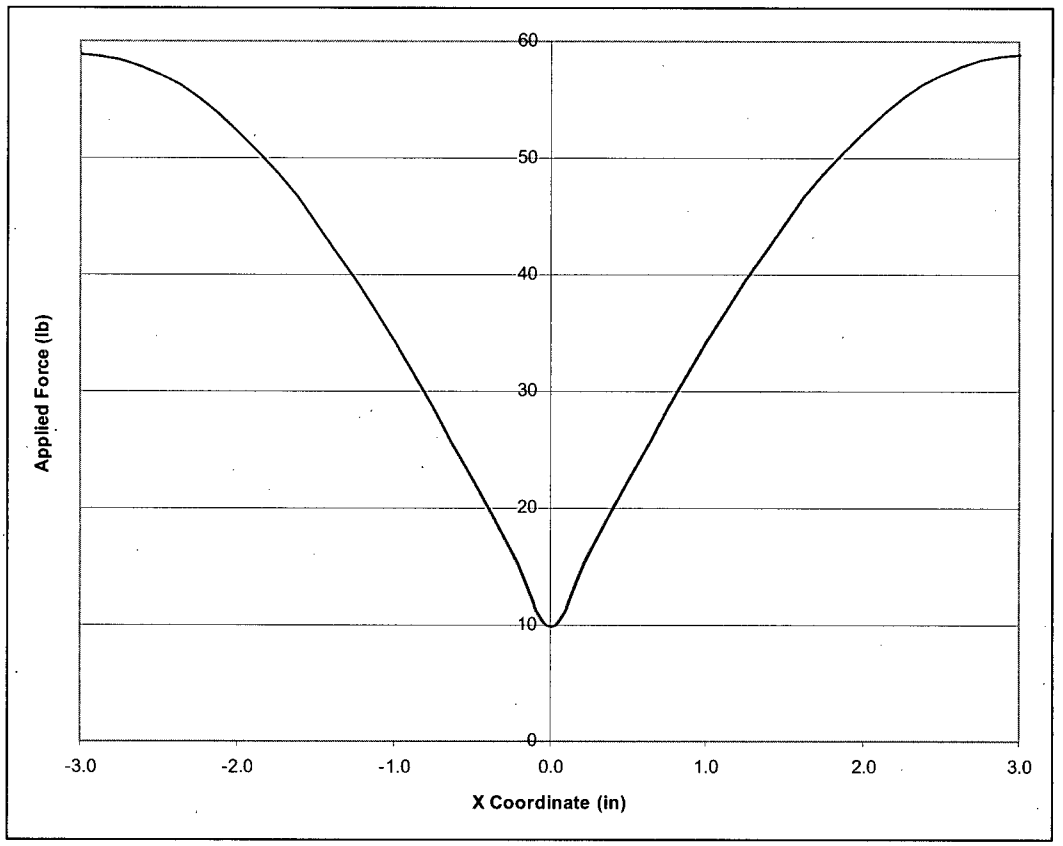

Figure 6-29
Submodel Analysis using Submodel #2
Applied Horizontal Loads for Load Case #2

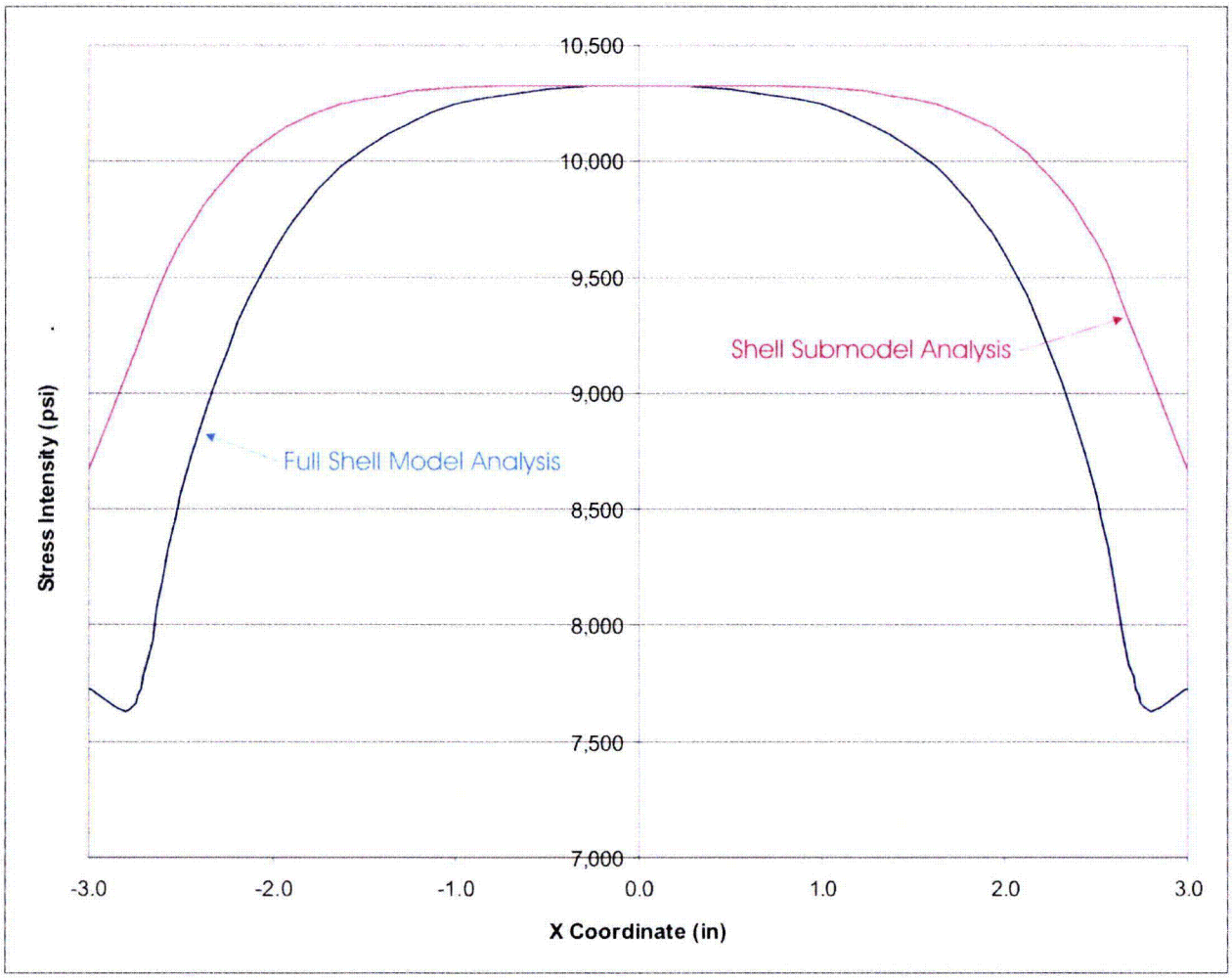

Figure 6-30
Submodel Analysis using Submodel #2
Stress Profile Comparison for Load Case #2

Stress Plot

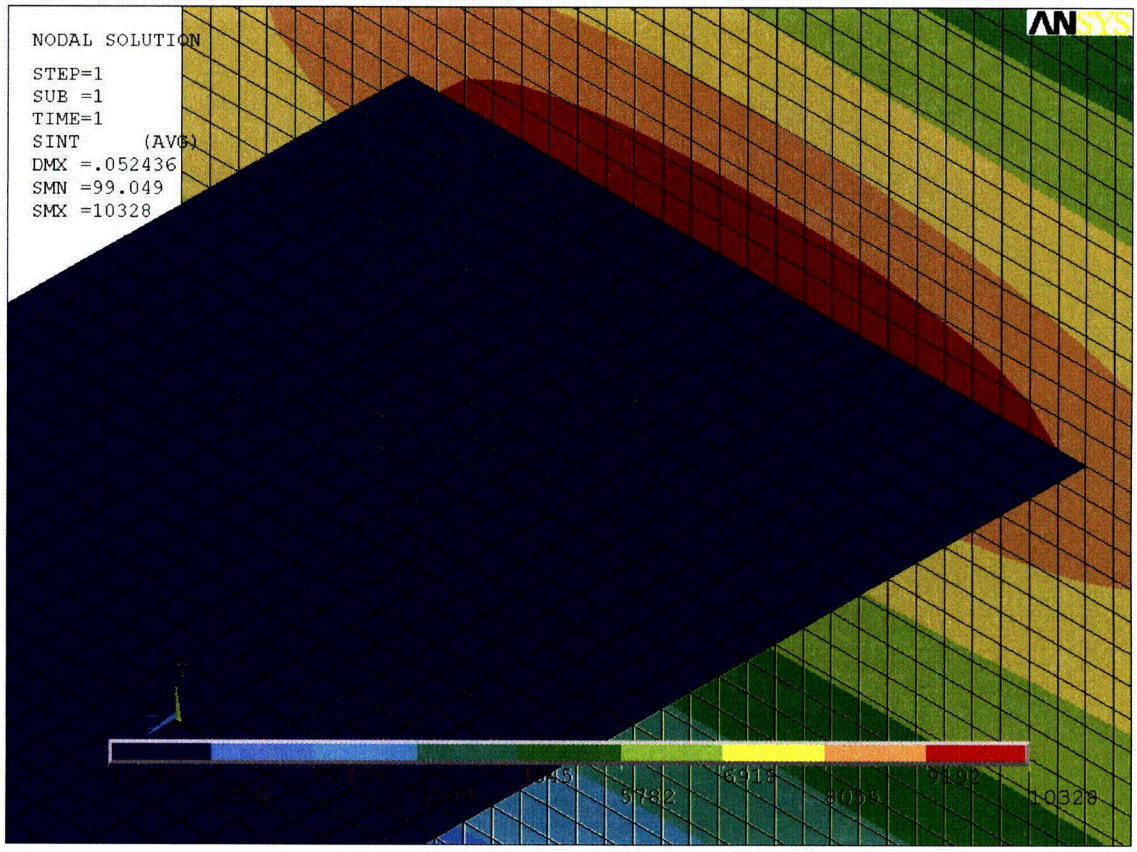

Figure 6-31
Submodel Analysis using Submodel #2
Shell Model Maximum Stress Intensity Plot for Load Case #2

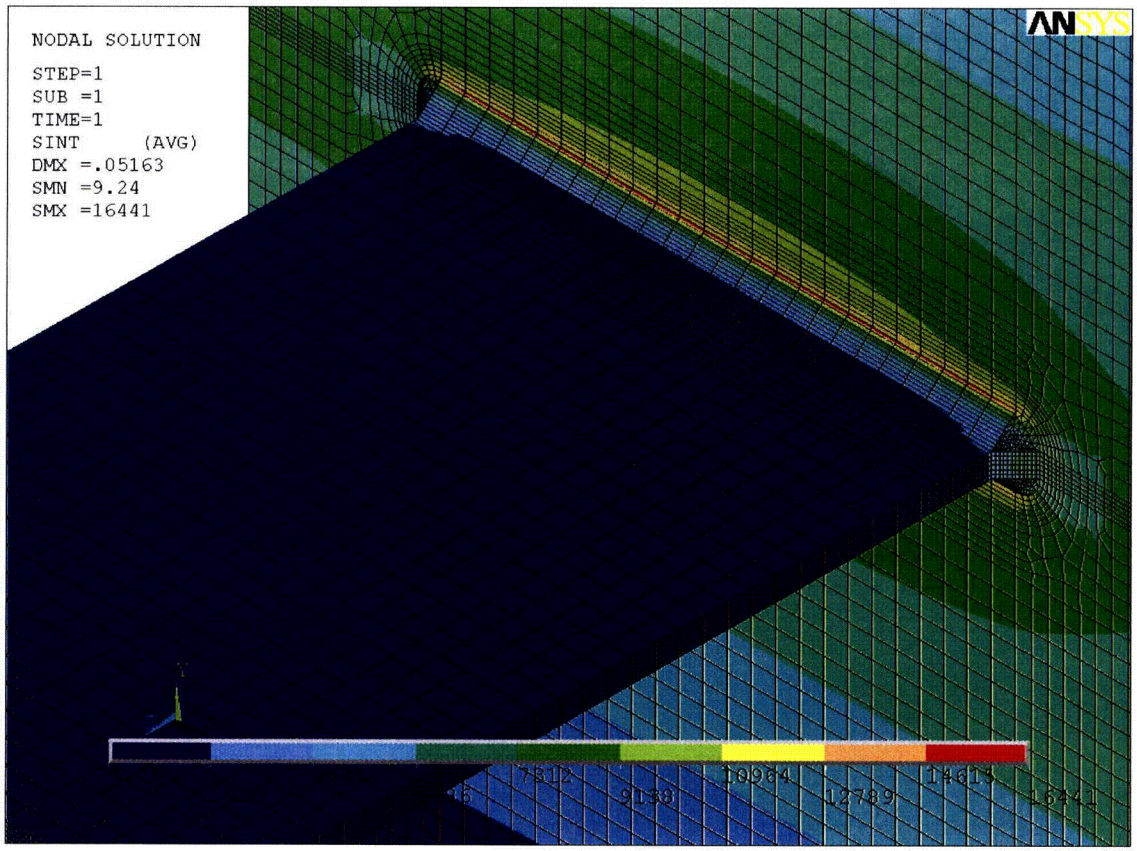

Figure 6-32
Submodel Analysis using Submodel #2
Solid Model Maximum Stress Intensity Plot for Load Case #2

SRF Table

Table 6-10
Submodel Analysis (Submodel #2) SRF
for Dynamic Load Case #2

Path #	Solid (psi)	Shell (psi)	SRF
1	5,898	10,328	0.57
2	5,944		0.58
3	9,012		0.87
4	5,898		0.57
5	5,944		0.58
6	9,012		0.87
7	2,771		0.27
8	9,191		0.89
9	7,413		0.72
10	7,413		0.72
11	9,191		0.89
12	8,611		0.83
13	5,821		0.56
14	5,505		0.53
15	5,667		0.55
16	8,078		0.78
		Maximum =	**0.89**

7.0 SUMMARY STRESS REDUCTION FACTORS

7.1 Static Analysis SRF

Static Load Case #1

Table 7-1
Summary SRF for Static Load Case #1

Analysis Approach	SRF
Full Solid Model Baseline Analysis	0.59
Substructure Analysis (Submodel #1)	0.74
Substructure Analysis (Submodel #2)	0.69
Submodel Analysis (Submodel #1)	0.68
Submodel Analysis (Submodel #2)	0.66

Static Load Case #2

Table 7-2
Summary SRF for Static Load Case #2

Analysis Approach	SRF
Full Solid Model Baseline Analysis	0.89
Substructure Analysis (Submodel #1)	0.92
Substructure Analysis (Submodel #2)	0.91
Submodel Analysis (Submodel #1)	0.89
Submodel Analysis (Submodel #2)	0.89

7.2 Dynamic Analysis SRF

Dynamic Load Case #1

Table 7-3
Summary SRF for Dynamic Load Case #1

Analysis Approach	SRF
Full Solid Model Baseline Time History Analysis	0.59
Substructure Time History Analysis (Submodel #2)	0.68
Submodel (Static) Analysis (Submodel #2)	0.66

Dynamic Load Case #2

Table 7-4
Summary SRF for Dynamic Load Case #2

Analysis Approach	SRF
Full Solid Model Baseline Time History Analysis	0.89
Substructure Time History Analysis (Submodel #2)	0.91
Submodel (Static) Analysis (Submodel #2)	0.89

8.0 DISCUSSIONS

The comparisons of the SRF and the different analyses lead to the following observations and deductions.

8.1 Static Analysis

Full Solid Model Baseline Analysis

The full solid model includes the detailed weld configuration, and this full solid model analysis provides the most accurate stress results, since this analysis does not include any inherent assumption or approximation associated with substructure or submodel analysis techniques. The resulting SRFs computed using this analysis provide an accurate baseline from which to determine the accuracy and conservatism of the submodel and substructure techniques.

Substructure Analysis Using Shell Submodels

The substructure analyses using the shell submodels show that the results are the same as the full shell model. The maximum stress intensities from both the shell submodel and the full shell model analyses are the same. The stress plots of both the submodel and full model analyses also show that the stress patterns are the same.

Substructure Analysis Using Solid Submodels

The substructure analysis using the solid submodel predicts higher SRF than the SRF computed in the full solid model baseline analysis (see Table 7-1 and Table 7-2). The reason that they are different is because the shell model is more flexible than the solid model, which models in the detailed weld configuration.

The local region of the solid model that models in the weld configuration becomes stiffer than the corresponding region in the shell model. When the displacements from the more flexible shell model analysis are applied onto the more rigid solid submodel, higher stresses are computed for the solid submodel.

To better predict the local stresses using the substructure analysis, the boundaries of the submodel need to be extended to a reasonable distance. This is evident when the submodel #1 and submodel #2 substructure analysis results are compared. When the boundaries are extended from submodel #1 to submodel #2, the SRF is lowered (see Table 7-1 and Table 7-2).

Submodel Analysis

The study shows that when the matching of the stress intensity profile along the high stress weld line is achieved, the submodel analysis is a reasonable approach for calculating the SRF. For Load Cases #1 and #2, the submodel analyses have computed SRFs that are conservative relative to the baseline full model and in good agreement with both the full model and the substructure analysis SRFs.

The SRFs computed using submodels #1 and #2 are very similar. This similarity in SRFs demonstrate that after satisfactory stress intensity profile matching, the computation of SRFs is not sensitive to the size of the submodel.

8.2 Dynamic Analysis

Full Solid Model Baseline Analysis

Similar to the static analysis, the full solid model includes the detailed weld configuration, and this full solid model analysis provides the most accurate stress results, since this analysis does not include any inherent assumption or approximation associated with substructure or submodel analysis techniques. The resulting SRFs computed using this analysis provide an accurate baseline from which to determine the accuracy and conservatism of the submodel and substructure techniques.

Substructure Analysis Using Shell Submodels

Similar to the static analysis, the substructure analysis using the shell submodel shows that the results are the same as the full shell model. The maximum stress intensities from both the shell submodel and the full shell model analyses are the same. The stress plots of both the submodel and full model analyses also show that the stress patterns are the same.

Substructure Analysis Using Solid Submodels

Similar to the static analysis, the substructure analysis using the solid submodel predicts higher SRF than the SRF computed in the full solid model baseline analysis (see Table 7-3 and Table 7-4). The reason that they are different is because the shell model is more flexible than the solid model, which models in the detailed weld configuration.

The local region of the solid model that models in the weld configuration becomes stiffer than the corresponding region in the shell model. When the displacements from the more flexible shell model analysis are applied onto the more rigid solid submodel, higher stresses are computed for the solid submodel.

Submodel Analysis

Consistent with the static analysis finding, the study shows that when the matching of the stress intensity profile along the high stress weld line is achieved, the submodel analysis is a reasonable approach for calculating the SRF. For Load Cases #1 and #2, the submodel analyses have computed SRFs that are conservative relative to the baseline full model and in good agreement with both the full model and the substructure analysis SRFs.

8.3 Submodeling Validity

Both the static and dynamic analyses show that the submodel analysis is a reasonable approach for establishing the SRF. Similar result trend has been observed for both the static and the dynamic analyses.

When the SRF computed using the submodeling analysis approach is compared with the SRF computed using the solid model, which is considered to be the most accurate baseline analysis, good agreement has been established for both the static and the dynamic analyses. The submodel SRF is either slightly more conservative or in exact agreement (up to 2 decimal places) with the solid model SRF (see Table 7-1 through Table 7-4).

Furthermore, the submodel approach SRF results are essentially identical for both static and dynamic analysis cases. This result substantiates that the submodel analysis technique does not ignore any inertial or body force loads. This is because the effect of these loads at the weld line is included in the full model stress that is matched in the shell submodel.

Based on these findings, it is reasonable to conclude that the SRFs computed using submodel analysis are valid and acceptable.

9.0 CONCLUSIONS

The comparison study documented in this calculation fully addresses the issues identified in the RAI 199/156 from NRC (Reference 3). In addition, this calculation also addresses the issues pertaining to the submodel analysis identified in the Draft RAI 201/162 from NRC (Reference 7).

Two Load Cases have been considered in this calculation:

Load Case #1

This load case examines the scenario where the weld is subjected to mainly bending action. To match the stress profile, imposed displacements are used. This is similar to the submodel analysis approach used to determine the stresses at the bottom of the skirt/drain channel junction in the BFN steam dryer stress analysis..

Load Case #2

This load case examines the scenario where the weld is subjected to mainly membrane action. To match the stress profile, imposed loads are used. This is similar to the submodel analysis approach used to determine the stresses at the intersection between the bottom of the inner hood, stiffener and base plate in the BFN steam dryer stress analysis..

Two analysis options have been evaluated: the static analysis and the dynamic time history analysis. Together these analyses show that the SRFs computed using the TVA's submodel analysis approach are accurate and acceptable.

In conclusion, this comparison study validates the submodel analysis approach adopted for the BFN steam dryer stress analysis.

10.0 REFERENCES

1. Email with attachments from George Nelson (TVA) to Marcos Herrera (SI) on 04/22/08 at 9:02 am, "Steam Dryer - Drain Channel," SI File No. BFN-15-224.
2. Email with attachment from Rick Cutsinger (TVA) to Soo Bee Kok (SI) on May 20, 2008 at 9:02 am, "RE: Weld Structure Evaluation," SI File No. BFN-15-227P.
3. Email with attachments from Denzel Housley (TVA) to Soo Bee Kok (SI) on 10/29/08 at 7:31 am, "RE: Editorial Changes to EMCB.199.156 R2", SI File No. BFN-15-229.
4. ANSYS Mechanical, Release 11.0 (w/ Service Pack 1), ANSYS, Inc., August 2007.
5. SI Calculation No. 0006982.302, Revision 0, "Project Specific Software Verification and Validation of ANSYS Release 11.0 (w/ Service Pack 1)".
6. Email with from Rick Cutsinger (TVA) to Soo Bee Kok (SI) on October 30, 2008 at 12:49 pm, "Re: SRF Calculation for RAI 199/156," SI File No. BFN-15-237.
7. Email with attachments from Ken Spates (TVA) to Soo Bee Kok (SI) on 12/08/08 at 6:06 am, "FW: REVISED DRAFT: BFN EPU Round 23 RAIs", SI File No. BFN-15-238.

Appendix A - Computer Files

General Application

Filename	Description
ShellFull.inp	Full shell finite element model development input file.
ShellSub1.inp	Shell submodel #1 finite element model development input file.
ShellSub2.inp	Shell submodel #2 finite element model development input file.
SolidFull.inp	Full solid finite element model development input file.
SolidSub1.inp	Solid submodel #1 finite element model development input file.
SolidSub2.inp	Solid submodel #2 finite element model development input file.
PPpath.mac	Stress path generation macro.

Static Load Case #1 Application

Filename	Description
T1E.inp	Full shell model baseline analysis for Load Case #1 input file.
C1E.inp	Substructure analysis using shell submodel #1 for Load Case #1 input file.
C2E.inp	Substructure analysis using shell submodel #2 for Load Case #1 input file.
T2E.inp	Substructure analysis using solid submodel #1 for Load Case #1 input file.
T2EPP.inp	Substructure analysis using solid submodel #1 for Load Case #1 post processing input file.
T2EPP.xls	Substructure analysis using solid submodel #1 for Load Case #1 SRF calculation spreadsheet.
T3E.inp	Substructure analysis using solid submodel #2 for Load Case #1 input file.
T3EPP.inp	Substructure analysis using solid submodel #2 for Load Case #1 post processing input file.
T3EPP.xls	Substructure analysis using solid submodel #2 for Load Case #1 SRF calculation spreadsheet.
T4E.inp	Full solid model baseline analysis for Load Case #1 input file.
T4EPP.inp	Full solid model baseline analysis for Load Case #1 post processing input file.
T4EPP.xls	Full solid model baseline analysis for Load Case #1 SRF calculation spreadsheet.
T5E.inp	Submodel stress intensity matching analysis using shell submodel #1 for Load Case #1 input file.
T6E.inp	Submodel analysis using solid submodel #1 for Load Case #1 input file.
T6EPP.inp	Submodel analysis using solid submodel #1 for Load Case #1 post processing input file.
T6EPP.xls	Submodel analysis using solid submodel #1 for Load Case #1 SRF calculation spreadsheet.
T7E.inp	Submodel stress intensity matching analysis using shell submodel #2 for Load Case #1 input file.
T8E.inp	Submodel analysis using solid submodel #2 for Load Case #1 input file.
T8EPP.inp	Submodel analysis using solid submodel #2 for Load Case #1 post processing input file.
T8EPP.xls	Submodel analysis using solid submodel #2 for Load Case #1 SRF calculation spreadsheet.

Static Load Case #2 Application

Filename	Description
T1D.inp	Full shell model baseline analysis for Load Case #2 input file.
C1D.inp	Substructure analysis using shell submodel #1 for Load Case #2 input file.
C2D.inp	Substructure analysis using shell submodel #2 for Load Case #2 input file.
T2D.inp	Substructure analysis using solid submodel #1 for Load Case #2 input file.
T2DPP.inp	Substructure analysis using solid submodel #1 for Load Case #2 post processing input file.
T2DPP.xls	Substructure analysis using solid submodel #1 for Load Case #2 SRF calculation spreadsheet.
T3D.inp	Substructure analysis using solid submodel #2 for Load Case #2 input file.
T3DPP.inp	Substructure analysis using solid submodel #2 for Load Case #2 post processing input file.
T3DPP.xls	Substructure analysis using solid submodel #2 for Load Case #2 SRF calculation spreadsheet.
T4D.inp	Full solid model baseline analysis for Load Case #2 input file.
T4DPP.inp	Full solid model baseline analysis for Load Case #2 post processing input file.
T4DPP.xls	Full solid model baseline analysis for Load Case #2 SRF calculation spreadsheet.
T5D.inp	Submodel stress intensity matching analysis using shell submodel #1 for Load Case #2 input file.
T6D.inp	Submodel analysis using solid submodel #1 for Load Case #2 input file.
T6DPP.inp	Submodel analysis using solid submodel #1 for Load Case #2 post processing input file.
T6DPP.xls	Submodel analysis using solid submodel #1 for Load Case #2 SRF calculation spreadsheet.
T7D.inp	Submodel stress intensity matching analysis using shell submodel #2 for Load Case #2 input file.
T8D.inp	Submodel analysis using solid submodel #2 for Load Case #2 input file.
T8DPP.inp	Submodel analysis using solid submodel #2 for Load Case #2 post processing input file.
T8DPP.xls	Submodel analysis using solid submodel #2 for Load Case #2 SRF calculation spreadsheet.

General Dynamic Analysis Application

Filename	Description
Thshell.inp	Full shell model modal analysis input file.
Thsolid.inp	Solid model modal analysis input file.
Damping(Rev1).xls	Alpha and beta damping coefficient calculation spreadsheet.

Dynamic Load Case #1 Application

Filename	Description
TH2B.inp	Full shell model baseline time history analysis for Load Case #1 input file.
TH2BP1.inp	Full shell model baseline analysis for Load Case #1, 1st post processing input file for generating time history displacements and stress intensities.
TH2BP2.inp	Full shell model baseline analysis for Load Case #1, 2nd post processing input file for generating displacements and stress intensities at time step = 0.052143 seconds.
TH2BP5.inp	Full shell model baseline analysis for Load Case #1, 3rd post processing input file for generating time history displacements used as input for subsequent submodel time history analyses.
TH30B.inp	Substructure time history analysis using shell submodel #2 for Load Case #1 input file.
TH30BP1.inp	Substructure time history analysis using shell submodel #2 for Load Case #1, 1st post processing input file for generating time history displacements and stress intensities.
TH30BP1.xls	Substructure time history analysis using shell submodel #2 for Load Case #1, displacements and stress intensities spreadsheet.
TH60B.inp	Substructure time history analysis using solid submodel #2 for Load Case #1 input file.
TH60BPP.inp	Substructure time history analysis using solid submodel #2 for Load Case #1 post processing input file.
TH60BPP.xls	Substructure time history analysis using solid submodel #2 for Load Case #1 SRF calculation spreadsheet.
TH9B.inp	Solid model baseline time history analysis for Load Case #1 input file.
TH9BPP.inp	Solid model baseline time history analysis for Load Case #1 post processing input file.
TH9BPP.xls	Solid model baseline time history analysis for Load Case #1 SRF calculation spreadsheet.
TH9BPP1.inp	Solid model baseline analysis for Load Case #1, 1st post processing input file for identifying which path has the maximum stress intensity.
TH9BPP2.inp	Solid model baseline analysis for Load Case #1, 2nd post processing input file for generating time history displacements and stress intensity.
TH4B.inp	Submodel stress intensity matching analysis using shell submodel #2 for Load Case #1 input file.
TH5B.inp	Submodel analysis using solid submodel #2 for Load Case #1 input file.
TH5BPP.inp	Submodel analysis using solid submodel #2 for Load Case #1 post processing input file.
TH5BPP.xls	Submodel analysis using solid submodel #2 for Load Case #1 SRF calculation spreadsheet.

Dynamic Load Case #2 Application

Filename	Description
TH2A.inp	Full shell model baseline time history analysis for Load Case #2 input file.
TH2AP1.inp	Full shell model baseline analysis for Load Case #2, 1st post processing input file for generating time history displacements and stress intensities.
TH2AP2.inp	Full shell model baseline analysis for Load Case #2, 2nd post processing input file for generating displacements and stress intensities at time step = 0.049857 seconds.
TH2AP5.inp	Full shell model baseline analysis for Load Case #2, 3rd post processing input file for generating time history displacements used as input for subsequent submodel time history analyses.
TH30A.inp	Substructure time history analysis using shell submodel #2 for Load Case #2 input file.
TH30AP1.inp	Substructure time history analysis using shell submodel #2 for Load Case #2, 1st post processing input file for generating time history displacements and stress intensities.
TH30AP1.xls	Substructure time history analysis using shell submodel #2 for Load Case #2, displacements and stress intensities spreadsheet.
TH60A.inp	Substructure time history analysis using solid submodel #2 for Load Case #2 input file.
TH60APP.inp	Substructure time history analysis using solid submodel #2 for Load Case #2 post processing input file.
TH60APP.xls	Substructure time history analysis using solid submodel #2 for Load Case #2 SRF calculation spreadsheet.
TH9A.inp	Solid model baseline time history analysis for Load Case #2 input file.
TH9APP.inp	Solid model baseline time history analysis for Load Case #2 post processing input file.
TH9APP.xls	Solid model baseline time history analysis for Load Case #2 SRF calculation spreadsheet.
TH9APP1.inp	Solid model baseline analysis for Load Case #2, 1st post processing input file for identifying which path has the maximum stress intensity.
TH9APP2.inp	Solid model baseline analysis for Load Case #2, 2nd post processing input file for generating time history displacements and stress intensity.
TH4A.inp	Submodel stress intensity matching analysis using shell submodel #2 for Load Case #2 input file.
TH5A.inp	Submodel analysis using solid submodel #2 for Load Case #2 input file.
TH5APP.inp	Submodel analysis using solid submodel #2 for Load Case #2 post processing input file.
TH5APP.xls	Submodel analysis using solid submodel #2 for Load Case #2 SRF calculation spreadsheet.

ENCLOSURE 3

TENNESSEE VALLEY AUTHORITY
BROWNS FERRY NUCLEAR PLANT (BFN)
UNITS 1, 2, AND 3

TECHNICAL SPECIFICATIONS (TS) CHANGES TS-431 AND TS-418
EXTENDED POWER UPRATE (EPU)

EVALUATION OF SUBMODEL APPROACH USED IN CDI REPORT 08-20P

The structural analysis considered in Calculation Package 0006982.304, "Comparison Study of Substructure and Submodel Analysis using ANSYS," (Enclosure 2 of this submittal) is revisited here using CDI's submodeling technology which was utilized in Appendix A of CDI Report No. 08-20P, "Stress Assessment of Browns Ferry Nuclear Unit 2 Steam Dryer with Outer Hood and Tie-Bar Reinforcements," (Enclosure 2 of the submittal dated November 14, 2008, "Supplemental Response to Rounds 19 and 22 RAI Regarding Steam Dryers," ML083250114). The geometry consists of a pair of welded plates. The first is a 1/2 inch thick vertical plate (40 inches tall and 10 inches wide). The second plate is 1/4 inch horizontal plate that is 20 inches long and 6 inches wide. The plates are joined by a 1/4 inch double sided fillet weld that wraps around the end of the horizontal plate. Ample depictions of the configuration are given in Calculation Package 0006982.304. The top and bottom edges of the vertical plate are fixed and a uniform force per unit length is applied along the tip edge of the horizontal plate. Two dynamic load cases shown in Figures 1a and 1b are considered here: (i) a transverse tip load that produces a predominantly bending stress at the root and, (ii) an in-plane tension force that induces a membrane stress. In both cases the force is a harmonic load with a frequency of 25 Hz. Since the stress reduction factor (SRF) is independent of the applied load magnitude (i.e., scaling the force does not change the SRF) a unit load is applied in each case.

Note too, that the current analysis is conducted using the same harmonic analysis and computational software used in the global steam dryer analysis. This implies several differences between the submodel analysis here and the one in Calculation Package 0006982.304. For example, the harmonic rather than Rayleigh damping model is employed. Also, the response represents the particular steady state or periodic solution due to the 25 Hz forcing; i.e., no transients are present. Therefore, the pair of times that produce the alternating stress will generally differ from those in Calculation Package 0006982.304 which adopted a transient-based simulation. In Calculation Package 0006982.304, the response still contained a noticeable transient as can be seen, for example, in the stress response of Figure 6-6 and the non-symmetric stress distribution of Figure 6-8. A related difference is that the submodel analysis in Calculation Package 0006982.304 was performed using the maximum stresses, whereas here the alternating stresses are evaluated. For a single frequency steady state response, however, this difference becomes immaterial since the maximum and alternating stress intensities become identical. Finally, it is pointed out that though the characteristic mesh spacings of the shell and solid models are similar to the ones in Calculation Package 0006982.304, the meshes were developed independently and so will differ from those in Calculation Package 0006982.304. Despite these differences, the results in Calculation Package 0006982.304 are in close agreement with those generated here.

For each load case, the full or global shell model is first subjected to the harmonic forcing. The maximum alternating stress intensity on the weld line is calculated and the location where it occurs is identified together with the pair of time steps in the time response that together produce the alternating stress intensity. The submodel is then generated by centering an 8 inch × 6 inch × 6 inch box at the high stress location. In both cases, the highest weld stresses occurs at the center of the weld line and the box is centered at the junction as indicated in Figures 1a and 1b. The same software and analysis procedures employed in Appendix A of CDI Report 08-20P are used in developing the results below.

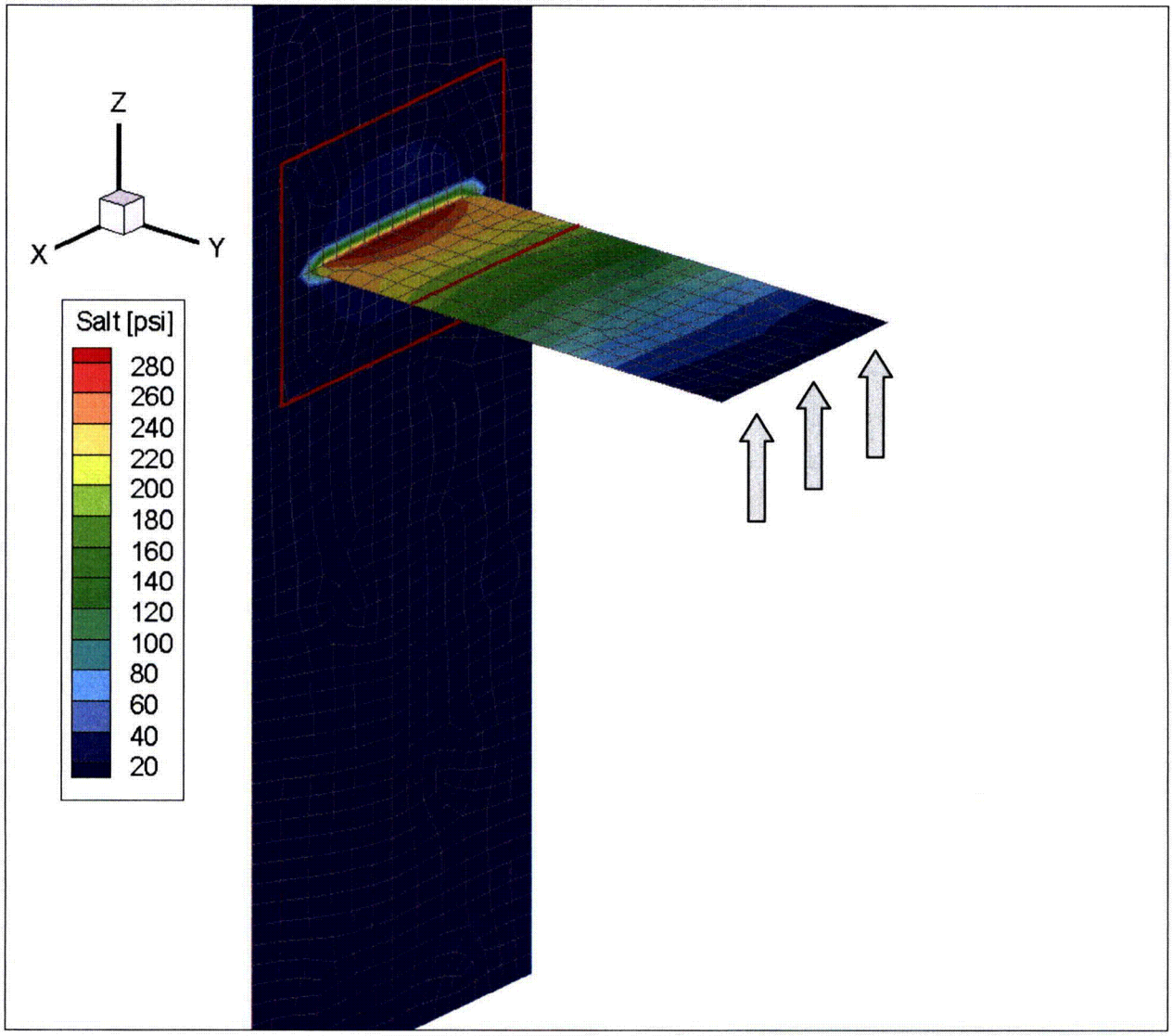

Figure 1a: Alternating stress intensity contours for the structure subject to transverse loading. The red lines represent the intersection lines of the 'cutting box' used to extract the submodel. The stresses along these lines are integrated to obtain the forces and moments along the intersection lines.

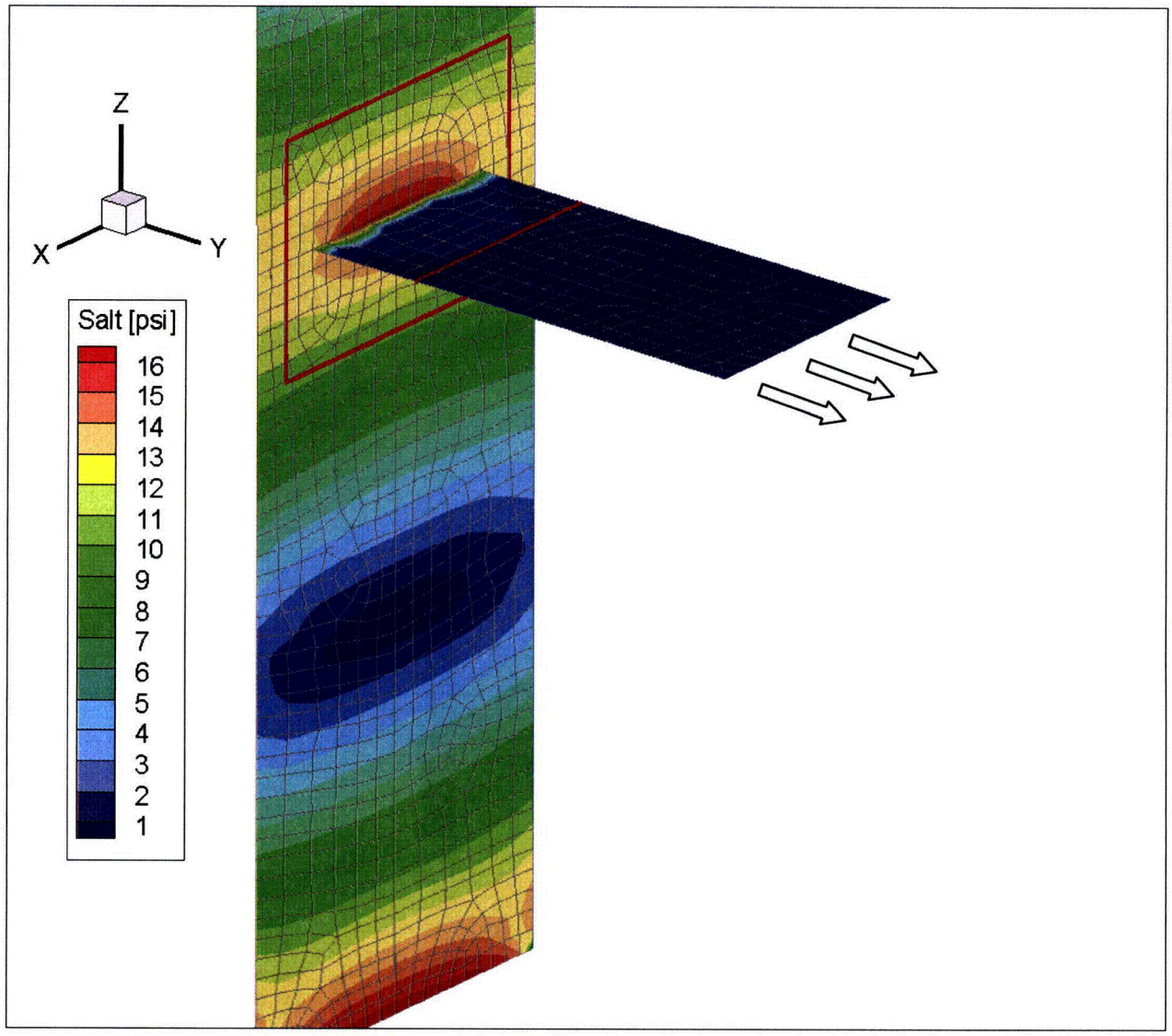

Figure 1b: Alternating stress intensity contours for the structure subject to in-plane loading. The red lines represent the intersection lines of the 'cutting box' used to extract the submodel. The stresses along these lines are integrated to obtain the forces and moments along the intersection lines.

Submodel Analysis for Bending Load

For this configuration, a transverse harmonic force of unit amplitude is distributed over the tip edge of the horizontal plate as indicated in Figure 1a. The resulting stress and displacements are shown in Figure 2. The maximum stress intensity in this case is 288.3 psi and occurs exactly halfway along the junction of the two plates.

The shell submodel was created centered at the mid-section of the plates' connection as shown in Figure 3a. The forces and moments at each edge of the submodel were adjusted to recover the stress field along the weld line and are shown in Figure 3b. The resulting stress distribution in the shell submodel is shown in Figure 3c. The maximum stress intensity in the shell submodel is 299.2 psi which closely matches the one in the global shell model (288.3 psi).

The solid submodel and associated mesh of the same junction are shown in Figure 4 and the stress distribution obtained when applying the same forces and moments used in the shell submodel is depicted in Figure 5. The stresses are linearized along the paths shown in Figure 6. The resulting linearized stresses along each path are summarized in Table 1. The largest linearized membrane + bending stress intensity is found to be 209.8 psi which, when compared against the corresponding value in the shell-based submodel (299.2 psi), yields a SRF of 209.8 / 299.2 = 0.7.

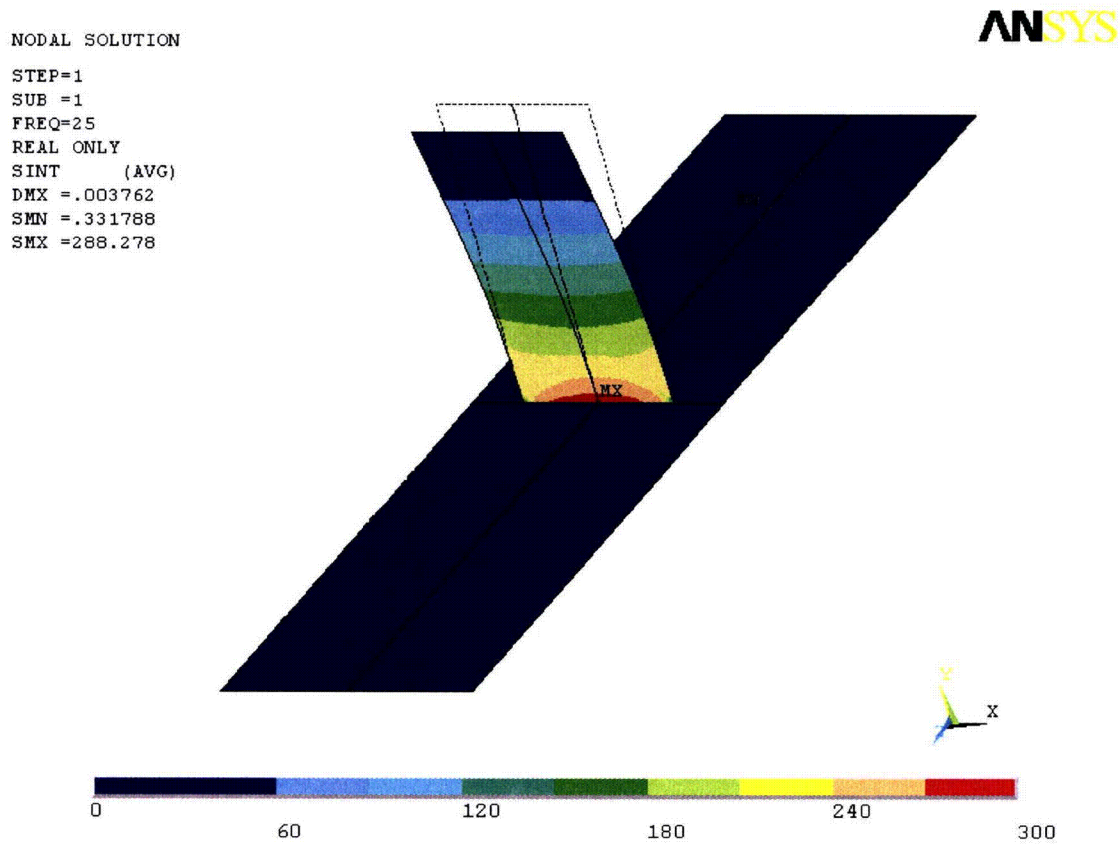

Figure 2: Stresses and displacements for bending loading in the global shell model.

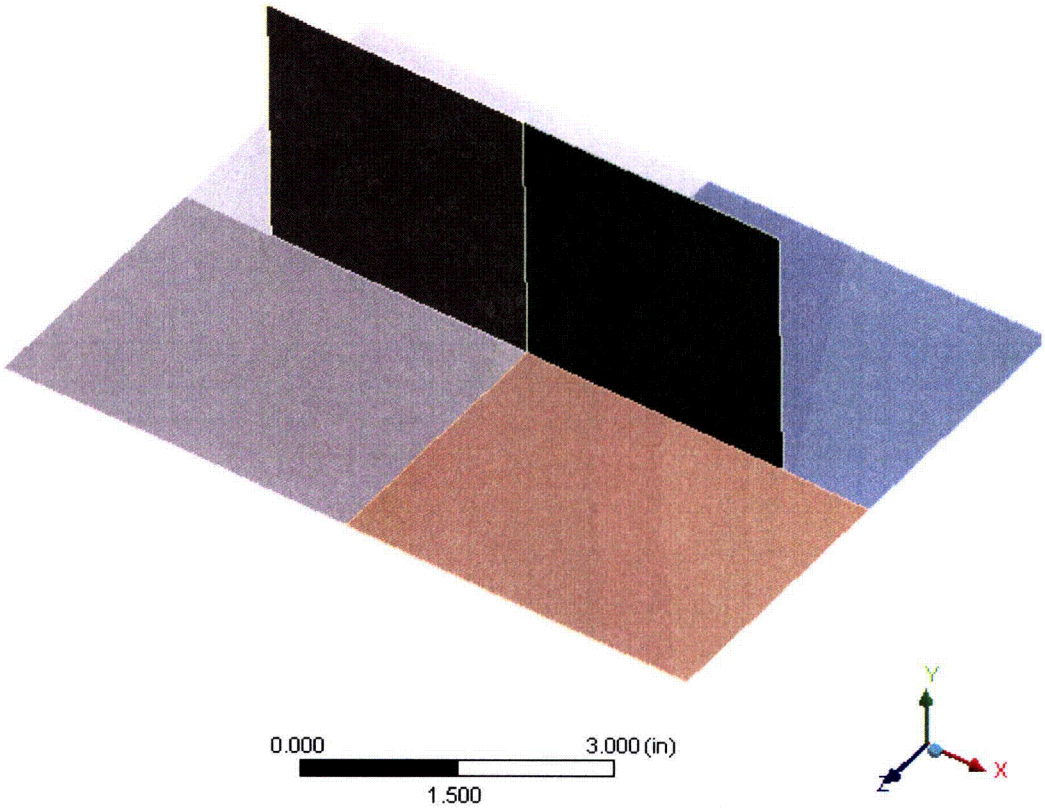

Figure 3a: Shell submodel.

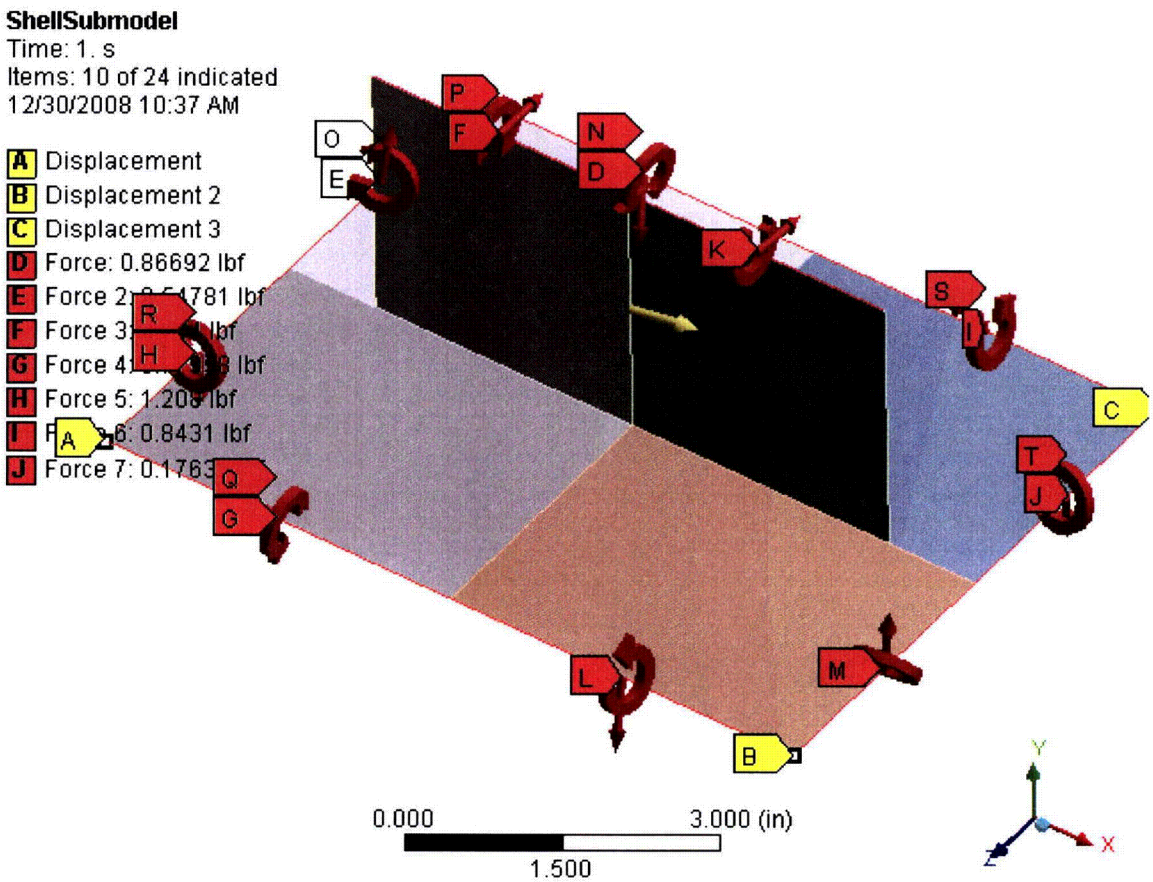

Figure 3b: Forces, moments, acceleration and constrained nodes imposed upon the submodel.

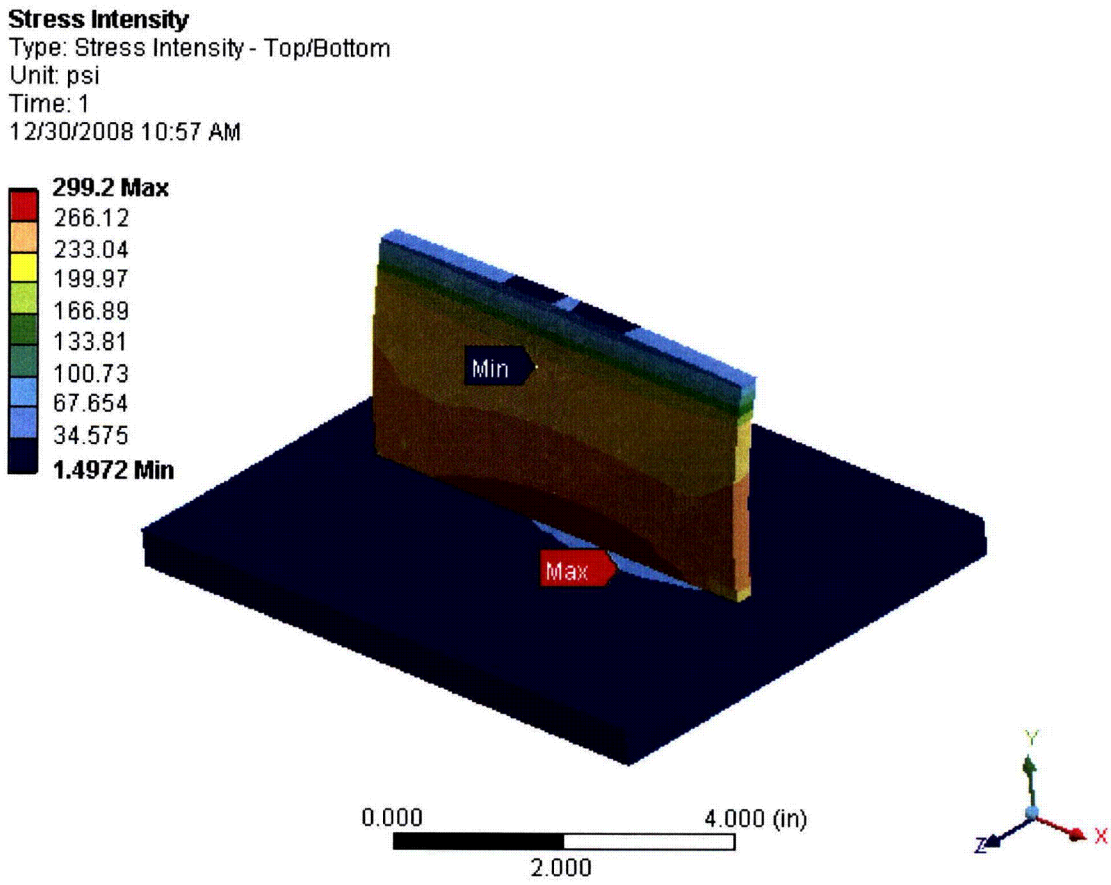

Figure 3c: Stresses in shell submodel.

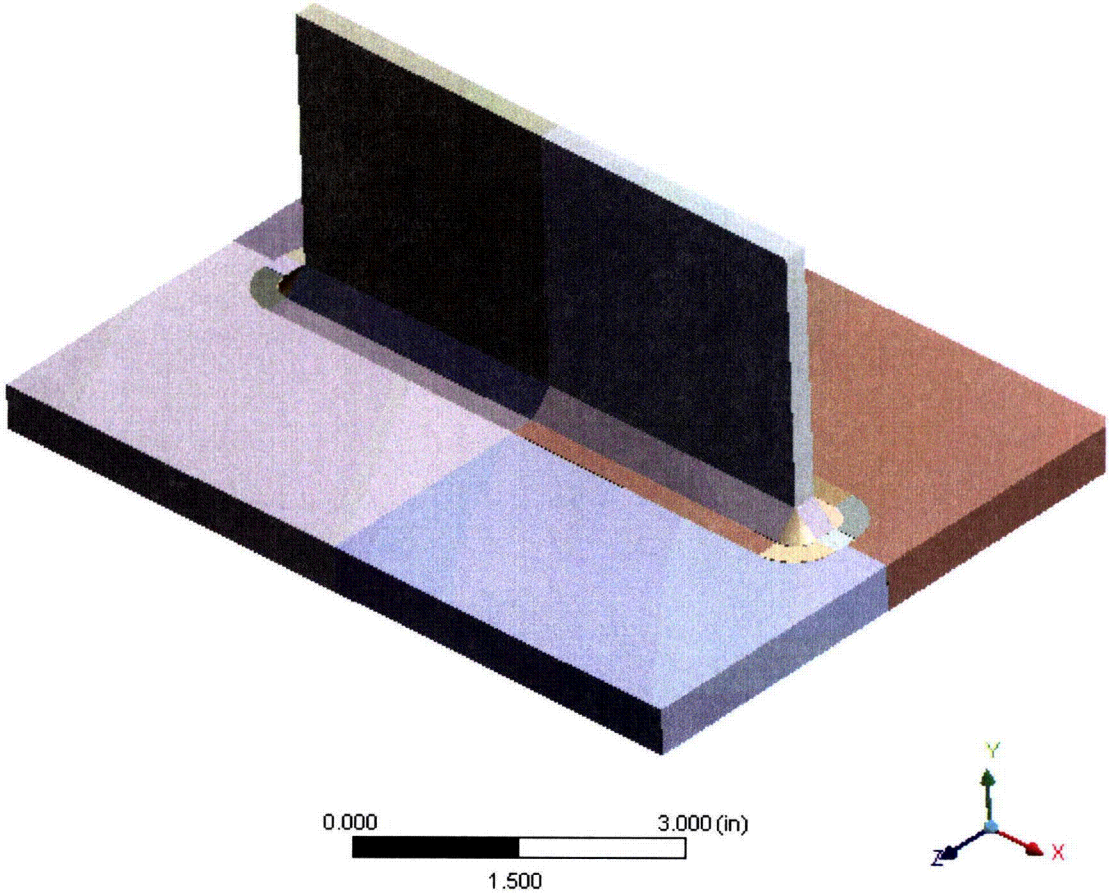

Figure 4a: Solid submodel.

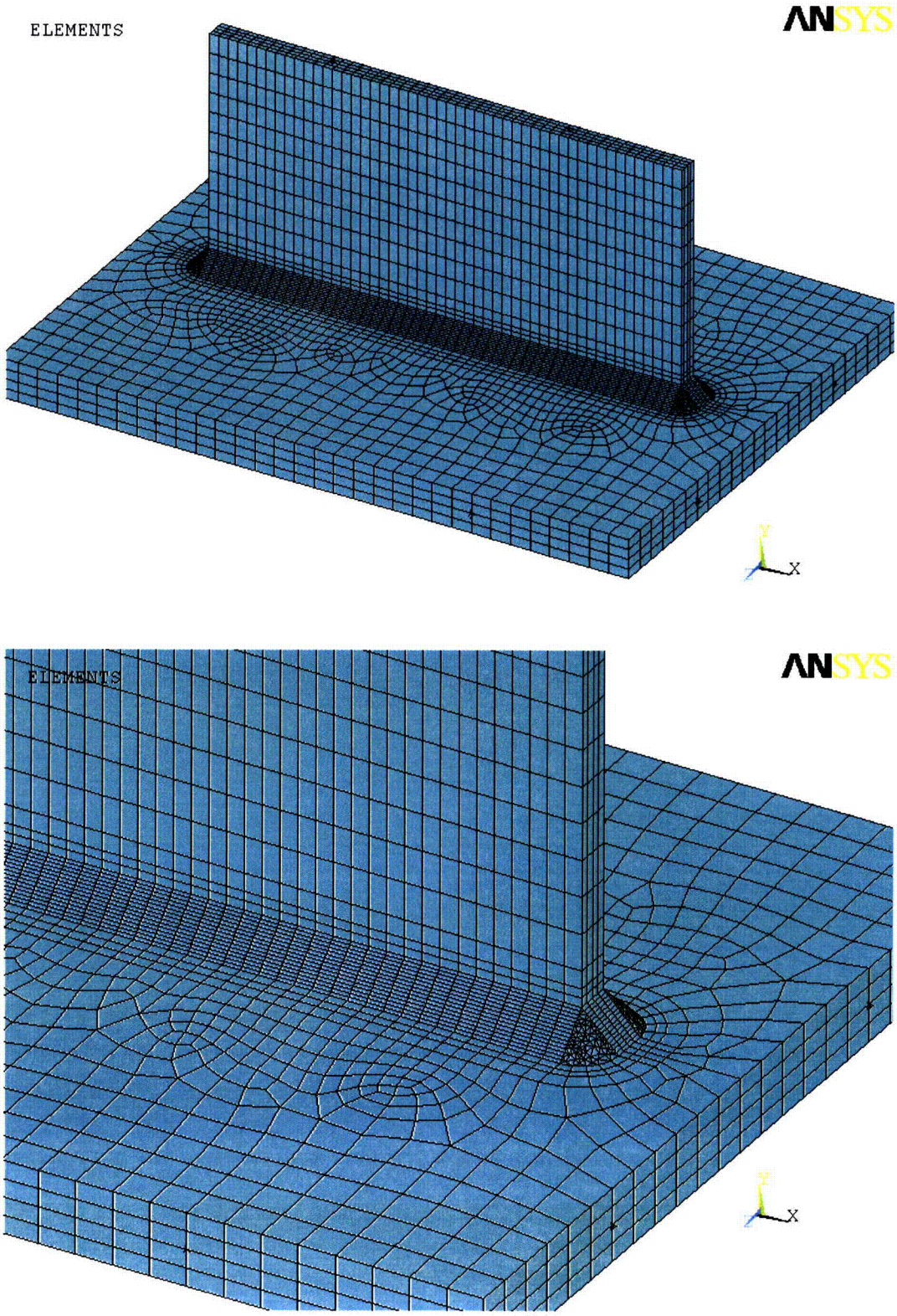

Figure 4b: Solid submodel mesh.

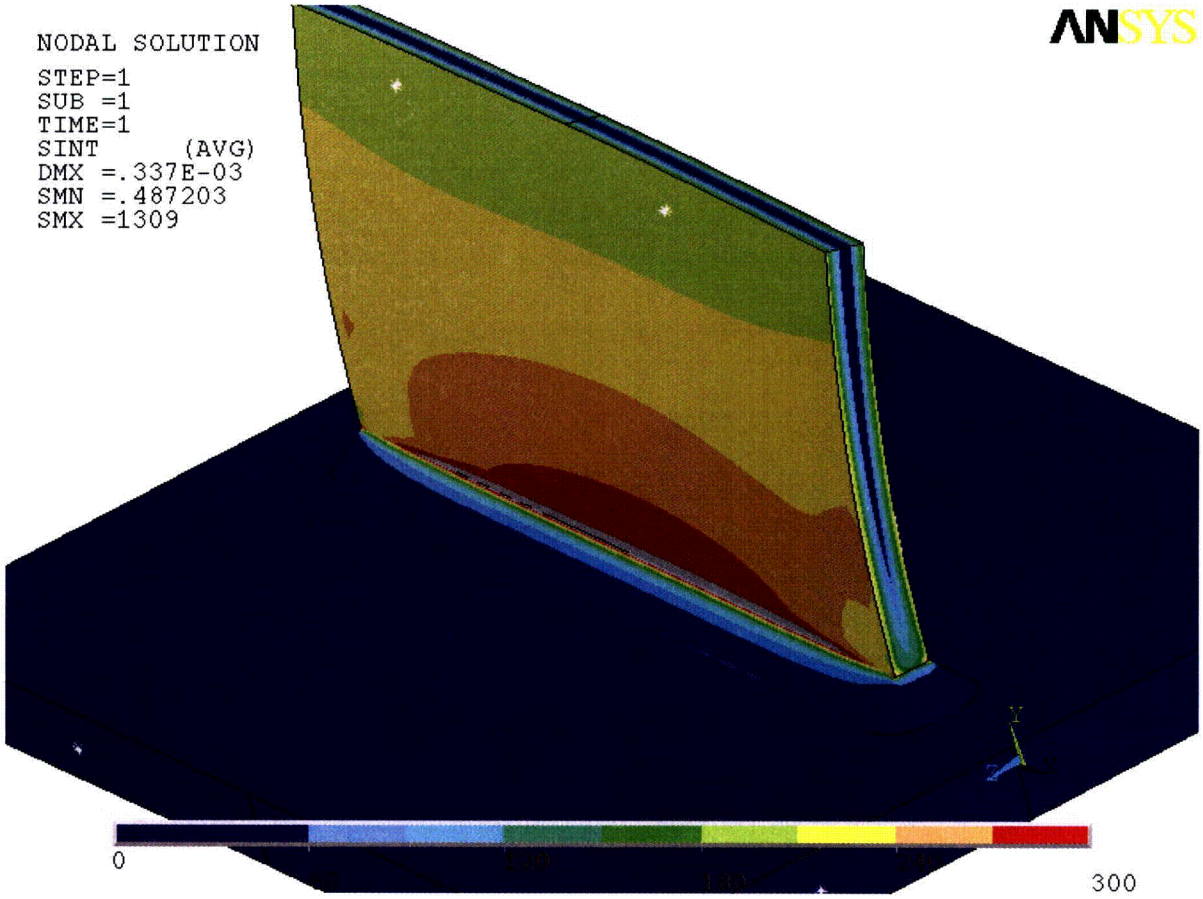

Figure 5a: Stresses in solid submodel.

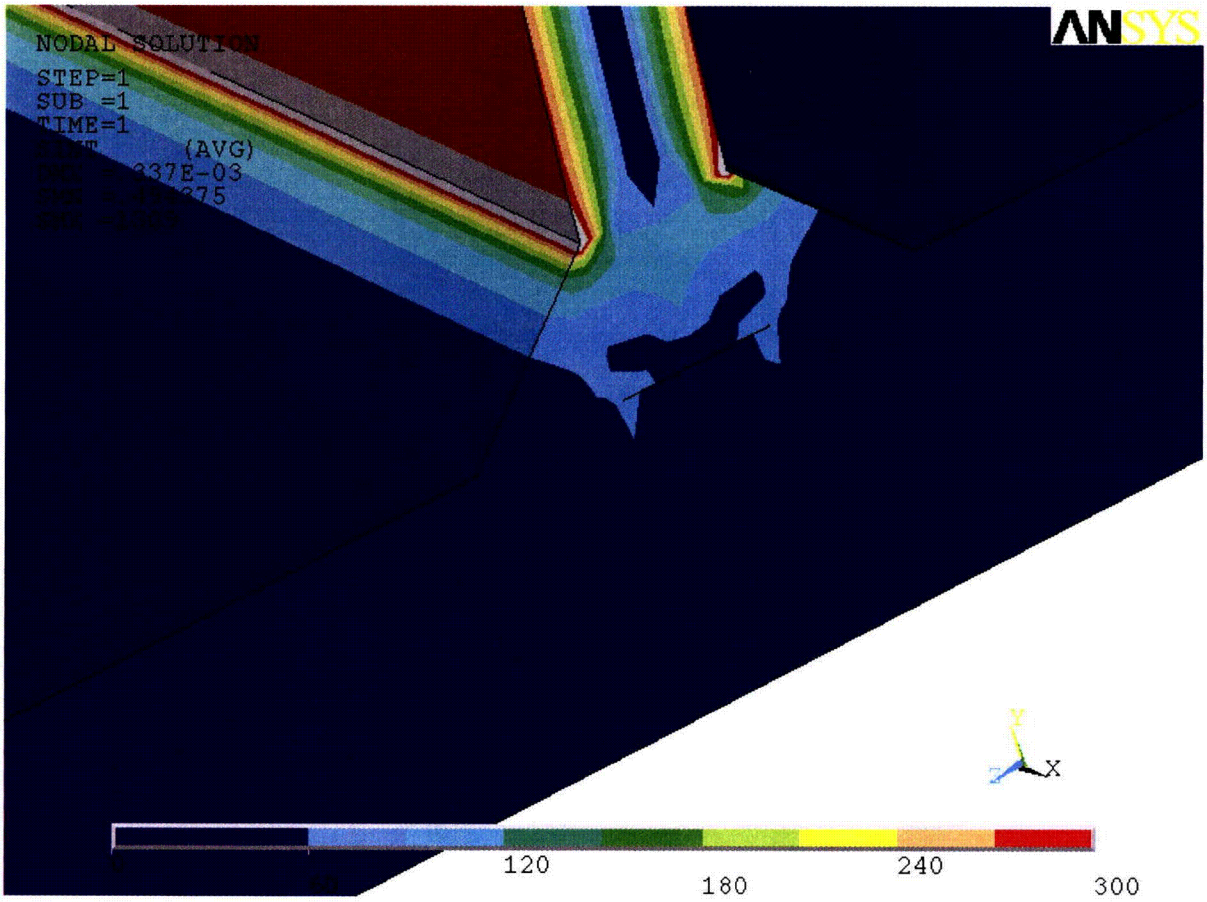

Figure 5b: Stresses in solid submodel across the weld.

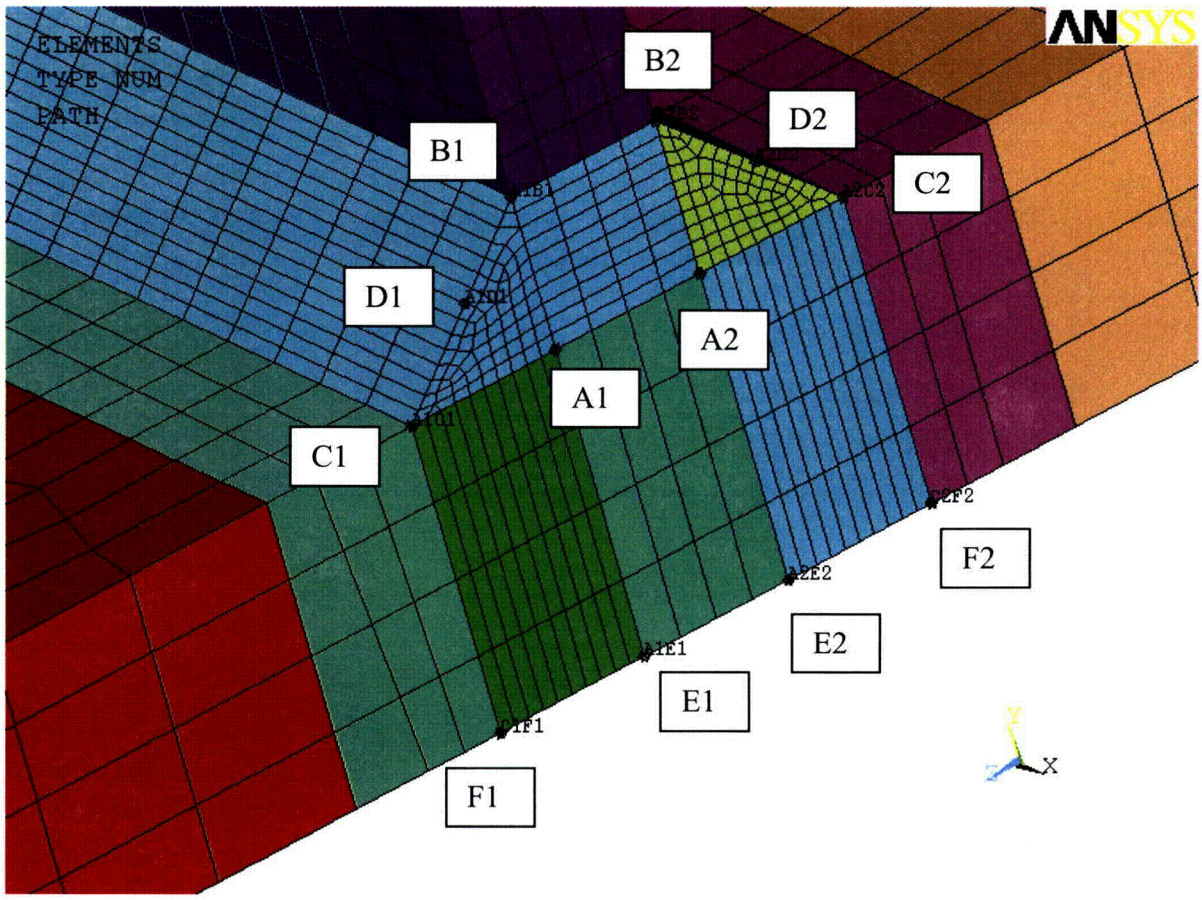

Figure 6: Linearization paths used to extract linearized stresses from the solid submodel.

Table 1: Linearized stresses extracted for the paths in Figure 6.

Path	Stress intensity, psi
A1-B1	**209.8**
A1-C1	54.35
A1-D1	84.31
A1-E1	61.6
C1-F1	34.75
B1-B2	206.4
A2-B2	201.8
A2-C2	54.32
A2-D2	80.82
A2-E2	60.84
C2-F2	35.25

Submodel Analysis for In-Plane or Membrane Load

In this case, the same structure is subjected to an in-plane harmonic force of unit amplitude distributed over the tip edge of the horizontal plate as indicated in Figure 1b. The resulting stress and displacements are shown in Figure 7. The maximum stress intensity on the weld line is 16.367 psi and occurs at the same node as for the bending load. (The highest stresses occur on the fixed edges of the vertical plate; however, these are not analyzed here). Therefore the same shell and solid submodels are reused here. Since the submodel geometry and mesh are the same, only the stress results are reported.

The forces and loads are derived in the same manner as for the bending problem and the resulting stress distribution in the shell submodel is shown in Figure 8. The maximum stress intensity in the shell submodel is 17.005 psi which closely matches the one in the global shell model (16.37 psi). Applying these same forces and moments to the solid submodel (Figure 4) produces the stress distributions shown in Figure 9. The linearized stresses calculated along the same paths used in the bending problem (Figure 6) are summarized in Table 2. The largest linearized membrane + bending stress intensity is found to be 15.98 psi which, when compared against the corresponding value in the shell-based submodel (17.005 psi), yields a SRF of 15.98 / 17.005 = 0.94.

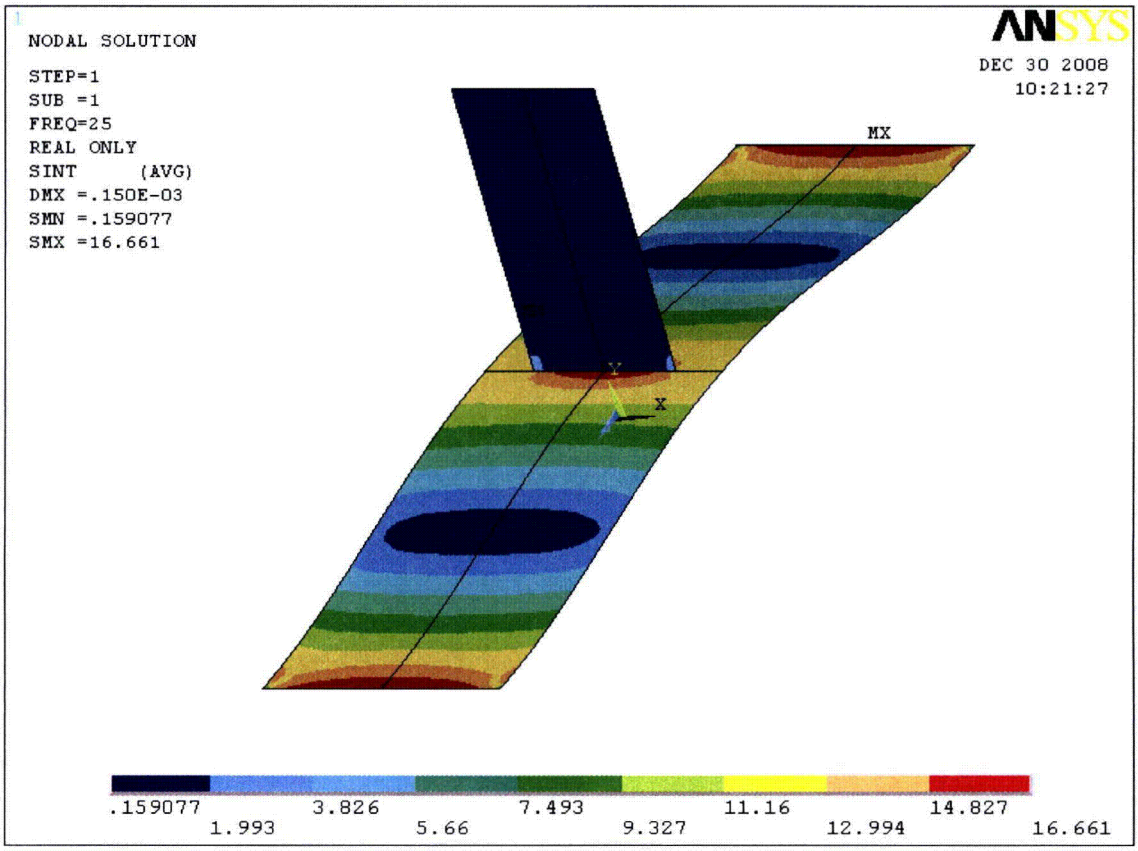

Figure 7: Stresses and displacements in the global shell model.

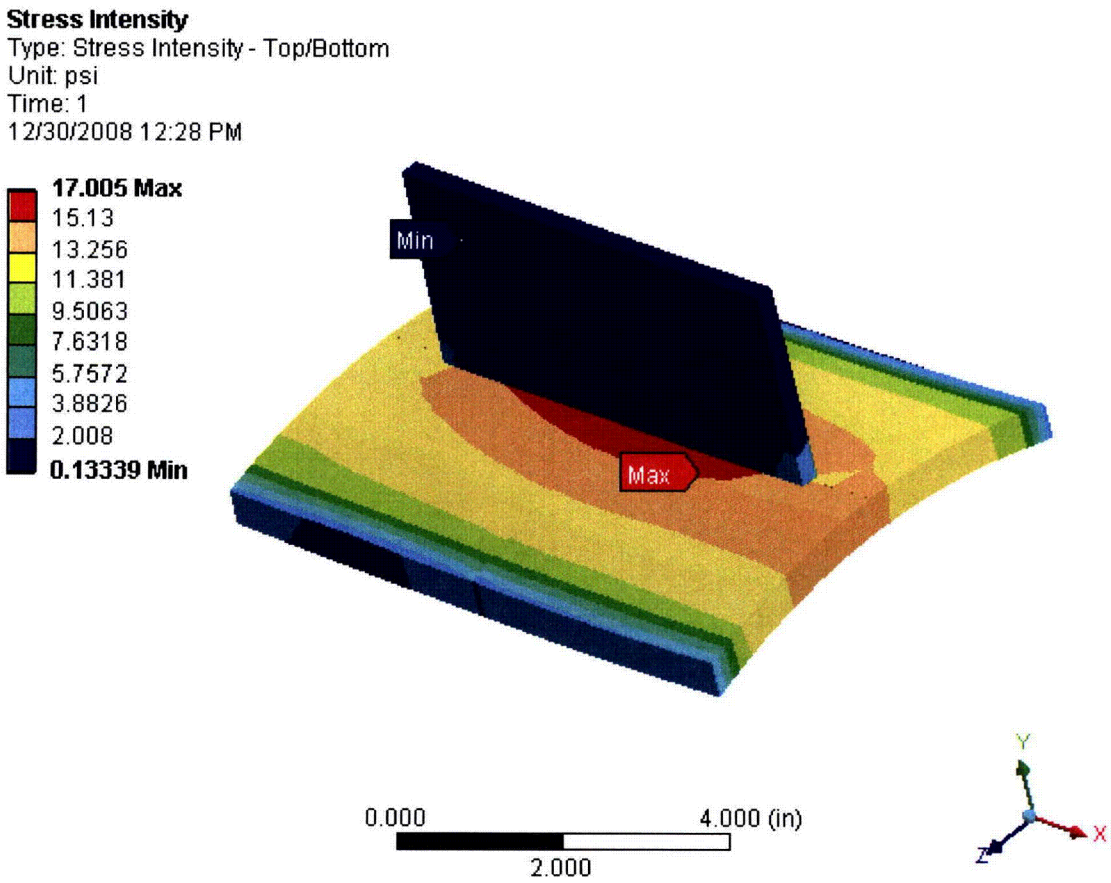

Figure 8: Stresses in shell submodel.

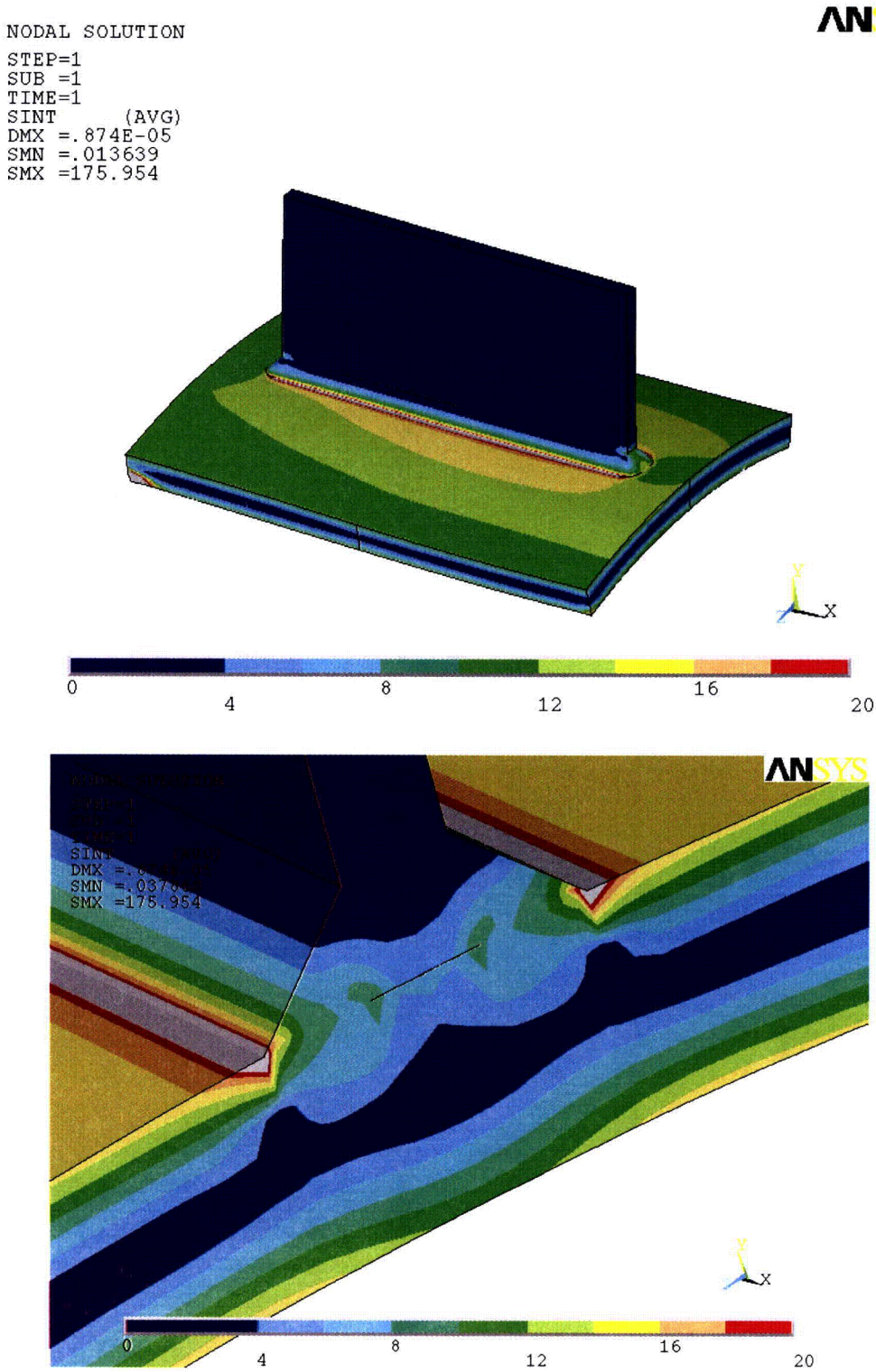

Figure 9: Stresses in solid submodel.

Table 2: Linearized stresses extracted for the paths in Figure 6.

Path	Stress intensity, psi
A1-B1	9.498
A1-C1	15.92
A1-D1	10.16
A1-E1	11.97
C1-F1	15.87
B1-B2	1.65
A2-B2	9.49
A2-C2	**15.98**
A2-D2	10.07
A2-E2	11.93
C2-F2	15.74

ENCLOSURE 4

TENNESSEE VALLEY AUTHORITY
BROWNS FERRY NUCLEAR PLANT (BFN)
UNITS 1, 2, AND 3

TECHNICAL SPECIFICATIONS (TS) CHANGES TS-431 AND TS-418
EXTENDED POWER UPRATE (EPU)

RESPONSE TO ROUND 23 REQUEST FOR ADDITIONAL INFORMATION (RAI)
REGARDING STEAM DRYER ANALYSIS SUBMODELING

(NON-PROPRIETARY VERSION)

Attached is the non-proprietary version of the Response to Round 23 Request for Additional Information (RAI) Regarding Steam Dryer Analysis Submodeling.

NRC RAI EMCB.201/162 (Units 1 and 2)

In Enclosure 6 to a letter dated October 31, 2008, TVA presented a response to EMCB.RAI 199/156 in the Structural Integrity Associates Calculation Package 0006982.304, *Comparison study of Substructure and Submodel Analysis using ANSYS*. The NRC staff finds the TVA's use of terms "substructure" and "submodel" confusing. For clarification, the NRC understands that the term "substructure" in the response implies a typical submodel as mentioned in the RAI, and the term "submodel" implies TVA's submodel.

TVA's response presents full-model and submodel analyses of a two-plate structure, with a horizontal plate welded to a vertical plate at the mid-height. The dynamic analysis of these plates with harmonic forces acting at the free end of the horizontal plate is presented in Section 6. Based on the analyses results presented in Sections 6.4.2 and 6.5.2, TVA concludes that the typical submodel analyses are invalid because they do not include inertia forces. Therefore, a justifiable stress reduction factor for the stresses at the weld during the dynamic analysis cannot be determined. Because of this, the accuracy of the stress reduction factors determined using the TVA's submodeling approaches (which are different from the typical submodeling approach) cannot be assessed. To address this concern, TVA is requested to provide the following:

a. A full solid finite element analyses for the two dynamic load cases listed in Section 4.2 of the SIA Calculation Package;

b. A comparison of resulting weld stresses with the corresponding stresses from the full shell finite element analyses presented in Sections 6.4.1 and 6.5.1 of the SIA Calculation Package and determination of stress reduction factors;

c. Submodel analyses for the two dynamic load cases considered in (a) using the approach presented in Appendix A of the CDI Report 08-20P. Provide a comparison of the resulting stress reduction factors with those obtained in (b). This comparison is requested to obtain a verification of the submodeling approach presented in Appendix A; and

d. A comparison of stress reduction factors obtained in (b) with those reported in Sections 6.4.4, and 6.5.4 of the SIA Calculation Package. This should include an assessment of the validity of the two TVA's submodeling approaches used in the stress analysis of Units 1 and 2 steam dryers.

Response to EMCB.201/162 (Units 1 and 2)

As clarified in the RAI request, the term "substructure" is used to indicate the typical analysis supported by computer programs such as ANSYS and "submodel" is used to indicate the method utilized by TVA which is based on basic engineering principles where loads or displacements are determined by matching the state of stress along the line of the joint under evaluation.

In order to assess the submodeling approaches utilized by TVA, the following actions/analyses have been performed.

- The substructure analyses that were performed in Sections 6.4 and 6.5 of Calculation Package 0006982.304 Revision 0 (Enclosure 6 of the submittal dated October 31, 2008, "Supplemental Response to Round 19 RAI and Response to Round 22 RAIs Regarding Steam Dryers," ML083120307), have been revised to provide dynamic results based on

the time history displacements from the full shell model at each of the 1400 time steps. These dynamic substructure results are provided in Revision 1 of Calculation Package 0006982.304 which is provided in Enclosure 2 of this submittal. This resolves the problem with inertia effects that was described in Revision 0 of the Calculation Package. The resultant stress and stress profiles for the substructure shell model accurately reflect the full shell model results.

Two additional changes were incorporated in Revision 1 of Calculation Package 0006982.304: 1) the structural damping used in the analyses has been changed from 4% to 1% to be consistent with the damping used in the steam dryer analyses, and 2) the inadvertent use of weight density instead of mass density in the dynamic analyses was corrected.

- Full solid model analyses have also been performed for the dynamic example load cases. The full solid model dynamic analyses are provided in Revision 1 of Calculation Package 0006982.304. Stress reduction factors (SRF) are computed based on the full solid model analyses which provide baseline SRFs that do not involve any submodeling or substructuring.

- The submodel approach utilized by CDI in Appendix A of CDI Report No. 08-20P, "Stress Assessment of Browns Ferry Nuclear Unit 2 Steam Dryer with Outer Hood and Tie-Bar Reinforcements," (Enclosure 2 of the submittal dated November 14, 2008, "Supplemental Response to Rounds 19 and 22 RAI Regarding Steam Dryers," ML083250114) was applied to the example structures from Calculation Package 0006982.304. The results of these analyses are provided in Enclosure 3.

The resultant SRFs from the full solid model and the submodel analyses are presented in Table EMCB.201/162-1. The SRFs computed from the full solid model provide a baseline that does not include any impact from either submodeling or substructuring. The analyses show that both of the submodeling approaches and the substructure approach provide conservative results compared to the baseline results of the full solid model.

Table EMCB.201/162-1: Comparison of Full Solid Model and Submodel SRFs

Approach	Stress Reduction Factors			
	Static Analysis		Dynamic Analysis	
	Load Case 1	Load Case 2	Load Case 1	Load Case 2
Full Solid Model	0.59	0.89	0.59	0.89
Substructure Model	0.74/0.69*	0.92/0.91*	0.68	0.91
SIA Submodel	0.68/0.66*	0.89/0.89*	0.66	0.89
CDI Submodel	-	-	0.70	0.94

*For the static analyses, two submodel sizes were analyzed.

In response to items a through d of the RAI, TVA has provided the requested information as follows:

(a) Full solid finite element model time history analyses for the two dynamic load cases listed in Section 4.2 of Calculation Package 0006982.304 have been performed. The analyses are performed using one half of the solid finite element model, with symmetric boundary conditions applied at the plane of half symmetry. The results of the analyses are provided in Sections 6.4.2 and 6.5.2 of Calculation Package 0006982.304 Revision 1.

(b) A comparison of the stresses from the full shell model and full solid model dynamic analyses and computed SRFs are provided in Tables 6-5 and 6-8 of Calculation Package 0006982.304 Revision 1 for dynamic load cases #1 and #2, respectively.

(c) An evaluation of the two dynamic load cases considered in Calculation Package 0006982.304 was performed utilizing the submodel approach presented in Appendix A of CDI Report 08-20P. The results of this evaluation are presented in Enclosure 3. The computed SRFs utilizing this submodel approach are presented in Table EMCB.201/162-1. The submodeling results are conservative relative to the SRFs determined from the full solid model baseline analyses that do not involve any submodeling or substructuring techniques.

(d) An evaluation of the two dynamic load cases presented in Sections 6.4.4 and 6.5.4 of Revision 0 of Calculation Package 0006982.304 has been reperformed and is presented in Sections 6.4.5 and 6.5.5 of Revision 1 of Calculation Package 0006982.304. The computed SRFs utilizing this submodeling approach are summarized in Tables 7-3 and 7-4 of the calculation package and presented in Table EMCB.201/162-1. The submodeling results are conservative relative to the SRFs determined from the full solid model baseline analyses that do not involve any submodeling or substructuring techniques. Furthermore, from Table EMCB.201/162-1, it may be observed that the SRFs computed for the static and dynamic cases provide consistent results.

Based on the results of the full model, submodel and substructure assessments described above, the following conclusions are evident:

- The full solid model dynamic solution clearly demonstrates the reduction in stress obtained from considering more realistic strain distribution behavior without any inherent analytical assumptions or adjustments associated with either a submodel or substructure approach. Accordingly, SRFs obtained from the full model solid element dynamic solution provide a sound basis from which to assess the accuracy and conservatism of both submodel analysis approaches and the substructure analysis approach.

- SRFs determined using either the submodel approach or the substructure approach are the same or conservative when compared to the full model solid element baseline. Accordingly, SRFs derived using either technique at specific locations on the BFN steam dryers are appropriate for fatigue evaluation at those locations.

NRC RAI EMCB.166 (Unit 2)

In Section 6.1 of the CDI Report 08-20P, "Stress Assessment of Browns Ferry Nuclear Unit 2 Steam Dryer with Outer Hood and Tie-Bar Reinforcements." TVA reports that the lowest alternating stress ratio calculated at EPU without considering filtering of the plant noise is 1.97.

The corresponding location is a weld between the dam plate and the new gusset (referred to as Dam Plate/New Gusset in Table 9c). For a more accurate estimate of the stresses at the weld, TVA considers typical submodeling for this location and determines that the stress reduction factor is 0.82 (see Appendix A of the CDI Report 08-20P). Application of this factor increases the alternating stress ratio from 1.97 to 2.40.

In the submodeling analysis mentioned above, TVA uses the known stresses from the global shell analysis to determine the forces and moments acting on the submodel boundary. In addition it simulates the acoustic pressures and inertial forces acting on the submodel by linearly varying body force. These forces and moments are applied to both shell submodel and the solid submodel, in which the welds are also modeled. The stress results from the analyses of these two submodels are used to determine the stress reduction factor. This submodeling approach is based on technically sound principles and is supported by the computer codes such as ANSYS and ABAQUS.

a) The global shell analysis is a dynamic analysis whereas the submodel analysis is a static analysis. Explain which instant of the global transient analysis is analyzed by the submodel analyses and why that instant is chosen for the analysis.

b) Explain whether the forces and moments acting on the submodel boundary were determined manually or by using the ANSYS Code capabilities.

c) Clarify the last two sentences in the third paragraph on p. 82 of the CDI report.

d) Table 10 in Appendix A of the CDI report provides the alternating stress intensity results for the global shell model. Discuss whether these stresses are related to those presented in the report.

e) Clarify the last two sentences in the fourth paragraph on p. 112 of the CDI report.

<u>TVA Response to EMCB.166 (Unit 2)</u>

a) The submodel stresses and forces are developed from the two time steps producing the highest alternating stress intensity at the node of interest. Recall that the alternating stress intensity is evaluated from the stress difference tensors, $\Delta\sigma_{nm} = \sigma(t^n) - \sigma(t^m)$ where $\sigma(t^n)$ is the 3×3 stress tensor evaluated at time $t=t^n$ and n refers to a time step number. In general for N time steps there will be N(N-1)/2 possible pairs n and m. The alternating stress intensity is calculated by considering every such pair and taking the pair that yields the highest stress intensity, i.e., the alternating stress intensity is defined as:

$$S_{alt} = \tfrac{1}{2}\max_{n,m}\{S(\Delta\sigma_{nm})\} \qquad (1)$$

where $S(\sigma)$ is the usual stress intensity (difference between the maximum and minimum principal stresses) of the argument, σ. Denoting the particular pair of time steps yielding the highest stress intensity by (n, m) = (n*, m*) then the stresses in the submodel are taken as:

$$\sigma^{sub-model} = \sigma_{n*} - \sigma_{m*} = \Delta\sigma_{n*m*} \qquad (2)$$

The submodel forces are formed in the same way. This pair of times is selected because it is the one that produces the limiting stress.

b) The forces and moments are obtained using a verified FORTRAN computer code developed by CDI that: (i) clips or intersects the global model with a cutting box and calculates the element stresses along the intersection lines at the indicated times and, (ii) integrates the stresses across the element thickness to obtain the distributed forces and moments along each edge.

c) The last sentences of this paragraph read:

When noise is retained "...the alternating stress ratios at all these nodes remain above 2.0 except for the leading node 92392 whose *calculated* alternating stress is only 1.5% below the target level. Note however, that at this location no stress reduction factor has been applied (this factor is used for the neighboring outboard gusset/steam dam junction only). Given the identical geometry and similar loading, it is expected that the analysis in Appendix A would produce a similar stress reduction factor of 0.82 which would result in a stress ratio of 2.40 – well above the target level."

The point made here is that the 0.82 SRF developed in Appendix A was only applied to the gussets next to the outermost steam dam gussets. These gussets contain location '4' in Figures 16e and 17e of CDI Report No. 08-20P, for example. The SRF has *not* been invoked for the gussets that are further inboard (for example, it is not applied to the gussets involving locations 1 and 12 in Figure 17e of CDI Report No. 80-20P). However, the junctions for these other gussets are geometrically identical and load conditions are very similar so one expects that a submodel analysis applied to these other inboard gussets would result in a similar SRF. In that case, the alternating stress ratio of the node 92392 would, assuming the same SRF of 0.82, increase from SR-a=1.97 to SR-a=1.97/0.82=2.40. The next lowest alternating stress ratio would then be SR-a=2.01 at node 92981. Therefore, Unit 2 would meet acceptance criteria without removal of low flow noise.

d) The stresses in Table 10 of Appendix A correspond to EPU loads with frequency shifting. Specifically, location 4 in Table 9b reporting alternating stresses at welds (page 87) reports an alternating stress intensity of 3075 pounds per square inch (psi) after application of the 0.82 SRF as indicated by the footnote (e). This corresponds to an alternating stress intensity of 3750 psi before application of the SRF which is the highest stress intensity at this node listed in the last column of Table 10.

e) [[

]]

NRC RAI EMCB.167 (Unit 2)

Explain why the submodeling approach discussed in Appendix A of the CDI Report 08-20P was not used for a more refined stress analysis of the two locations evaluated in Structural Integrity Associates Calculation package, 0006982.301.

TVA Response to EMCB.167 (Unit 2)

The selection of submodeling approaches utilized by TVA was based upon resource availability of the two companies performing steam dryer analysis. As shown in the response to RAI EMCB.201/162, both submodeling approaches provide conservative results.

ENCLOSURE 5

TENNESSEE VALLEY AUTHORITY
BROWNS FERRY NUCLEAR PLANT (BFN)
UNITS 1, 2, AND 3

TECHNICAL SPECIFICATIONS (TS) CHANGES TS-431 AND TS-418
EXTENDED POWER UPRATE (EPU)

CDI AFFIDAVIT

Attached is the CDI affidavit for the proprietary information contained in Enclosure 1.

Continuum Dynamics, Inc.

(609) 538-0444 (609) 538-0464 fax 34 Lexington Avenue Ewing, NJ 08618-2302

AFFIDAVIT

Re: BROWNS FERRY NUCLEAR PLANT (BFN) – UNITS 1, 2, AND 3 – TECHNICAL SPECIFICATIONS (TS) CHANGES TS-418 AND TS-431 – EXTENDED POWER UPRATE (EPU) – RESPONSE TO ROUND 23 REQUEST FOR ADDITIONAL INFORMATION (RAI) REGARDING STEAM DRYER ANALYSIS SUBMODELING (TAC NOS. MD5262, MD5263, AND MD5264)

I, Alan J. Bilanin, being duly sworn, depose and state as follows:

1. I hold the position of President and Senior Associate of Continuum Dynamics, Inc. (hereinafter referred to as C.D.I.), and I am authorized to make the request for withholding from Public Record the Information contained in the documents described in Paragraph 2. This Affidavit is submitted to the Nuclear Regulatory Commission (NRC) pursuant to 10 CFR 2.390(a)(4) based on the fact that the attached information consists of trade secret(s) of C.D.I. and that the NRC will receive the information from C.D.I. under privilege and in confidence.

2. The Information sought to be withheld, as transmitted to TVA Browns Ferry as attachment to C.D.I. Letter No. 09003 dated 9 January 2009, BROWNS FERRY NUCLEAR PLANT (BFN) - UNITS 1, 2, AND 3 – TECHNICAL SPECIFICATIONS (TS) CHANGES TS-418 AND TS-431 – EXTENDED POWER UPRATE (EPU) – RESPONSE TO ROUND 23 REQUEST FOR ADDITIONAL INFORMATION (RAI) REGARDING STEAM DRYER ANALYSIS SUBMODELING (TAC NOS. MD5262, MD5263, AND MD5264).

3. The Information summarizes:

   (a) a process or method, including supporting data and analysis, where prevention of its use by C.D.I.'s competitors without license from C.D.I. constitutes a competitive advantage over other companies;
   (b) Information which, if used by a competitor, would reduce his expenditure of resources or improve his competitive position in the design, manufacture, shipment, installation, assurance of quality, or licensing of a similar product;
   (c) Information which discloses patentable subject matter for which it may be desirable to obtain patent protection.

   The information sought to be withheld is considered to be proprietary for the reasons set forth in paragraphs 3(a), 3(b) and 3(c) above.

4. The Information has been held in confidence by C.D.I., its owner. The Information has consistently been held in confidence by C.D.I. and no public disclosure has been made and it is not available to the public. All disclosures to third parties, which have been limited, have been made pursuant to the terms and conditions contained in C.D.I.'s Nondisclosure Secrecy Agreement which must be fully executed prior to disclosure.

5. The Information is a type customarily held in confidence by C.D.I. and there is a rational basis therefore. The Information is a type, which C.D.I. considers trade secret and is held in confidence by C.D.I. because it constitutes a source of competitive advantage in the competition and performance of such work in the industry. Public disclosure of the Information is likely to cause substantial harm to C.D.I.'s competitive position and foreclose or reduce the availability of profit-making opportunities.

I declare under penalty of perjury that the foregoing affidavit and the matters stated therein are true and correct to be the best of my knowledge, information and belief.

Executed on this 9th day of JANUARY 2009.

Alan J. Bilanin
Continuum Dynamics, Inc.

Subscribed and sworn before me this day: January 9, 2009

Eileen P. Burmeister, Notary Public

EILEEN P. BURMEISTER
NOTARY PUBLIC OF NEW JERSEY
MY COMM. EXPIRES MAY 6, 2012